Three Open Reading Frames Involved with Carbohydrate Transport in *Pseudomonas aeruginosa*.

BY

Karen LoVetri

A Thesis submitted to
the Faculty of Graduate Studies
In Partial Fulfillment of the Requirements for the Degree of

MASTER OF SCIENCE

Department of Microbiology
University of Manitoba
Winnipeg, Manitoba

THE UNIVERSITY OF MANITOBA

FACULTY OF GRADUATE STUDIES

*****

COPYRIGHT PERMISSION

Three Open Reading Frames Involved with Carbohydrate Transport in *Pseudomonas aeruginosa*

BY

Karen LoVetri

A Thesis/Practicum submitted to the Faculty of Graduate Studies of The University of Manitoba in partial fulfillment of the requirement of the degree

Of

Master of Science

Abstract

The research presented herein builds on previous research done in the Worobec laboratory wherein a knockout mutant strain (WMA200) was designed from wildtype *Pseudomonas aeruginosa* PA01, in which three open reading frames (orf's) over 1.5 million bases upstream from the genes in the glucose high affinity pathway operon were deleted. The deletion of these three orf's gave a carbohydrate uptake profile which was considerably different from wildtype. In the case of the carbohydrate glucose, a five-fold decrease in the rate of uptake was observed for the mutant as compared to the wildtype. In the cases of carbohydrates fructose and mannitol, a five-fold increase in uptake was observed in the mutant compared to the wildtype. In the case of carbohydrate glycerol, the uptake remained constant (high) for both the mutant and wildtype strains. The characterization of each of the three orf's is undertaken in this thesis.

Initially WMA200 was tested via polymerase chain reaction (PCR) with each set of orf primers and it was shown that each gene in the knockout mutant strain was amplified. This finding lead to experiments designed to recreate the original mutant (WMA200), which were unsuccessful. Insertion mutants were obtained from the University of Washington Genome Center.

This thesis uses insertion mutants for each orf and generates the following data with each mutant. Each mutant was confirmed via PCR and transformed with its appropriate

gene using plasmid pUCP20/21. Growth curves were performed with each mutant and wildtype using four carbohydrates (glucose, fructose, mannitol and glycerol) as substrate. Carbohydrate uptake assays were performed on the mutant, transformed mutant and wildtype after growth in four carbohydrates. A protein BLAST (pBLAST) analysis was performed on each orf. The pBLAST gave strong protein homology for two of the three orf's. *OrfB* has a high homology to *E. coli* MdoB protein and *orfD* has a high homology to *E. coli* spermidine synthase. Mutant B had a significantly different growth rate in glucose and glycerol compared to wildtype. Mutants C and D had significantly different growth rate in glycerol compared to wildtype. Mutant B had reduced uptake of glucose, mannitol and glycerol. Partial complementation of mutant B was only for glycerol uptake. Mutant C showed a reduced uptake of glucose and glycerol. Full complementation was seen only in the case of glycerol uptake. Mutant D showed a reduced uptake of glucose, mannitol and glycerol. Full complementation was seen with both mannitol and glycerol uptake.

Acknowledgments

I would like to sincerely thank my supervisor Dr. E. A. Worobec for her moral and financial support throughout my work on my Master's thesis. I would also like to acknowledge my fellow graduate students particularly Ayush Kumar and Kari Kutcher for all their words of wisdom, feedback and ideas when things were and were not working. A special thank you to Dr. R. Habibian for the pUCP20/*orfC* and pUCP20/*orfD* constructs. More thanks to Olasunkanmi (Suki) Famobio and Sanela Begic for their support during my time in the Worolab, along with summer students, Bonnie Solylo and Ian MacArthur. Finally all would be for naught without the neverending support of my husband, Joe and our children, Natalie, Peter, Silvana, Carmela and our two, four footed companions Guido (Miniature Pinscher) and Latifa (Neapolitan Mastiff).

Table of Contents

Chapter 3

List of Figures

List of Tables

Abbreviations

a. a. - amino acids

ABC - ATP binding cassette

ADC - arginine decarboxylase

AMP - adenosine monophosphate

Ap - ampicillin

ATP - adenosine triphosphate

bla - β - lactam

BLAST - basic local alignment search tool

BM - basal medium

bp - base pair

C - Celsius

cAMP - cyclic AMP

CAPS - cyclophexylamine-1-propanesulfonic acid

CF - Cystic Fibrosis

CRC - catabolite repression control

DMSO - dimethyl sulfoxide

DNA - deoxyribonucleic acid

Edd - 6-phosphogluconate dehydrogenase

EDP - Entner-Doudoroff Pathway

EDTA - ethylene-diaminetetraacetic acid

EMP - Embden-Meyerhoff-Parnas

Eda - 2-keto-3-deoxy-6-phosphogluconate aldolase

Fba - fructose 1,6-bisphosphate aldolase

Fpk - fructose 1-phosphate kinase

FPTS - fructose phosphotransferase system

Frk - fructokinase

g - gravity

Gad - gluconate dehydrogenase

Gap-NAD - glyceraldehyde 3-phosphate dehydrogenase-nicotinamide adenine dinucleotide

Gbp - glucose binding protein

GC - guanine/cytosine

Gcd - glucose dehydrogenase

Glk - glucokinase

GlpD - glycerol P-dehydrogenase

GlpF - glycerol facilitator protein

GlpK - glycerol kinase

Gm - gentomicin

GnuK - gluconate kinase

His - histidine

hr - hour

IM - inner membrane

IPTG - isopropylthio-β-D-galactoside

kb - kilobases

kDa - kilodaltons

Kgk - 2-ketogluconate kinase

Kgr - 2-keto-6-phosphogluconate reductase

K_m- the substrate concentration for getting half maximum velocity

LB - Luria Bertani

lacZ - β-galactosidase

M - molar

Mbp - mannitol binding protein

MCS - multicloning site

Mdh - mannitol dehydrogenase

MDO - membrane derived oligosaccaride

MdoB - phosphoglycerol transferase I

NRC - National Research Council

mg - milligram

min - minute

ml - milliliter

mM - milliMolar

M_r - molecular weight

N - amino

NCBI - National Centre for Biotechnology Information

nm - nanometer

OD - optical density

OM - outer membrane

orf - open reading frame

OPG - osmoregulated periplasmic glycan

oprB - outer membrane porin B

oprD - outer membrane porin D

oriT - origin of transfer

PA - *Pseudomonas aeruginosa*

PAGE - polyacrylamide gel electrophoresis

PCR- polymerase chain reaction

PEP - phosphoenolpyruvate

Pgi - phosphoglucoisomerase

P-GRO - phosphatidyl glycerol

phoA - alkaline phosphatase

pI - isoelectric point

PMF - proton motive force

pmol - picomole

PTS - phosphotransferase system

PVDM -polyvinylidene difluoride membrane

RBS - ribosome binding site

RNA - ribonucleic acid

RNase - ribonuclease

s - seconds

sacB - gene encoding levansucrase

SDS - sodium dodecyl sulfate

Sm - streptomycin

spp. - species

TCA - tricarboxylic acid cycle

Tc - tetracycline

UDP - uridine diphosphate

V - volt

V_{max} - maximum velocity

v/v - volume per volume

w/v - weight per volume

w/w - weight per weight

X-gal - 5-bromo-4-chloro-indoyl-β-D-galactopyranoside

XP - 5-bromo-4-chloro-3-indoyle phosphate

Zwf - glucose 6-phosphate dehydrogenase

Chapter 1

Introduction and Literature Review

1.1 General Introduction

1.1.1 Pseudomonas aeruginosa

P. aeruginosa is a gram-negative, rod shaped bacterium equipped with a polar flagella used for motility. *P. aeruginosa* is particularly adept at using a vast array of sugars, fatty acids, di- and tri-carboxylic acids, alcohols, polyalcohols, glycols, amino acids, *etc.*, as food sources and electron donors for energy generation. *P. aeruginosa* produces a blue pigment called pyocyanin, and a yellowish green fluorescent pigment called pyoverdin which is used as an iron transporter. It also has the ability to produce a very potent toxin called Exotoxin A, which works by blocking protein synthesis in the cell it enters (Brock *et al.*, 1984, Mims *et al.*, 1993).

P. aeruginosa is easily isolated from the soil but is also prominent in hospital settings where it plays the role of an opportunistic pathogen. An opportunistic pathogen is one which is usually present in the external and internal environment of a person but will not be detrimental unless the immune system is breached in some manner, *e.g.* surgical wounds, burns, infections, radiation or disease, *etc.*

P. aeruginosa has a natural antibiotic resistance that is of particular concern for burn patients and cystic fibrosis (CF) patients. Its antibiotic resistance is one of the most significant features which complicates the treatment of this infection. In the case of patients with CF the disease causes very viscous bronchial secretions in the lungs of the patient. This viscosity leads to stasis in the lungs and predisposes the patient to infection by *P. aeruginosa.* Once *P. aeruginosa* takes hold it is difficult to control due to the innate antibiotic resistance.

P. aeruginosa has a genome of over 6 million base pairs. The complete genome sequence has been reported (Stover *et al.*, 2000) and the genome database is maintained by the *Pseudomonas* Community Annotation Project collaborators (PseudoCAP.http// www.pseudomonas.com). The large size of the genome gives this bacterium considerable versatility in its ability to adapt to the varying environmental conditions it may encounter. *P. aeruginosa* can be found in various places such as soil, water, homes, hospital, inside human lungs, burns, wounds or blood. These are all challenging environments (Brock *et al.*, 1984). Its gene clustering ability is greater than required by the operon model. This clustering is seen in functionally related, but independently regulated genes, such as the carbohydrate catabolism genes (Rosenberg and Hegeman, 1971, Roehl *et al.*, 1983, Cuskey *et al.*, 1985a).

1.2 Literature Review

1.2.1 P. aeruginosa carbohydrate transport systems

An important initial point to note regarding carbohydrate use in *P. aeruginosa* is that it differs from *Escherichia coli* in that metabolism of glucose is not preferred by *P.*

aeruginosa but succinate and other tricarboxylic acid (TCA) cycle intermediates are used before glucose (Blevins *et al.*, 1975, Hylemon and Phibbs, 1972, Midgley and Dawes, 1973).

The Entner-Duodoroff Pathway (EDP), also referred to in Fig. 1-1 as the central cycle, and lower Embden-Meyerhoff-Parnas (EMP) pathway are the main cycles used in *P. aeruginosa* for carbohydrate catabolism (Blevins *et al.*, 1975, Cuskey *et al.*, 1985a). Both of these pathways are essential for aerobic and anaerobic catabolism of carbohydrates (Hunt and Phibbs, 1983). In the EDP the following enzymes, glucose 6-phosphate dehydrogenase (Zwf), 2-keto-3-deoxy-6-phosphogluconate aldolase (Eda), glucokinase (Glk), and 6-phosphogluconate dehydrogenase (Edd) are coinducible by the presence of: glucose, gluconate, mannitol, fructose, glycerol or glycerol-3-phosphate (Blevins *et al.*, 1975, Phibbs *et al.*, 1978). These enzymes are subject to catabolite repression control (CRC) by the TCA cycle intermediates which in *P. aeruginosa* is cyclic adenosine monophosphate (cAMP) independent in contrast to *E. coli* where growth in glucose results in repression of other catabolic pathways via changes in levels of cAMP (Tiwari and Campbell, 1969, MacGregor *et al.*, 1991). It has been shown that the *hexR* (PA 3184) gene product is a negative control protein and when bound represses the expression of the following EDP enzymes: Glk, Zwf, Edd, Eda and Gap-NAD of the lower EMP pathway. With the number of genes involved in carbohydrate catabolism in *P. aeruginosa* it is easy to see the complexity of regulation (Temple *et al.*, 1990).

Fig. 1-1 is a summary of what is known about carbohydrate transport and catabolism in *P. aeruginosa*. Appendix A contains a table that cross references the components in Fig. 1-1 with *P. aeruginosa* (PA) numbers from the *P. aeruginosa* genome site, gene name,

beginning and end of gene (indicated via base pair numbers), a short description of the gene and a color coding system to enable easy visual identification of gene clusters specific to particular carbohydrate systems.

Table 1-1. Abbreviation table for Fig. 1-1

Section *	Abbreviation	Full name	Section *	Abbreviation	Full name
A	OM	outer membrane	**E**	Fpk	fructose1-phosphate kinase
A	CM	cytoplasmic membrane	**F**	GlpF	glycerol uptake facilitator protein
A	PP	periplasm	**F**	GlpK	glycerol kinase
B	OprD	outer membrane porin D	**F**	GlpD	glycerol 3-phosphate dehydrogenase
B	Gcd	glucose dehydrogenase	**G**	Zwf	glucose 6-phosphate dehydrogenase
B	Gad	gluconate dehydrogenase	**G**	Edd	6-phosphogluconate dehydratase
B	GnuT	gluconate permease	**G**	Eda	2-keto-3-deoxy-6-phosphogluconate aldolase
B	GnuK	gluconate kinase	**G**	Fba	fructose1, 6-bisphosphate aldolase
B	Kgk	2-ketogluconate kinase	**G**	Tpi	triose phosphate isomerase
B	Kgr	2-keto-6-phosphogluconate reductase	**G**	Fbp	fructose 1,6-bisphosphatase
C	OprB	outer membrane porin B	**G**	Pgi	phosphoglucoisomerase
C	Gbp	glucose binding protein	**H**	Gap	glyceraldehyde 3-phosphate dehydrogenase
C	Glk	glucokinase	**H**	Pgk	3-phosphoglycerate
D	Mbp	mannitol binding protein	**H**	Pgm	phosphoglucomutase/ phosphoglucoisomerase
D	Mdh	mannitol dehydrogenase	**H**	Eno	enolase
D	Frk	fructokinase	**H**	Pyk	pyruvate kinase
E	EnzII	enzyme II of PTS system	**I**	Pyc	pyruvate carboxylase
E	PTS	phosphotransferase system	**I**	TCA	tricarboxylic acid cycle
E	EnzI	enzyme I of PTS system			

* In Fig. 1-1 letters are given to sections which correspond to various aspects of carbohydrate transport and catabolism

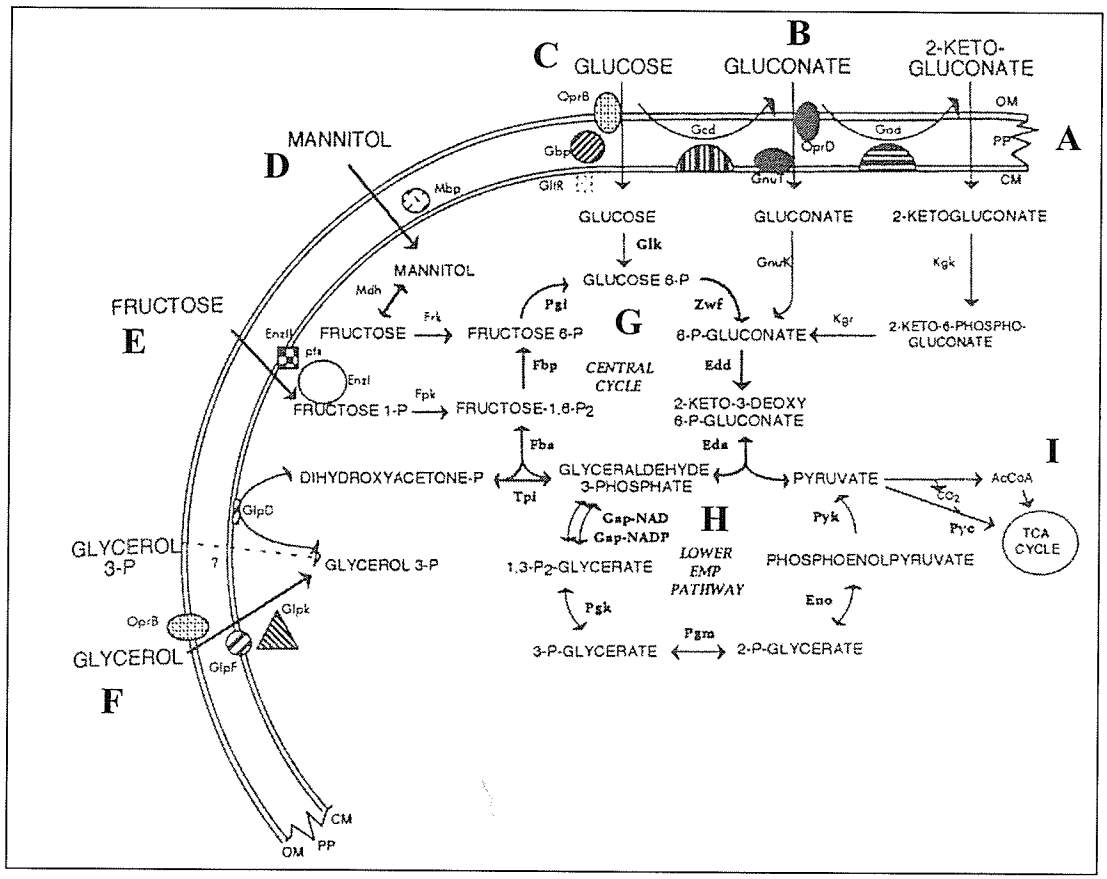

Figure 1-1. Carbohydrate transport and catabolism overview

Letters are given to corresponding sections **A** - components of the cell wall in *P. aeruginosa*, **B** - components of the glucose oxidative system, **C** - components of the glucose phosphorylative system, **D** - components of the mannitol phosphorylative system, **E** - components of the fructose phosphotransferase system, **F** - components of the glycerol dual uptake system, **G** - components of the EDP, **H** - the lower EMP pathway, **I** - the TCA cycle (Reproduced from Temple *et al.*, 1998).

1.2.1.1 Glucose transport

Glucose has two ways of entering the cell. One way is by the oxidative pathway (Eagon and Phibbs, 1971, Midgley and Dawes, 1973) which is activated when concentrations of extracellular glucose are high (K_m = 2.8 mM). Another is by the phosphorylative pathway which uses active transport to take up glucose when extracellular concentrations of glucose are low (K_m = 8 μM, Eagon and Phibbs, 1971, Midgley and Dawes, 1973, Guymon and Eagon, 1974). Eagon and Phibbs, (1971) also showed that glucose enters by a diffusion process which is constant and unsaturable. The proteins needed for glucose utilization in *P. aeruginosa* are always available but are subject to metabolic regulation (Eagon and Williams, 1960, Midgley and Dawes, 1973). Glucose induces EDP enzymes but glucose limitation has no affect on the EDP enzymes except for isocitrate dehydrogenase (not shown) of the TCA cycle which falls by 70% (Whiting *et al.*, 1976a).

A. Oxidative pathway

The oxidative pathway (Fig. 1-1, B), also referred to as the low affinity system, converts glucose to gluconate by the inner membrane bound glucose dehydrogenase (Gcd) (Stinnett *et al.*, 1973). Gluconate can enter into the cell by OprD, the major porin for gluconate transport, or further be catalyzed to 2-ketogluconate by the inner membrane bound enzyme gluconate dehydrogenase (Gad, Huang and Hancock, 1993, Temple *et al.* 1998, Whiting *et al.*, 1976a,b). When glucose is converted to gluconate the extracellular medium increases in the concentration of gluconate. The abundance of gluconate is a major factor in repressing the phosphorylative transport system, but also induces components for the oxidative pathway (Whiting *et al.*, 1976a,b, Hunt and Phibbs, 1983). For the oxidative transport systems to be induced glucose must be converted to gluconate and 2-

ketogluconate. Once gluconate enters into the cell it is then converted to 6-P-gluconate by gluconate kinase (GnuK) which in turn enters the EDP. 2-keto-gluconate enters the cell and is reduced to 2-keto-6-phosphogluconate by its reductase (Kgr) to 6-phosphogluconate and enters into the EDP. The advantage for *P. aeruginosa* to quickly convert high levels of glucose into gluconate or 2-ketogluconate is to sequester the available glucose and make it unusable to other competing organisms (Whiting *et al.*, 1976b). The availability of oxygen is also a factor for *P. aeruginosa* glucose metabolism. When concentrations of oxygen are high, the oxidative pathway is used and when concentrations of oxygen are limiting it uses the phosphorylative pathway. The change is caused by a decrease in activity and expression of enzymes (Gcd, Gad, GnuK, Kgr) responsible for glucose conversion and catabolism in the oxidative pathway (Mitchell and Dawes, 1982). The EDP and the EMP pathway are essential for both aerobic and anaerobic catabolism of these carbohydrates by *P. aeruginosa* (Hunt and Phibbs, 1983).

B. Phosphorylative pathway

When glucose is taken up by the phosphorylative pathway (Fig. 1-1, C) it is transported in an unaltered state (Phibbs and Eagon, 1970) through the outer membrane by OprB, a carbohydrate specific porin. Glucose is then transported through the periplasmic space by a glucose binding protein (Gbp). Glucose is then recruited from the Gbp by the ATP binding cassette (ABC) transporter which uses adenosine triphosphate (ATP) to deliver the glucose into the cytosol (Temple *et al.*, 1998). Once in the cytoplasm, glucose is phosphorylated by glucokinase (Glk), an enzyme which is induced by growth on glucose (limited amounts), to glucose 6-phosphate, the intermediate used in the EDP of catabolism (Eagon and Phibbs, 1971, Blevins *et al*, 1975, Whiting *et al.*, 1976a).

There are aspects of regulation of the phosphorylative pathway which involve glucose, oxygen and gluconate. Glucose limitation results in decreased levels of gluconate dehydrogenase (Gad), glucose dehydrogenase (Gcd), gluconate kinase (GnuK), 2-ketogluconate kinase (Kgk), and 2-keto-6-phosphogluconate reductase (Kgr). All of these enzymes are required for the oxidative system. Glucose limitation also results in increased levels of glucokinase (Glk) and glucose 6-phosphate dehydrogenase (Zwf) (Whiting *et al.*, 1976b, Phibbs and Eagon, 1970). These enzymes are required for glucose catabolism via EDP. Oxygen limitation results in the obligatory use of the phosphorylative pathway (Mitchell and Dawes, 1982, Hunt and Phibbs, 1983). The phosphorylative system is repressed by high concentrations of gluconate produced by glucose dehydrogenase (Gcd) (Whiting *et al.*, 1976a).

The high affinity system (Fig. 1-2) is composed of four known components: an outer membrane carbohydrate selective porin called OprB (Wylie and Worobec, 1995), a periplasmic glucose-binding protein (Gbp) which transfers glucose from OprB to other components of the system located in the bacterial inner membrane. Gbp is thought to transport glucose across the periplasm to the cytoplasmic membrane components of the system (Stinson *et al.*, 1977). An ATP binding cassette (ABC) transporter actively transports glucose across the cytoplasmic membrane. The ABC transporter is composed of GltF and GltG, two proteins, which have amino acid sequences that implicate them as transmembrane proteins transversing the inner membrane (Kutcher, 2004). On the cytoplasmic side of GltF and GltG is the ATP binding protein component, GltK (Adewoye and Worobec, 1999). In the cytoplasm a glucose-catabolizing glucokinase (Glk) catalyses phosphorylation of cytoplasmic glucose into glucose-6-phosphate (Cuskey *et al.*, 1985a).

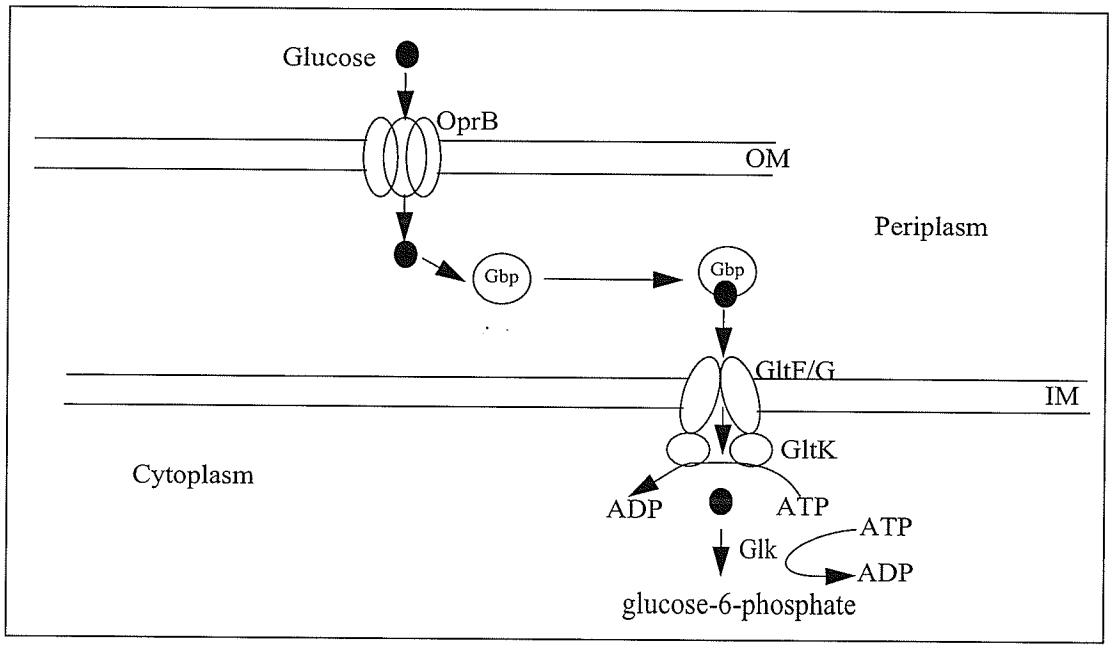

Figure 1-2. Schematic of high affinity glucose transport system of *P. aeruginosa*

Glucose (●) enters the outer membrane (OM) through the OprB porin. The glucose binding protein (Gbp) binds glucose in the periplasm and transports it to the inner membrane (IM) where glucose is transversed through with the assistance of the ATP binding cassette (composed of GltF & GltG). GltK breaks down ATP to ADP. Glucose is then phosphorylated by glucokinase (Glk) into glucose-6-phosphate (diagram adapted from Kutcher, 2004).

B.1 OprB

The OprB porin is located in the outer membrane of *P. aeruginosa* (Hancock and Carey, 1980). This porin is involved in the transport of glucose as demonstrated via liposome swelling assay (Trias *et al.*, 1988) and by black lipid bilayer analysis (Wylie *et al.*, 1993). The OprB porin is expressed when either the glucose or glycerol high affinity uptake systems are induced (Hancock and Carey, 1980, Williams *et al.*, 1994). It is also responsive to environmental factors such as pH, temperature, salicylate, osmolarity and various carbohydrate sources (Adewoye and Worobec, 1999). It is anion selective, in contrast to other carbohydrate specific porins which are cation selective. This ion selectivity may be determined by residues at or near the exterior of the pore away from the binding site residues (Wylie *et al.*, 1993). OprB can transport other sugars such as fructose, mannitol and glycerol in addition to glucose (Wylie *et al.*, 1993, Wylie and Worobec, 1994, 1995, Williams *et al.*, 1994). The OprB porin has been cloned and sequenced and it was demonstrated to be present in all members of the *Pseudomonadaceae* family (Wylie and Worobec, 1994, Saravolac *et al.*, 1991).

B.2 Glucose binding protein

The glucose binding protein (Gbp) is found in the periplasm of *P. aeruginosa.* It has a molecular weight of 44,000 and is specific for glucose (Stinson *et al.*, 1977, Wylie and Worobec, 1993). The synthesis of Gbp and the glucose high affinity transport system are coregulated (Stinson *et al.*, 1976, 1977). The Gbp is an essential component of glucose active transport system (Cuskey *et al.*, 1985a, Sly *et al.*, 1993). Gbp is involved and required for glucose chemotaxis (Stinson *et al.*, 1977, Sly *et al.*, 1993).

B.3 ABC transport systems

The ABC transporter is split into two components, a transmembrane permease and an ATPase. GltF and GltG proteins are the putative transmembrane components of the *P. aeruginosa* glucose ABC transporter (Kutcher, 2004). These two highly hydrophobic membrane proteins are thought to function as a heterodimer (Higgins *et al.*, 1990, Kutcher, 2004). Glucose uptake assays performed using GltF and GltG insertion mutants demonstrated that these two proteins have a definite role in the high affinity glucose uptake system (Kutcher, 2004). It is thought that the hydrophilic regions of GltF and G facing the cytoplasm interact peripherally with GltK, the ATP binding component. Studies show that the portion of the protein facing the periplasm space interacts with the Gbp in the periplasm. Little is known about how the translocation of glucose through the cytoplasmic membrane is achieved. It is thought that these proteins have substrate specificity but location(s) of this specificity is unknown. The GltK of the system binds ATP and couples ATP hydrolysis to the transport process. It is though that two polypeptides together function as a heterodimer, supporting the fact that two ATP molecules may be hydrolyzed per transport event. (Stinson *et al.*, 1976, Higgins *et al.*, 1990, Adewoye, 1999).

B.4 Glucokinase

Glucokinase is the enzyme which catalyzes the phosporylation of glucose to glucose-6-phosphate in the cytoplasm of the cell. Glucokinase is expressed coordinately with four other EDP enzymes: Zwf, Edd, Eda and Gap-NAD of the lower EMP pathway (Temple *et al.*, 1990, Cuskey *et al.*, 1985a).

B.5 Glucose transport regulator (GltR)

A specific glucose transport regulator (GltR) has been identified (Cuskey *et al.*, 1985a, Sage *et al.*, 1996). This regulator is required for glucose transport by *P. aeruginosa*. This regulator has a 46.6% identity and 70.1% similarity to OmpR, a known response regulator protein in *E. coli* (Powell *et al.*, 1989). This protein has highly conserved residues Asp-13, Asp-56 and Lys-108 of which have recognized functions in phosphorlyation of response regulator proteins. The OmpR subfamily of these proteins control a variety of systems in bacteria some of which include response to medium osmolarity, phosphate uptake, virulence and antibiotic resistance. It is known that both OprB and Gbp are regulated by GltR (Sage *et al.*, 1996).

1.2.1.2 Mannitol transport and catabolism

Mannitol (Fig. 1-1, D) passes through OprB porin into the periplasm (Wylie and Worobec, 1993). Once in the periplasm, mannitol is bound by a mannitol binding protein (Mbp), and transported via an ABC transporter into the cytoplasm (Eisenberg and Phibbs, 1982, Davis and Robb, 1985). The Mbp has a molecular weight of 37,000 and an isoelectric point (pI) of 8.3. Inhibition studies were done on the Mbp and it was determined that glucose and glycerol did not affect mannitol binding but fructose caused a 20% inhibition of binding to mannitol (Eisenberg and Phibbs, 1982). Once mannitol is in the cytoplasm the enzyme mannitol dehydrogenase (Mdh), which is required and induced when grown in mannitol only, converts mannitol to fructose (Phibbs and Eagon, 1970, Phibbs *et al.*, 1978, Davis and Robb, 1985). This conversion demands an increased level of fructokinase (Frk) (Phibbs and Eagon, 1970). The Frk converts the fructose into fructose 6-phosphate which is incorporated in the EDP. Important to note, rapid mannitol uptake must be induced, in

uninduced cells mannitol enters via passive diffusion, but cannot be utilized due to lack of (Frk) fructokinase (Phibbs and Eagon, 1970, Eagon and Phibbs, 1971). Mannitol uptake induces the glucose enzyme glucokinase and glucose 6-phosphate, the first intermediates of the EDP (Eagon and Phibbs, 1971, Phibbs *et al.*, 1978).

1.2.1.3 Fructose transport and catabolism

Unlike other carbohydrates transported via *P. aeruginosa,* the uptake of fructose (Fig 1-1, E) is driven by the phosphoenolpyruvate (PEP) - (PTS) phosphotransferase system (Baumann and Baumann, 1975, Sawyer *et al.*, 1977, Van Dijken and Quayle, 1977, Phibbs *et al.*, 1978, Roehl and Phibbs, 1982). This is the only known PTS system in *P. aeruginosa* (Phibbs *et al.*, 1978, Durham and Phibbs, 1982, Roehl and Phibbs, 1982). This system uses the OprB porin (Wylie and Worobec, 1993) for fructose to enter into the periplasm. The membrane associated Enzyme II is located in the periplasm (Roehl and Phibbs, 1982). Enzyme II forms a complex with cytoplasmic soluble Enzyme I (Roehl and Phibbs, 1982, Durham and Phibbs, 1982). Soluble Enzyme I phosporylates fructose to give fructose 1-P which is further phosphorylated to fructose-1,6-P_2 by fructose 1- phosphate kinase (Fpk). It was shown in *P. duodorffii* that the phosphorylation of fructose by Enzyme I is induced by the enzyme Fba (fructose 1,6-bisphosphate aldolase) of the EMP (Baumann and Baumann, 1975). It is important to note that rapid fructose uptake must be induced (Durham and Phibbs, 1982, Eagon and Phibbs, 1971, Phibbs and Eagon, 1970, Phibbs *et al.*, 1978, Eagon and Williams, 1960) and in uninduced cells fructose enters via diffusion (Phibbs and Eagon, 1970). Note also that fructose obtained externally is catabolized via a different pathway than fructose originating intracellularly through mannitol catabolism as discussed above.

1.2.1.4 Glycerol transport and catabolism

Fig. 1-1 F, shows that glycerol has two ways to enter into the cell. Glycerol is transported into the cell unaltered (Tsay *et al.*, 1971) via the OprB porin (Wylie *et al.*, 1993, Williams *et al.*, 1994). There is an inducible glycerol binding protein (Tsay *et al.*, 1971) not depicted in Fig. 1-1 but has been shown to transport glycerol through the periplasm to the cytoplasmic glycerol facilitator protein (GlpF) which is regulated by catabolite repression control (Weissenborn *et al.*, 1992, Schweizer *et al.*, 1997). Glycerol is shuttled into the cytoplasm where glycerol kinase (GlpK) phosphorylates it to glycerol 3-phosphate which is oxidized to dihydroxyacetone phosphate by glycerol-P dehydrogenase (GlpD). It then enters into the EDP. The alternate case for glycerol transport is still unknown at this time.

The identity of a glycerol regulatory unit called GlpR (not shown in Fig 1-1) was demonstrated by Cuskey and Phibbs, 1985b. It was further determined that this regulator was responsible for glycerol transport of both pathways. Glycerol-3-P is the inducer metabolite which causes expression of glycerokinase (GlpK) and subsequent uptake of glycerol in the cell (Cuskey and Phibbs, 1985b).

1.2.2 Identity of a trans-regulatory locus involved in carbohydrate transport

Initially, a gene located upstream of the *oprB* gene, a porin involved in high-affinity carbohydrate transport, was identified. It was observed that mutations in this gene caused significant reduction in glucose transport. Upon further investigation it was discovered that this region was composed of a three orf cluster called *orfBCD*. Fig. 1-3 shows the three orfs

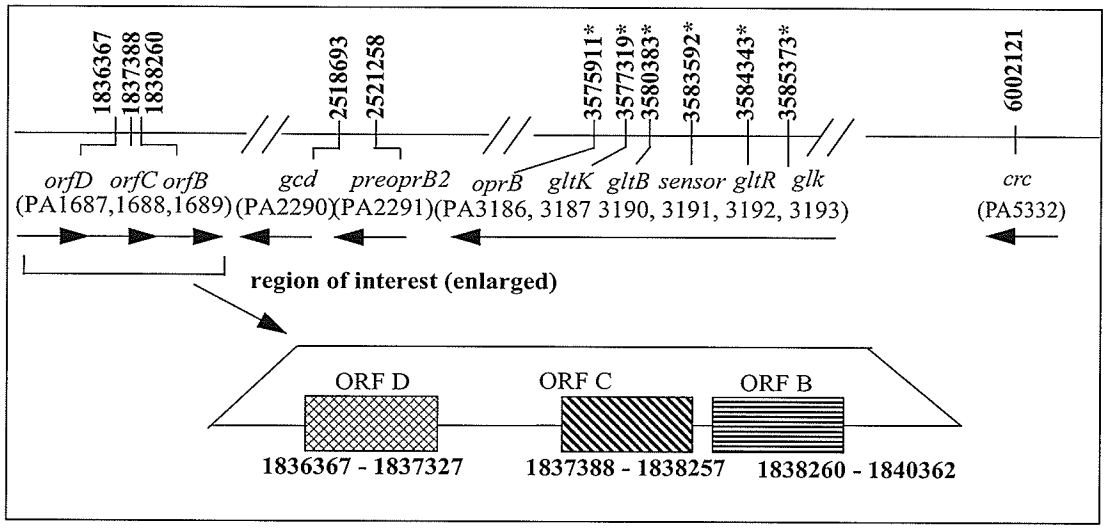

Figure 1-3. Genome representation of *orfBCD* in reference to the components of the glucose transport cluster

The bold numbers indicate nucleic acid base number in *P. aeruginosa* genome. Names of *orfs* are in italics. *P. aeruginosa* genome numbers are in brackets. Arrows indicate direction of gene transcription. Glucose transport cluster (indicated by * after nucleic acid base number) runs from PA3186-PA3193. Adapted from Stover *et al.*, 2000.

of interest of which *orfBCD* region is located 1.5 million bases upstream of the operon which is associated with the high-affinity glucose transport system (Adewoye, 1999). *P. aeruginosa* genome has a significant amount of gene clustering as is demonstrated by Fig. 1-3 and Appendix A [which illustrates gene clustering in the various carbohydrate uptake systems (Cuskey *et al.*, 1985a)]. The *orfBCD* cluster was cloned, sequenced and a deletion mutant called WMA200 was constructed and confirmed via Southern blot. It was reported by Adewoye (1999) that one or a combination of all the orf's play a role in high affinity carbohydrate uptake. Fig. 1-4A shows that WMA200 had a five fold decrease of [^{14}C] glucose uptake compared to wildtype. Fig. 1-4B shows that wildtype and WMA200 had equal uptake of [^{14}C] glycerol. Fig. 1- 4C & D show that deletion mutant WMA200 had a seven-fold increase in [^{14}C] mannitol uptake and a five-fold increase in the [^{14}C] fructose uptake compared to wildtype. This uptake data demonstrated the effect of the *orfBCD* deletion on glucose, mannitol, glycerol and fructose transport systems suggesting that these *orfs* may encode a regulatory protein which affects the carbohydrate ABC transporters as well as the phosphoenolpyruvate-dependent fructose phosphotransferase system. The binding of glucose to OprB porin and the periplasmic Gbp of the transport system were not affected. The expression level of the periplasmic Gbp component was not altered in the mutant (Adewoye, 1999, Adewoye *et al.*, 1999). This data supported the idea that one or all of the orf's were working in *trans* to control one or more aspects of the high affinity uptake system.

In summary, the work of Adewoye indicates that the products of *orfBCD* locus in *P. aeruginosa* may act in *trans* to regulate the glucose high affinity transport system to increase glucose uptake rates. Similarly, the products of the *orfBCD* locus may be working

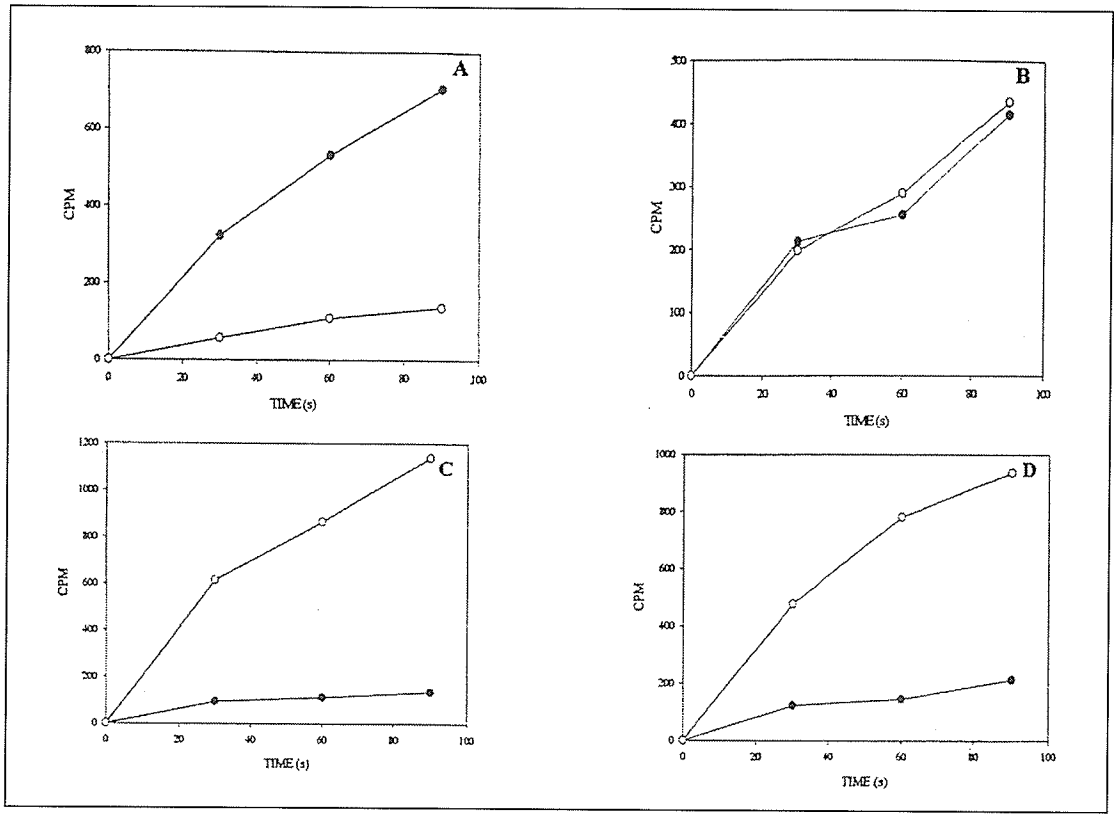

Figure 1-4. [^{14}C] carbohydrate uptake studies of *P. aeruginosa orfBCD* mutant and wildtype *P. aeruginosa* PA01

Panel **A**, [^{14}C] glucose uptake; Panel **B**, [^{14}C] glycerol uptake, Panel **C**, [^{14}C] mannitol uptake; Panel **D**, [^{14}C] fructose uptake. Wildtype (●), *orfBCD* mutant (○). Uptake of 2.4 mM of [^{14}C] sugar was studied at a cell density, OD_{600} = 0.04, in order to ensure a linear initial uptake of radiolabelled sugar by starved cells of *P. aeruginosa* PAO1 wildtype and *orfBCD* mutant. Data are representative of at least three independent assays (Adewoye, 1999).

to decrease mannitol and fructose uptake in wildtype.

The preliminary work of Adewoye (1999) showed that *orfBCD* had an effect on the high affinity glucose uptake system. The discovery of the role that each of the open reading frames has on the high affinity glucose uptake system of *P. aeruginosa* was the basis of this thesis.

1.2.2.1 Open reading frame B

The *orfB* consists of 2,102 bases and encodes a 700 a. a. polypeptide with an expected size of 77,984 Da. The protein has a pI = 6.46. The gene has a GC content of 65.6% (Stover *et al.,* 2000). It has a putative secretory signal sequence. Using various computer programs three possible predicted cleavage sites were determined. These predicted cleavage sites were at residue 26, 44 or 55, and the approximate size of the predicted protein after cleavage would be from 68 to 75 kDa which agrees with the database protein size stated above. The prediction of hydropathy character is used to determine putative membrane spanning regions (Von Heigne, 1986). Various programs were used to predict that *orfB* could encode for a protein having four transmembrane helices, thus indicating a probable cytoplasmic membrane location (Adewoye, 1999, Stover *et al.,* 2000, Kyte and Doolittle, 1982). Sequence analysis revealed a putative rho-independent terminator following the *orfB* translational stop signal suggesting that this gene is not involved in any operonic arrangement with downstream genes. A protein BLAST (pBLAST) revealed a 23% identity to *E. coli* MdoB spanning 211 amino acids (Adewoye, 1999).

1.2.2.2 Open reading frame C

The *orfC* consists of 869 bases and encodes a 289 a. a. polypeptide with the expected size of 31,750 Da. The protein has a pI = 5.06. The gene has a GC content of 67.2%. It has a signal sequence, as determined by various programs of which all were in agreement, that is cleaved at the 36th residue from the N-terminus (Stover *et al.*, 2000). The orf has one predicted transmembrane region and a possible periplasmic or outer membrane location (Adewoye, 1999, Stover *et al.*, 2000). A pBLAST showed some homology to serine/ threonine protein kinase of *Mycobacterium* spp. (Adewoye, 1999).

1.2.2.3 Open reading frame D

The *orfD* consists of 860 bases and encodes a 286 residue protein with the expected size of 32,238 Da. This protein has a pI = 4.93. The gene has a GC content of 64.5%. The protein has a predicted cytoplasmic location. There was a consensus among various computer programs that no signal sequence cleavage site is present in *orfD*. A pBLAST showed a 60% identity to *E. coli* spermidine synthase (Adewoye, 1999).

1.3 Objectives

The objective of this thesis was to see if any or all of the *orfB*, *C* or *D* contribute independently to the phenotype initially described by Adewoye (1999). This was approached as follows:

1 - pBLAST search of each *orf*,

2 - verification of insertion mutants,

3 - construction of pUCP21/*orfB*,

4 - transformation of each insertion mutant with the appropriate pUCP20-21/*orf* construct to complement the mutation,

5 - generation of growth curve data for each mutant,

6 - generation of uptake assay data for each mutant and putative complemented mutant.

Chapter 2

Materials and Methods

2.1 Bacterial Strains, Plasmids and Growth Conditions

All bacterial strains, plasmid constructs used in this study are listed in Tables 2-1 and 2-2. *Pseudomonas aeruginosa* PA01 strain H103 (Hancock and Carey, 1979) was the source of the cloned *orfB*, *orfC*, *orfD*. *P. aeruginosa* MPA01 wildtype strain and mutant strains (Jacobs *et al.*, 2003) were used to overexpress the gene products from *orfB*, *orfC* and *orfD* following transformation with plasmid pUCP20 (*orfC, D*) or pUCP21 (*orfB*) with the cloned orf's genes (West *et al.*, 1994). All bacterial strains were routinely maintained on Luria-Bertani (LB), [20 g/L LB broth (Difco)] medium at 37°C. To induce the high affinity glucose transport system of *P. aeruginosa*, bacterial strains were grown overnight in Basal Medium 2 (BM2: 40 mM K_2HPO_4, 22 mM KH_2PO_4, 7mM $(NH_4)_2SO_4$, 0.5 mM $MgSO_4$, 10 μM $FeSO_4$), (Hancock and Carey, 1979) supplemented with 0.4% D-glucose (w/v), 0.4% D-fructose (w/v), 0.4% D-glycerol (w/v) or 0.4% D-mannitol (w/v), depending on the system to be induced. For long term storage of bacterial cultures (-70°C), dimethyl sulfoxide (DMSO) was added to overnight cultures to a final concentration of 7% (v/v). Transformed bacterial cultures were maintained in the presence of appropriate antibiotics. Ampicillin (100 μg/ml), streptomycin (25 μg/ml), or tetracycline (60 μg/ml) were added to cultures of *E. coli* strains harbouring Ap^r, Sm^r, Tc^r markers, respectively. Cultures of

Pseudomonas spp. were supplemented with carbenicillin (500 μg/ml), streptomycin (500 μg/ml) or tetracycline (500 μg/ml) depending on antibiotic resistance genes carried by these strains.

Table 2-1. Bacterial strains used in this study

Strain	Relevant characteristic(s)	Source or reference
Pseudomonas aeruginosa		
H103	Wildtype PA01 prototroph	Hancock and Carey (1979)
MPA01	Wildtype PA01(from B. Iglewski)	Jacobs *et al.*, 2003
Insertion mutants		
Mutant B_A	MPA01 *orfB* Ω *phoA,Tc*^{r}	Jacobs *et al.*, 2003
Mutant C_B	MPA01 *orfC* Ω *lacZ,Tc*^{r}	Jacobs *et al.*, 2003
Mutant D_D	MPA01 *orfD* Ω *lacZ,Tc*^{r}	Jacobs *et al.*, 2003
WMA200	H103 Δ *orfBCD*	Adewoye, 1999
Escherichia coli		
NM522	*supE thi* Δ (*lac-proAB*)*hsd5 F*'[*proAB*± *lacI*^{q} *lacZ*Δ M15]	Promega
K12CC118 (λ pir)	*araD*139Δ (*ara,leu*) 7697 Δ *lacX*74 *phoA* Δ 20 *galE galK thi rpsE rpoB argE*$_{am}$ *recA*1	C. Manoil (Seattle,USA)
Abbreviations: Tc^r - tetracycline resistance, Ω - gene insertion, Δ - gene deletion		

Table 2-2. Plasmids used in this study

Plasmid reference	Relevant characteristic(s)	Source or reference
pBL100	pTZ18U derivative carrying a 5.2kb *Bgl II* genomic fragment from pE6 cosmid clone	Adewoye and Worobec (1999)
pUCP20/21	3.8 kb ColEI cloning vector, Ap^r	West *et al.*, 1994
pUCP20/*orfD*	pUCP18 + 1.9 kb *Pst*I fragment from pRO1600[1], *orfD*,	West *et al.*, 1994, R. Habibian
pUCP20/*orfC*	pUCP18 + 1.9 kb *Pst*I fragment from pRO1600[1], *orfC*	West *et al.*, 1994, R. Habibian
pUCP21/*orfB*	pUCP19 + 1.9 kb *Pst*I fragment from pRO1600[1], *orfB*,	This study
pBON	pBL100 with a deletion of *Stu*I fragments (Δ *orfC* and partial of *orfD* and *orfB*)	This study
pEX18Tc	Tc^r, *sacB* - containing replacement vector with MCS from pUC18	Hoang *et. al.*, 1998
pKNG101	Sm^r, *sacB* - containing replacement vector with *E. coli* plasmid R6K origin, defective pir gene, RK2/ RP4	Kaniga *et al.*, 1991
pBL102	pTZ18U derivative containing ~ 1.0kb *Hind III-EcoRI* fragment obtained from pBL100 following a deletion of a 4.2 kb *Bam HI* fragment	Adewoye and Worobec, 1999
pAK18Tc	pEX18Tc plus insert of a 2.0 kb *BamHI* fragment from pBON	This study
pKK101	pKNG101 vector plus insert of a 2.0 kb *Bam HI* fragment from pBON	This study

[1] - This fragment encodes part of *bla* gene and unknown functions which confer to pMB1(COL1) replicons the ability to replicate in Pseudomonas (Olsen *et al.*, 1982).
Abbreviations: MCS - multi-cloning site, Ap^r - ampicillin resistance, Sm^r - streptomycin resistance, *sacB* - levansucrase gene, Tc^r - tetracycline resistance, Δ - gene deletion.

2.2 Nucleic acid isolation

Plasmid deoxyribonucleic acid (DNA) isolation, restriction enzyme digestion, agarose gel electrophoresis, DNA fragment purification, ligation, preparation of competent *E. coli* and competent *P. aeruginosa* were all performed by standard procedures (Ausubel *et al.*, 1989). Genomic DNA isolation of *P. aeruginosa* was performed using the boiling preparation method (Pitout *et al.*, 1998). High quality sequencing grade plasmid DNA was routinely prepared by the alkaline lysis method (Ausubel *et al.*, 1989)

2.3 DNA sequencing

DNA sequencing was performed using the automated DNA sequencing facility of the National Research Council/Plant Biotechnology Institute in Saskatoon, Saskatchewan.

2.4 Gene cloning

Cloning procedures involved standard recombinant DNA techniques as described by Sambrook *et al.*, 1989. Plasmid pBL100 harbouring *orfBCD* (Adowoye, 1999) was originally obtained from a cosmid genomic library of *P. aeruginosa* H103. Deletion subclones were obtained by digesting 1-5 μg of plasmid DNA with 5 units of restriction enzyme for 3 hours at 37°C (or 28°C for *SmaI* digestion). The digestion was carried out in a total volume of 20 μl in the presence of 1x React Buffer (Gibco BRL) and 1 μl of 1 mg/ml RNaseA. An aliquot of digested DNA was mixed with 2 μl of loading buffer [0.025% (w/v) bromophenol blue, 0.25% (w/v) xylene cyanol, 40% (w/v) sucrose in water] and electrophoresed on 0.8 % agarose gel in 1x TAE buffer (0.4 M Tris-acetate, 0.1 mM EDTA). Ligation product (10 μl) was transformed via heat shock method detailed below, into 200 μl of competent *E. coli* NM522.

orfC and *D* were cloned into pUCP20 by Dr. R. Habibian (Appendix C). *orfB* gene was cloned into pUCP21 (Results Section 3.5).

2.5 *E. coli* competent cell production and transformation

E. coli competent cells were prepared by the $CaCl_2$ method (Ausubel *et al.*, 1989). Cells were grown overnight in LB broth at 37°C. Fresh LB broth was inoculated with a 1% (v/v) of the overnight culture, and incubated with shaking to an $OD_{600} = 0.3$ at 37°C. Cells were harvested by centrifugation in a Sorvall centrifuge at 1000 x g for 5 mins at 4°C, and were resuspended in 1/10 of the original culture volume of 0.1 M ice cold $CaCl_2$. Following 30 min incubation on ice, cells were harvested by centrifugation at 1000 x g for 5 min at 4°C, and resuspended in 1/25 volume of ice cold 0.1 M $CaCl_2$. Glycerol was added to a final concentration of 23% (v/v), and 200 µl aliquots were stored at -60°C.

For transformation, approximately 10 ηg to 1 µg DNA in a volume of 10 µl was added to 100 µl of competent cells. After incubation on ice for 30 min, the mixture was heat-shocked at 42°C for 3 min, and cold-shocked on ice for 5 min. Room temperature LB broth (700 µl) was added, and the cells were incubated without shaking for 50 min at 37°C. Aliquots (100 µl) were plated in duplicate on selective media, and the remainder of cells were pelleted and resuspended in 100 µl of fresh room temperature LB and plated. The direct blue/white colony screening was done with the addition of 0.5 mM IPTG (isopropylthio-β-D-galactoside, Sigma) and 40 µg/ml of X-gal (5-bromo-4-chloro-3-indolyl-β-D-galactopyranoside) to the appropriate antibiotic-containing (ampicillin, 100 µg/ml) LB agar plates. The appropriate colonies were then subjected to plasmid preparations and the plasmid was screened for the appropriate recombinant by restriction

digestion of plasmid DNA in all cases and PCR in the case of *orfB* and *D* only. In the case of *orfC* PCR was not applicable, since the *orfC* PCR product was initially digested before ligation into the pUCP20 vector, this eliminated the majority of the forward and reverse primer binding sites.

2.6 Generation of deletion subclones

PCR experiments revealed that the WMA200 mutant no longer was void of *orfBCD* (Results Section). To regenerate the WMA200 mutant, pEX18Tc and pKNG100 suicide knock out systems was used. The knock-out system called for a new plasmid, called pBON to be made. pBON was generated by initial digestion of pBL100 with *Stu*I restriction enzyme. This was followed by a digest of pBON using *Bam*HI restriction enzyme to remove flanking regions of the genes of interest which were to be cloned into the gene replacement vector, pKNG101 (Kaniga *et al.*, 1991) and pEX18TC (Hoang *et al.*, 1998) at the unique *Bam*HI site present on these suicide vectors. The new names for these tools are pKK101 and pAK18Tc (see Appendix B for construction details). These constructed replacement vectors were to be used to create a knockout in wildtype *P. aeruginosa* H103 by homologous recombination (Schweizer and Hoang, 1995). This approach was aborted when a new source of mutants was identified as described below.

2.7 Transposon Mutants

A number of different transposon mutants for *orfB*, *C* and *D* were received from the University of Washington Genome Centre in Seattle, Washington (Jacobs *et al.*, 2003). These mutations were generated using modified Tn*5* transposons which generate *lacZ* or *phoA* gene fusions and internal His epitope/affinity purification tags. These mutants were

engineered to be non-polar. Insertion locations were mapped using a high throughput two stage semi-degenerate PCR method, automated sequencing and sequence analysis tools.

The insertion deletions used in the thesis (obtained from M. Jacobs) were derived by the following method. Transposon mutagenesis was carried out on the whole *P. aeruginosa* PA01 genome (from B. Iglewski lab, referred to as MPA01). Insertions were either IS*phoA*/hah insertions or IS*lacZ*/hah insertions as seen in Fig. 2-1. Mutagenized cells were selected by plating on LB with tetracycline (60 μg/ml), chlorampenicol (10 μg/ml) for counterselection against the donor strain, and either 5-bromo-4-chloro-3-indoyl phosphate (XP) (40 μg/ml) for detection of active *phoA* fusions or 5-bromo-4-chloro-3-indolyl-β-D-galactoside (X-gal) for active *lacZ* fusions. Transposon mutagenesis created a mutant library consisting of whole genome transposon insertion mutants which were identified by PCR.

The initial identification PCR was performed using a specific primer for the transposon and a semidegenerate primer with a defined tail. The second round of PCR used round one PCR product as template with a nested transposons primer and a primer targeted at the tail portion of semidegenerate primer. This was followed by sequencing and the sequences compared to the *P. aeruginosa* genome site. This was followed up by confirmation of positions by PCR to specifically designed primers to gene and insert and known PCR product would be generated if the position was correct (Jacobs *et al.*, 2003).

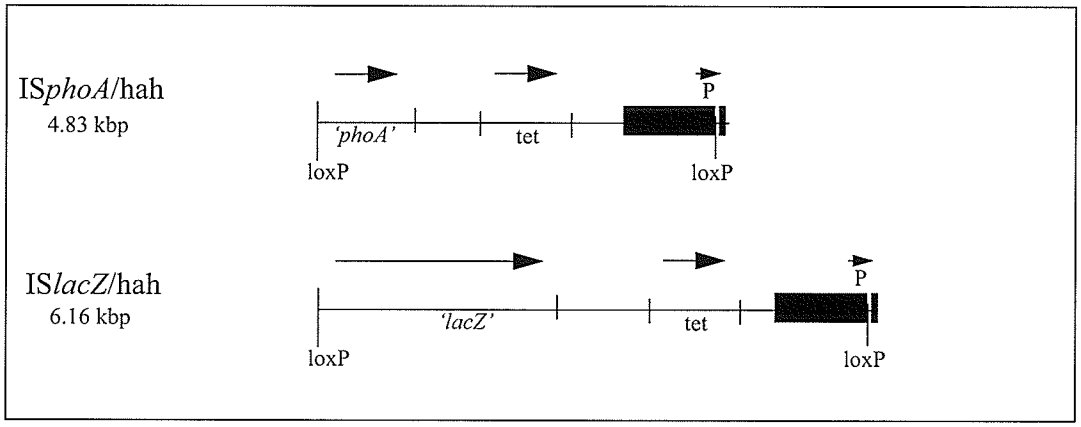

Figure 2-1. Insertion mutations using IS*phoA*/hah and/or IS*lacZ*/hah

Transposons used for insertion mutagenesis. '*phoA*' - alkaline phosphatase, '*lacZ*' - β - galactosidase, tet - tetracycline resistance marker, loxP - Cre recognition sequence, P - neomycin phosphotransferase promoter (Jacobs *et al.*, 2003).

2.8 Transformation of *P. aeruginosa* insertion mutants

The *P. aeruginosa* insertion mutants B, C and D were transformed with each of their specific genes using pUCP21/*orfB,* pUCP20/*orfC* or pUCP20/*orfD*, respectively.

The pUCP20/21 cloning vectors were designed from the pUCP18/19 vectors. Only the orientation of the multiple cloning site (MCS) differs between pUCP18 and pUCP19. pUCP18 and 20 share the same MCS as pUCP19 and 21. pUCP20/21 are unique, in that they contain a 1.9 kb *Pst*I fragment from pR01614 (originally from pRO1600). This 1.9 kb fragment encodes part of the *bla* gene and additionally confers other unknown functions, which allow the plasmid to replicate in *Pseudomonas* (National Centre for Biotechnology Information site www.ncbi.nlm.nih.gov/entrez/viewer.fcgi?db=nucleoide&val=460937, West *et al.*, 1994). pUCP20/21 allows for direct blue/white colony screening with the addition of 0.5 mM IPTG (isopropylthio-β-D-galactoside, Sigma) and 40 μg/ml of X-gal (5-bromo-4-chloro-3-indolyl-β-D-galactopyranoside) to the appropriate antibiotic-containing LB agar plates. This plasmid has a versatile MCS, small size and makes 8 to 10 copies in *P. aeruginosa*.

Competent *P. aeruginosa* cells were prepared by the method of Olsen *et al.*, (1982) with modifications. Briefly, cells were grown overnight in TN broth [5% (w/v) tryptone, 1% (w/v) glucose, 2.5% (w/v) yeast extract] at 37°C. Fresh TN broth was inoculated with a 1% inoculum of the overnight culture, and incubated with shaking to an OD_{600} = 0.3 at 30°C. Cells were harvested by centrifugation at 1000 x g for 5 min at 4°C, and were resuspended in one half of the original culture volume of cold transformation buffer (10 mM Tris, pH 8.0, 50 mM $MgCl_2$, 10 mM $CaCl_2$). Following a 10 min incubation period on ice, cells were again pelleted and resuspended in one half of the original culture volume of transformation

buffer. Cells were incubated for 20 min on ice, harvested, and resuspended in 1/10 of the original culture volume of 0.1 M $MgCl_2$ with 15% (v/v) glycerol and 10 mM PIPES (piperazine-N,N'-bis[2-ethanesulfonic acid]), pH 7.0. Cells were stored at -60°C in 200 µl aliquots.

For transformation of *P. aeruginosa* insertion mutants, approximately 0.2 µg of plasmid in a volume of 25 µl was added to 200 µl of competent cells. After incubation on ice for 1 hr, the mixture was heat-shocked at 42°C for 3 min, and cold-shocked on ice for 5 min. Room temperature LB broth (500 µl) was added, and the cells were incubated without shaking for 2 hours at 37°C. Aliquots (100 µl) were plated in duplicate on selective media, and the remainder of the cells were pelleted and resuspended in 100 µl of fresh room temperature LB broth and plated. The screening was done by plating on LB agar containing tetracycline (60 µg/ml) and carbenicillin (500 µg/ml). The colonies were subjected to plasmid preparation and the extracted plasmid was processed via restriction digest and PCR to verify that the appropriate plasmid was in the *P. aeruginosa* insertion mutant.

2.9 PCR detection

Selected oligonucleotide primers (Table 2-3, Figs. 2-2 and 2-3) specific for the *P. aeruginosa orf B*, *C* and *D* gene, were used for PCR amplification using a PTC-150 minicycler (Techne). Conditions for the PCR were: 50 ηg genomic DNA template, 2.5 mM dNTPs, 1.5 mM $MgCl_2$, 1x PCR buffer (Gibco-BRL), 1 unit Taq-DNA polymerase (Gibco-BRL), 10 pmol of each primer, 95°C 1min, 54°C (63°C for *orfB* primers, 61°C for *sacB* primers, 56°C for Hah-166 and lacZ-211 primers) 1 min, 72°C (1.0 - 1.5 min), 30 cycles. The reactions began with a 3 min cycle of 95°C to ensure separation of the double stranded

DNA, and ended with an additional 7 min extension at 72°C to ensure that fragments were all amplified.

Table 2-3. PCR primers used in this study

Primer Name	Sequence (5′ → 3′)	Anneal-ing Temp. (C.)	Paired with primer	orf amplif-ied	Product size	Figs. 2.2 & 2.3 Code #
LacZ-211	cgggcctcttcgctatta	56°	F primer *orfC*	*orfC*	964 bp	1
			R primer *orfD*	*orfD*	725 bp	
Hah-166	tcacccgttaaacggcga	55°	F primer *orfB*	*orfB*	780 bp	2
			F primer *orf D*	*orfD*	920 bp	
$B_{1(forward)}$	caccctgcagatgttgct	54°				3
$B_{2(reverse)}$	cgccgaattcctgcgct	54°	$B_{1(forward)}$	*orfB*	1.4 kbp	4
$C_{1(forward)}$	tactacaacgcc**ggatcc**[1]	54°				5
$C_{2(reverse)}$	ggtggttcggaattccgt[2]	54°	$C_{1(forward)}$	*orfC*	1.1 kbp	6
$D_{1(forward)}$	tggtggaattcgcgccatt[2]	54°				7
$D_{2(reverse)}$	caggca**ggatcc**tactacg[1]	54°	$D_{1(forward)}$	*orfD*	1.3 kbp	8
$B_{1(forward)}$	ctacaaccgcgaactgatcg	63°				9
$B_{2(reverse)}$	gtattctccagcaggctcttg	63°	$B_{1(forward)}$	*orfB*	2.0 kbp	10
*IDF_1 (forward)	aagggatcgaaggccaccgg	66°	$IDR_{2(reverse)}$	confirm WMA 200	1.2 kbp	11
*IDF_2 (forward)	gcatgttcgccaccatggcc	66°	IDR_1 (reverse)	confirm pBL100 & wild-type	2.5 kbp	12
*IDR_1 (reverse)	tggagggcagtccggagatc	66°	IDF_1 (forward)	confirm WMA 200	3.3 kbp	13
*IDR_2 (reverse)	accccaggcgaaggtcatgg	66°	IDF_1 (forward)	confirms pBL100 & wild-type	2.5kbp	14

* these primers were designed to be used to identify deletion mutant WMA200 which has portions of *orfD* and *orfB* present. $IDF_{1(forward)}$located on pBL100, base #381-400, $IDF_{2(forward)}$ located on pBL100, base #3901-3920, $IDR_{1(reverse)}$ located on pBL100, base #5361-5380 $IDR_{2(reverse)}$located on pBL100, base #1590-1610. pBL100 see Appendix B.

[1] - *Bam*HI restriction site in bold.

[2] - *Eco*RI restriction site underlined.

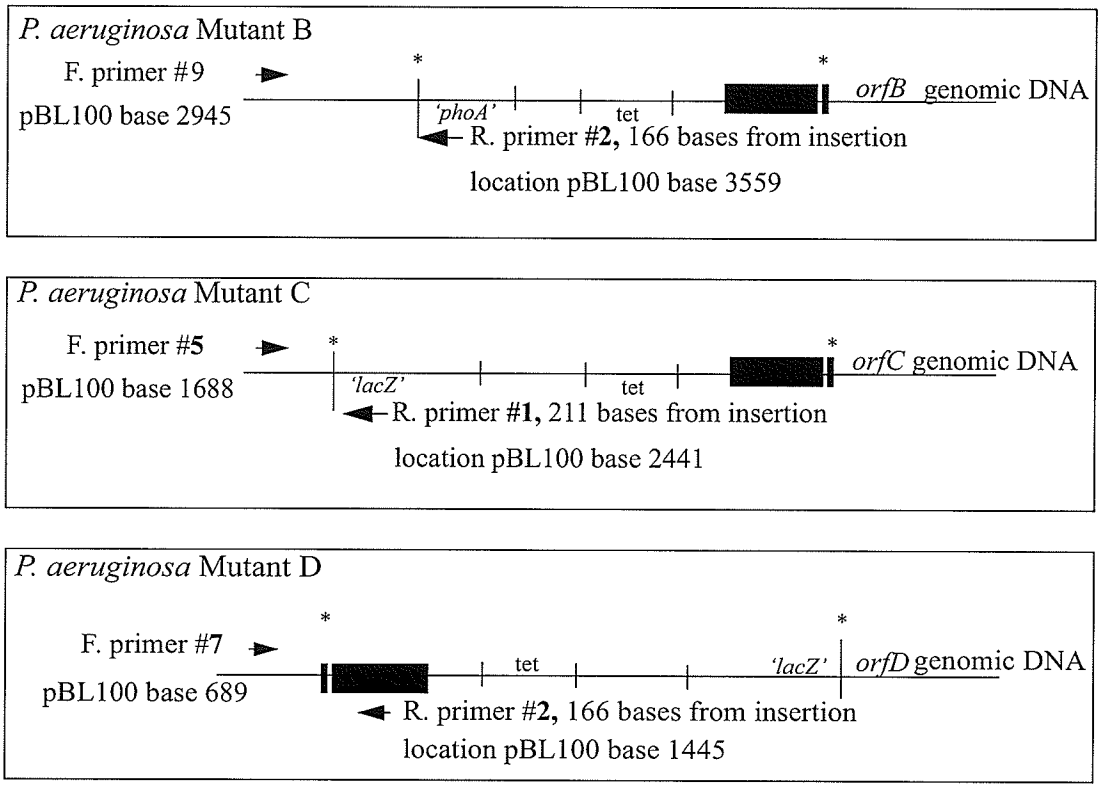

Figure 2-2. Primer binding sites on insertion mutants

Each of the insertion mutants are shown above and the positions where each of the primers would bind in each specific case. Insertion cassette is between *. '*phoA*' - alkaline phosphatase, '*lacZ*' - β-galactosidase, tet - tetracycline resistance marker. The bold numbers preceded by a # sign correspond to the specific primer code in Table 2-3. The arrows show direction of primer extension.

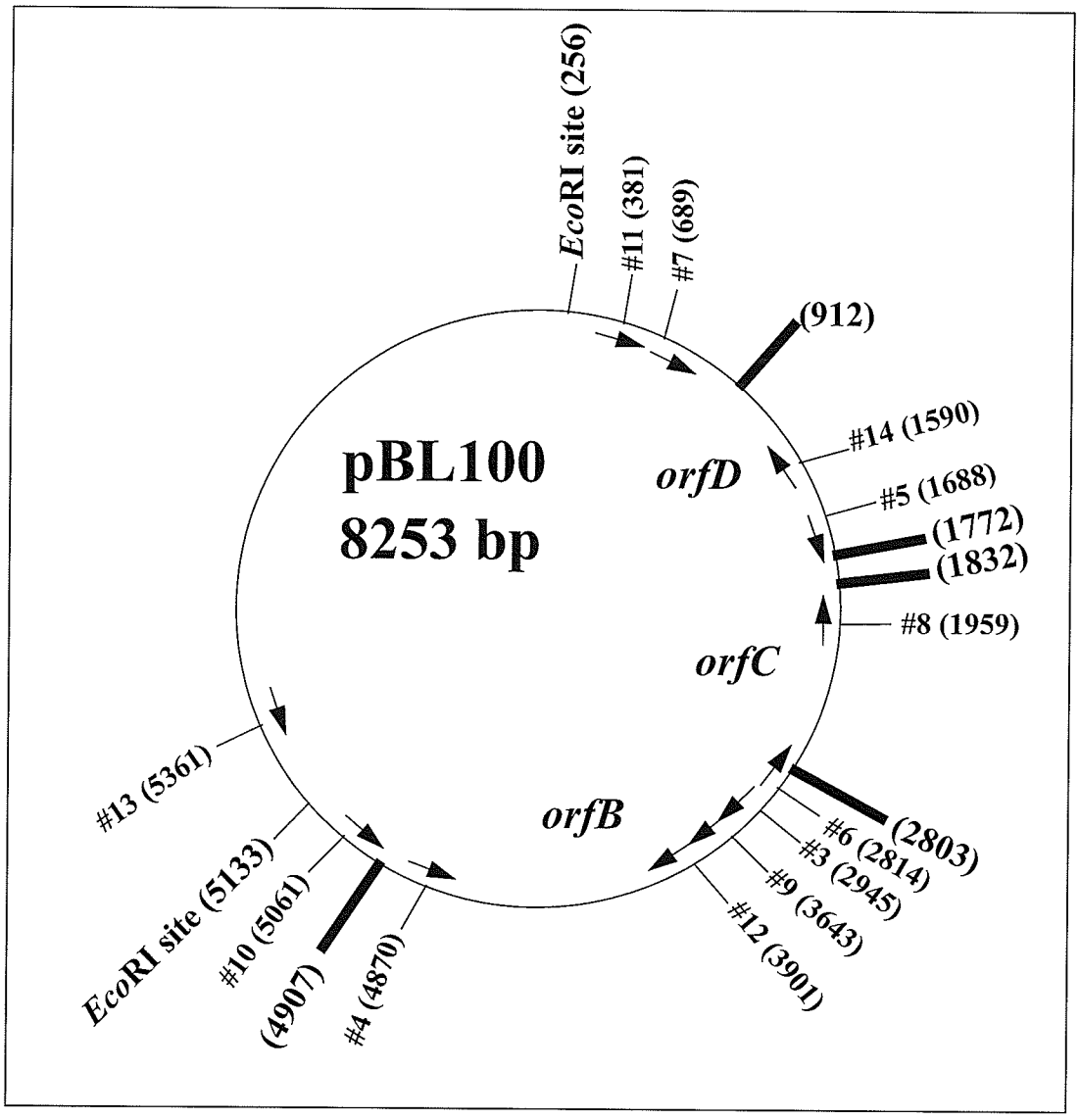

Figure 2-3. Primer binding sites on pBL100

The thick lines represent the beginning and ends of the three *orfsB*, *C* and *D* all are transcribed in the clockwise direction (Adapted from OMIGA 2.0 software of Oxford Moleculars). The numbers in brackets state base of pBL100. The numbers preceded by a # sign correspond to the specific primer code in Table 2-3. The arrows show direction of primer extension.

2.10 Whole cell lysis

The expression vectors pUCP18 & 19, pUCP20 & 21 were used to clone genes for protein expression in *E. coli* NM522 and *P. aeruginosa* MPA01, respectfully. For rapid verification of gene expression at a mini scale, an overnight culture of the bacterial strain harbouring the desired recombinant plasmid was inoculated into 50 ml of LB medium supplemented with ampicillin (100 μg/ml) and grown to OD_{600} = 0.3 - 0.5. Aliquots (5 ml) were withdrawn into two sterile test tubes and isopropylthio-β-D-galactoside (IPTG, Sigma) was added to one of the tubes to a final concentration of 0.4 mM. Tubes were incubated for another 3 hours to allow IPTG-inducible expression of the cloned gene. An aliquot (1.5 ml) of each culture was centrifuged at 12,000 x g for 30 s and cells were resuspended in 100 μl of cell lysis buffer [2% (w/v) SDS, 4% (v/v) DTT, 10% (w/v) glycerol and 1M Tris-HCl, pH 6.8]. Protein samples (5 μl) were heated at 100°C for 5 - 10 min prior to running on 11% polyacrylamide gel.

2.11 Sodium dodecyl sulphate-polyacrylamide gel electrophoresis

Sodium dodecyl sulphate (SDS) polyacrylamide gel electrophoresis (PAGE) was performed using the 11% gel system of Lugtenberg and VanAlpen, 1983. Protein samples were solubilized in buffer containing 0.4% (w/v) SDS, 12 mM Tris-HCl, pH 8.0, 2% (w/v) glycerol and 1% (v/v) β-mercaptoethanol. Samples were heated at 100°C for 10 mins prior to loading. Electrophoresis of protein samples was conducted in the presence of prestained broad-molecular weight range SDS-PAGE standards (Bio-Rad) at 40-120V with a 2.98% (w/v) acrylamide stacking gel over the 11% (w/v) running gel. Gels were stained overnight with Coomassie Blue Solution [0.4% (w/v) Coomassie Brilliant Blue R-250, 30% (v/v)

isopropanol, 10% (v/v) acetic acid] and subsequently destained for 5-8 hours in 20% methanol/7.5% acetic acid.

2.12 Growth curves

The growth curves were generated by initially growing cultures in 1 ml of LB supplemented with tetracycline (60 μg/ml) where appropriate to maintain the insertion in the mutant and incubated at 37°C shaking for 7 hours. This volume was subcultured into 50 ml of minimal media supplemented with tetracycline and 20 mM of appropriate carbohydrate, to induce the low affinity uptake system and mimic conditions used in the carbohydrate uptake assays (see below) then incubated at 37°C shaking overnight. The overnight was cultured into 50 ml of fresh minimal media supplemented with 20 mM of appropriate carbohydrate and tetracycline then inoculated with a volume of overnight culture to get an OD_{600} of approximately 0.1. The culture was incubated at 37°C shaking and OD_{600} was taken at 1 hour intervals for a total of 7 hours.

2.13 Whole cell carbohydrate uptake assays

Incorporation of [U-^{14}C] glucose (3.7 MBq), [U-^{14}C] mannitol (1.85 MBq), [U-^{14}C] fructose (9.25 MBq) and [U-^{14}C] glycerol (1.85 MBq) was studied using a modified membrane filtration assay of Eagon and Phibbs (1971) as described by Wylie and Worobec (1993). Briefly, fresh basal medium 2 (BM2) supplemented with appropriate carbohydrate (20 mM) was inoculated with a 1% inoculum of the overnight culture. The cells were grown with shaking at 37°C, until OD_{600} = 0.5. Cells were pelleted at 10,000 x g for 10 min. Harvested cells were washed twice with 10 ml of carbon substrate-free BM2 and resuspended to an absorbance of 0.04 at 600nm. Cell suspensions were prewarmed to 37°C

for 10 min prior to initiation of uptake assays. Calculated amounts of labelled carbohydrate (0.33 μM glucose, 2.4 μM fructose, mannitol or glycerol, DuPont Canada Inc., Markam, Ont.) were added to resuspended prewarmed cells, aliquots (0.5 ml) were removed at 20, 40, 60s, 2, 5, 8, 16 and 24 min and filtered through a 25 mm, 0.45 μM membrane filter (Gelman Sciences, Ann Arbor, Michigan) in a Millipore manifold (Millipore Corp., Bedford, Mass.). Filters were promptly washed with 5 ml of substrate free BM2. Uptake data from formalin killed cells was used to account for non-specific filter binding. Each assay was repeated at least three times. The results graphed were the mean of at least three replications.

2.14 Computer analysis of DNA and protein sequences

DNA sequences of *orfBCD* from the *P. aeruginosa* database (http:// www.pseudomonas.com) were analyzed as follows. Putative polypeptides were compared with sequences in the GenBank/Swissprot database using the pBLAST 2.6 algorithm (Altschul *et al.*, 1997) of the National Centre for Biotechnology Information (NCBI). Profiles of the predicted amino acid sequences were analyzed via OMIGA 2.0 (software of Oxford Moleculars) programs to determine Kyte-Doolittle hydropathy, Argos transmembrane helices, von Heijne transmembrane helices and hydrophobicity and Goldman/Engelman/Steitz hydrophobicity (Adewoye, 1999).

Chapter 3

Results and Discussion

Various analyses (computer and experimental) were performed to attempt to account for the correlation between the deletion of *orfsB*, *C* and *D* and the carbohydrate uptake profiles presented by Adewoye (1999).

3.1 pBLAST search results

In order to assess the role of the gene products of each of *orfB*, *C* and *D* extensive pBLAST analyses were performed.

3.1.1 pBLAST of orfB

A pBLAST search using the predicted OrfB protein sequence from the *P. aeruginosa* genome site resulted in 342 hits. Fig. 3-1 shows five significant alignments accompanied by each alignments score (bits) and E value. The score (bits) is a value that is derived by calculating the summing of scores for each letter-to-letter and letter-to-null position in the alignment (the higher this value the better the match). The E value represents the number of times this match or a better one would be expected to occur purely by chance in a search of the entire database (the lower the value means an increase in the confidence of the match). Initially in trying to analyze which alignment to pay attention to one must understand how the BLAST programs are designed. The pBLAST looks for local

similarity, these are regions of perfect match between the query and subject sequences. It then spans the whole sequence and will report a global alignment, it is this alignment which is the preferred result for protein identification (www.ncbi.nlm.nih.gov/Class/BLAST/blast_course.short.html). In Fig. 3-1 it is shown that even though the sulfatase is the first hit the fact that the second hit has more similarity over a larger portion of the protein plus a higher score (307) leads one to think that OrfB protein may function in a manner similar to MdoB. In the subsequent significant alignments we see the score is decreasing significantly giving these matches a decreased level of homology. Fig. 3-2 shows the amino acid comparisons of the query protein (OrfB) against the top two significant alignments. In the first comparison there is an 87.8% alignment with 283 residues of the total 700 residues of the OrfB query sequence. Whereas in the second comparison there is a 94.2% alignment with 647 residues of the total 700 residues of the orfB query sequence. This provides one with some confidence that OrfB is an MdoB-like protein. The following two sections will describe facts and functions associated with membrane derived oligosaccharides (MDOs) and MdoB.

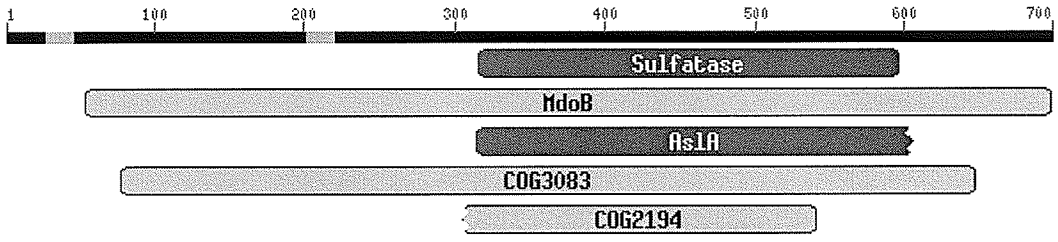

PSSMs producing significant alignments:	Score (bits)	E value
gnl|CDD|25643 pfam00884, Sulfatase, Sulfatase..	179	7e-46
gnl|CDD|11084 COG1368, MdoB, Phosphoglycerol transferase and related protein...	307	3e-84
gnl|CDD|12458 COG3119, AslA, Arylsulfatase A and related enzymes [Inorganic ...	61.7	3e-10
gnl|CDD|12422 COG3083, COG3083, Predicted hydrolase of alkaline phosphatase ...	51.1	4e-07
gnl|CDD|11902 COG2194, COG2194, Predicted membrane-associated, metal-depende...	50.0	9e-07

Figure 3-1. pBLAST showing significant alignments for the predicted OrfB protein

Number line at top corresponds to the 700 a. a. from the putative OrfB protein. The bars below number line show the hits and where they are homologous in comparison to the 700 a. a. of the putative OrfB protein. Red - denotes sequences with high homology. Grey - denotes sequences with decreased homology. PSSM - position specific scoring matrix. Score (bits) - this value is derived by calculating the summing of scores for each letter-to-letter and letter-to-null position in the alignment. E value - represents the number of times this match or a better one would be expected to occur purely by chance in a search of the entire database. Blue letter number sequence - locus identification.

gnl|CDD|25643, pfam00884, Sulfatase, Sulfatase.

```
              CD-Length = 329 residues,  87.8% aligned
              Score =  179 bits (456), Expect = 7e-46

Query:  314   IRNVVVVLLESFAGHYVGALGAPGNITPYFDKLSKEGLLFTQFFSNGTHTHQGMFATMAC  373
Sbjct:  2     PPNVVLVLGESLRAGDMGLYGYPRETTPFLDRLAEEGLLFTNFYSSGPLTAPSRAALLTG  61

Query:  374   FPNLPGFEYLMQTPEGGHKFSGLPQLLSARQYEDVYVYNGDFAWDNQSG---FFSNQGMT  430
Sbjct:  62    RYPHNTGMYLNTGNLGGTF---LPDLLKKAGYQTGLVGKWHLGWLSNQSGEKGVCASVIA  118

Query:  431   TFIGRNDYVDPVFSDPTWGVSDQDMFARGNEELDKLASTGKPFYALLQSLSNHVPYAL--  488
Sbjct:  119   KQPDERGF--PPPYENNGGVLDELLLDKALEFLDQL--EGKPFFLVLHLLGSHGPAPTCD  174

Query:  489   -PKDLPVERVTGYGSLDEHLTAMRYSDWALGQFFEKAKKSPYYKDTLFVVVGDHGFG---  544
Sbjct:  175   ANDEFLGKSCSQEDLVGAYDNTILYTDDLIGRVIDKLKDSGLLDNTLVIYTSDHELGENG  234

Query:  545   ---SPEQLTEMDLHRFNVPLLLIAPGIQEKFGTHLPTVGTQVDIVPTIMGLLGGET  597
Sbjct:  235   GYLHGGKYAIAPEGGTRVPLLVWWPGVLKAKGKVIEELVSHVDLFPTLLGLAGVEL  290
```

gnl|CDD|11084, COG1368, MdoB, Phosphoglycerol transferase and related proteins, alkaline phosphatase superfamily [Cell envelope biogenesis, outer membrane]

```
              CD-Length = 650 residues,  94.2% aligned
              Score =  307 bits (787), Expect = 3e-84

Query:  52    LIGATPASTFLEAFGNGVRFDLRVVVYAVAPLVLSLFAVRAMAARGLFRTWLTLFASITL  111
Sbjct:  39    LGFVLPILLLFQGLR---LLFSLPILFIVSLLLLLLFKG-VDALNIFRLILALLIS---  91

Query:  112   FLGVLELDFYREFHQRLNSLVFQYMSEDPKTVMSMLWYGFPVVRYLLAWAFATWVLYRVF  171
Sbjct:  92    ILLILDILFYRFF-IDFLTIPNALLIEDFNLGK----LGFSALSLLYPEDILFVVDLILL  146

Query:  172   KAIDLVTRPSQRKPREDSVIARPSAAAPWY*VRGVVLFLCVLVCVLAARGTLRQGPPLRWG  231
Sbjct:  147   ILLLVFYWRLAGLTSKLIPLFVRLLVL----------ALLLYLFLQLLFLGEILDPALLA  196

Query:  232   DAFTTESMFANQLGLNGTLTLVKAAKERFSEDRANIWKATLDDKVALETTRQMLLTFNDK  291
Sbjct:  197   AAFDR-LYIAPYLGLDNFLIYDGNAFLYASKQRALAAVKGLLTDVANYI-KASLTAPNSK  254

Query:  292   LVDADEAAVRREFTPPAANTLPIRNVVVVLLESFAGHYVGALGAPGNITPYFDKLSKEG-  350
Sbjct:  255   LF----------------GEAKGPNVIVIQLESFQGFLINPKVNGIEVTPNLNKLQKGGV  298

Query:  351   -LLFTQFFSNGTHTHQGMFATMACFPNLPGFEYLMQTPEGGHKFSGLPQLLSARQYEDVY  409
Sbjct:  299   SLLFSNFFGGVTAGSTFDAETGVLSSLFPAARGSVFQTYGDNKYSSLPAILKQQGYKTAA  358

Query:  410   VYNGDFAWDNQSGFFSNQGMTTFIGRNDYVDPVFSDPTWGVSDQDMFARGNEELDKLAST  469
Sbjct:  359   LHGGDGSFWNRKSFYKIFGFDDFFDLESFDGNADSEIGWGLSDKDLF---KESLPLLKKL  415

Query:  470   GKPFYALLQSLSNHVPYALPKDLPVERVTGYGS----LDEHLTAMRYSDWALGQFFEKAK  525
Sbjct:  416   KKPFFSFVITLSNHGPFELPEGKRNELLEEPLSASTALANYLQAVHYADEALGQFIDKLK  475

Query:  526   KSPYYKDTLFVVVGDHGFGSPEQLTEMDLHR----------FNVPLLLIAPGIQEKFGTHL  576
Sbjct:  476   KSGLYKNSVIVLYGDHYGISGNQNLAMPKFLGKSYDIDMLQRVPLLIHAPGI--KNKKKI  533

Query:  577   PTVGTQVDIVPTIMGLLGGET-VHQCWGRDLLNLPEGDTGFGVIKPSGSEQNVAIVSGNR  635
Sbjct:  534   DTVGGQLDIAPTILGLLGISTKSYAFFGRDLLGDEPYKVPF-RNGSFGTDAKGYSVGDNR  592

Query:  636   ILVRPKDGDVRVYDYQLGGDAKAVITKEVPDQAELQKKLESFIQTATKSLLENTAGVVHG  695
Sbjct:  593   MYDTRTGNEILDLQLD------KVKPKKLKANAELELSDLLINGDLLRSYAEKNFLGVSP  646

Query:  696   IPDK  699
Sbjct:  647   AKLK  650
```

Figure 3-2. Individual protein sequence comparisons for the top two hits for the predicted OrfB protein

The top line of the alignment is the description of subject sequence. Red letters - identical residues, blue letters - similar, nonidentical residues with positive alignment scores, dashes (-) - are gaps in the alignment, query - OrfB a. a. sequence, sbjct - database sequence with homology to query.

3.1.1.1 Membrane derived oligosaccarides (MDOs)

Membrane derived oligosaccarides (MDOs) are also referred to as osmoregulated periplasmic glycans [(OPGs), Debarbieux *et al.*, 1997, Lacroix *et al.*, 1999]. MDOs of *E. coli* have 8 to 10 glucose units/molecule in a highly branched structure which are localized in the periplasmic space (Schneider *et al.*, 1979, Schulmann, and Kennedy, 1979). The biosynthesis of MDOs (Fig. 3-3) is initiated at the cytoplasmic side of the inner membrane and completed at its external side, which results in a release of soluble polymers into the periplasmic space. These periplasmic polymers of glucose, which become abundant under low osmolarity growth conditions, play a significant but undefined role in osmotic adaptation of bacterial cells by reducing the turgor pressure exerted against the inner membrane (Kennedy, 1982, Delcour *et al.*, 1992). These molecules have also been shown to regulate the degree of openness of bacterial porins by promoting closing of the channels in addition to their modulatory effects on porin osmoregulation (Geiger *et al.*, 1992, Delcour *et al.*, 1992). There are many functions associated with MDOs in *E. coli*: cell to cell signalling, chemotaxis, lysis induction by bacteriophages, regulation of capsular polysaccharide synthesis, osmoregulation of outer membrane protein expression (Geiger *et al.*, 1992). *E. coli* with defects in enzymes involved in MDO production have their MDO composition altered compared to wildtype (Jackson *et al.*, 1984). The blocking of MDO synthesis has no effect on porin production as porin production is linked to the ionic strength of the periplasm. For example, in *P. aeruginosa* OprB porin expression increased when osmolarity of growth medium increased (Adewoye *et al.*, 1999). Structural genes of enzymes for MDO synthesis are not regulated by the osmolarity of the growth medium. It

is suspected that feedback inhibition may be a factor in MDO regulation (Jackson, *et al.*, 1986, Rumley *et al.*, 1992, Lacroix *et al.*, 1999).

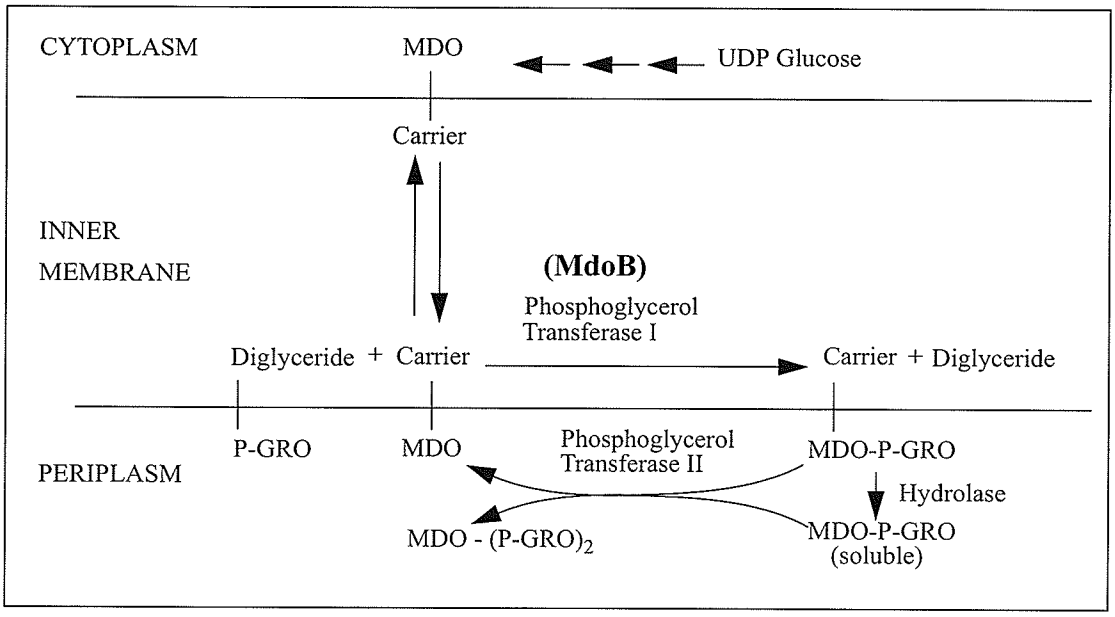

Figure 3-3. Model of MDO synthesis

UDP-glucose is an essential precursor of the polyglucose backbones of MDO molecules. The oligosaccharide chains are bound to a carrier. Phosphoglycerol transferase I (MdoB) catalyzes the transfer of *sn*-1-phosphoglycerol headgroups from donor phosphatidyl glycerol (P-GRO) to MDO. The phosphoglycerol transferase II, a soluble, periplasmic enzyme equilibrates phosphoglycerol residues among soluble species of MDO in the periplasm, leading to formation of multiple substituted oligosaccarides (Bohin and Kennedy, 1984).

3.1.1.2 MdoB protein

MdoB is the specific enzyme phosphoglycerol transferase I (Fig. 3-3) which is involved in the biosynthesis of MDOs (Fiedler and Rotering, 1985, Bohin and Kennedy, 1984, Jackson and Kennedy, 1983, Delcour *et al.*, 1992). MdoB is an integral membrane protein containing four potential transmembrane regions located at the N-terminal half of the protein molecule (Delcour *et al.,* 1992). Phosphoglycerol transferase I (MdoB) transfers phosphoglycerol residues from phosphatidylglycerol to soluble forms of MDO (*in vivo*). When concentrations of MDO are high this transfer is done poorly. This loss of transfer ability blocks the utilization of phosphatidyl glycerol which may be a form of regulation (Jackson *et al.*, 1984). MdoB mutants lack the phosphoglycerol transferase I active site on the outer side of cytoplasmic membrane (Bohin and Kennedy, 1984). Regulation before the MdoB step of synthesis showed that MDO production was limited by availability of polyglucose acceptor. This acceptor limitation is the rate limiting step for MdoB. The polyglucose acceptor may respond to the action of an effector which in turn is immediately responsive to osmolarity (Bohin and Kennedy, 1984, Jackson *et al.*, 1986).

E. coli MdoB mutants have been implicated in slow growth rates (Jackson, *et al.*, 1986), along with decreases and loss of virulence in the cases of *Salmonella typhimurium* and *Erwinia chrysanthemi* (Page *et al.*, 2001, Valentine *et al.*, 1998). Mutants have shown a hypersensitivity to sodium dodecyl sulphate (SDS), an anionic detergent. Wildtype can repel SDS by the abundance of negatively charged MDO's in the periplasm (Rajagopal *et al.*, 2003).

3.1.2 pBLAST of orfC

The pBLAST search using the predicted OrfC protein sequence from the *P. aeruginosa* genome site resulted in 107 hits. Fig. 3-4 shows three significant alignments accompanied by each alignments score (bits) and an E value. Fig 3-5 shows the amino acid comparisons of the query protein (OrfC) against the top three significant alignments. In the first comparison there is an 36.5% alignment with 125 residues of the total 289 residues of the OrfC query sequence. In the second comparison there is a 64.3% alignment with 267 residues of the total 289 residues of the OrfC query sequence. In the final comparison there is a 43.6% alignment with 115 residues of the total 289 residues of the OrfC query sequence. The sequence which would be the most relevant in this case (highest score) is the second alignment. Unfortunately at this time it is an uncharacterized alignment which gives no information. The next two choices are strictosidine synthase (score 43.0) and gluconolactonase (score 35.7, E value close to 1) which have fairly low scores that must be taken into account. Aligning OrfC putative protein with either of these proteins is very weak until more information becomes available. These two proteins will be briefly described in the following sections.

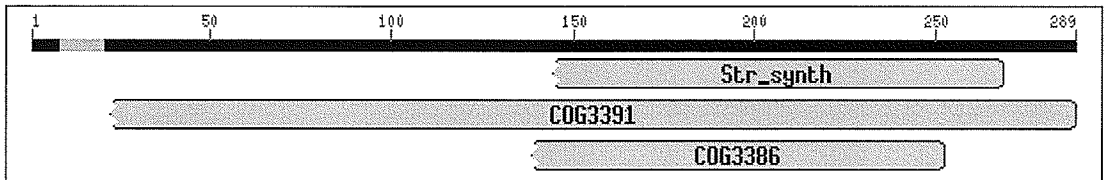

PSSMs producing significant alignments:	Score (bits)	E value
gnl|CDD|26018 pfam03088, Str_synth, Strictosidine synthase. Strictosidine sy...	43.0	4e-05
gnl|CDD|12723 COG3391, COG3391, Uncharacterized conserved protein [Function ...	111	1e-25
gnl|CDD|12718 COG3386, COG3386, Gluconolactonase [Carbohydrate transport and...	35.7	0.006

Figure 3-4. pBLAST showing significant alignments for the predicted OrfC protein

Number line at top corresponds to the 289 a. a. from the putative OrfC protein. The bars below number line show the hits and where they are homologous in comparison to the 289 a. a. of the putative OrfC protein. Grey - denotes sequences with decreased homology. PSSM - position specific scoring matrix. Score (bits) - this value is derived by calculating the summing of scores for each letter-to-letter and letter-to-null position in the alignment. E value - represents the number of times this match or a better one would be expected to occur purely by chance in a search of the entire database. Blue letter number - locus identification.

gnl|CDD|26018, pfam03088, Str_synth, Strictosidine synthase. Strictosidine synthase (E.C. 4.3.3.2) is a key enzyme in alkaloid biosynthesis. It catalyses the condensation of tryptamine with secologanin to form strictosidine.

```
            CD-Length = 364 residues, only 36.5% aligned
            Score = 43.0 bits (101), Expect = 4e-05

Query:  144   YLYAAEDRDLDGRILRYDPETGGLTVLREGLQRSEGVAACPDGS-VFYTEKKRGHVMRLH  202
Sbjct:  182   FIFAMLEGDPTGRLLKYDPSTKVTTVLLDELYFPNGLALSPDGSFVLVAETPMARIRKYW  241

Query:  203   EGAED----EVVLNGL-NAPSFLLCDSEG-LWITEDSTHNARALLLPPDGPLQVIVRRLR  256
Sbjct:  242   LKGPKAGTSEVFAEGLPGYPDNIRRDGDGHFWVALVSHRSTLWRLLMSYPWVRKFLAKLL  301

Query:  257   SAQSLLPIGPGRY  269
Sbjct:  302   KLEVLPLLPLNGK  314
```

gnl|CDD|12723, COG3391, COG3391, Uncharacterized conserved protein [Function unknown]

```
            CD-Length = 381 residues, only 64.3% aligned
            Score = 111 bits (277), Expect = 1e-25

Query:  22    FIALAFLGWQRFAPAATVSGWTYRVVLEDIPHVSALARDPDGLLYVSQELQDGKGLVFRI 81
Sbjct:  120   GLAVDPDGKYVYVANAG-NGNNTVSVIDAATN-KVTATIPVGN----------TPTGVAV 167

Query:  82    AADGSRDTVLDGLSKPDGMASFRDGIAISQEQGASPVFWWHAQQARPLFDGIQVEGVASD 141
Sbjct:  168   DPDGNKVYVTN---SDDNTVSVIDTSGNS-------VVRGSVGSLVGVGTGPAGIAVDPD 217

Query:  142   GRYLYAAEDRDLDGRILRYDPETGGLTVLRE--GLQRSEGVAACPDGSVFYTEKKRGHVM 199
Sbjct:  218   GNRVYVANDGSGSNNVLKIDTATGNVTATDLPVGSGAPRGVAVDPAGKAAYVANSQGGTV 277

Query:  200   RLHEGAEDEVVLNGLNAPSFLLCDSEGLWITEDSTHNARALLLPPDGPLQVIVRRLRSAQ 259
Sbjct:  278   SVIDGATDRVVKTGPTGNEALGEPVSIAISPLYDTNYVSVKVVPST---TVSLQAIHVVQ 334

Query:  260   SLLPIGPGRYLLAEQGRDRILEIERQKSEL 289
Sbjct:  335   EAVGIGYPVQLAEVPDAAYLLAISVSDNDV 364
```

gnl|CDD|12718, COG3386, COG3386, Gluconolactonase [Carbohydrate transport and metabolism]

```
            CD-Length = 307 residues, only  43.6% aligned
            Score = 35.7 bits (82), Expect = 0.006

Query:  138   VASDGRYL-----YAAEDRDLD---GRILRYDPETGGLTVLREGLQRSEGVAACPDGSVF  189
Sbjct:  118   VDPDGRIWFGDMGYFDLGKSEERPTGSLYRVDPDGGVVRLLDDDLTIPNGLAFSPDGKTL  177

Query:  190   Y-TEKKRGHVMRLH--------EGAEDEVVLNGLN-APSFLLCDSEG-LWI-TEDSTHNA  237
Sbjct:  178   YVADTPANRIHRYDLDPATGPIGGRRGFVDFDEEPGLPDGMAVDADGNLWVAAVWGG--G  235

Query:  238   RALLLPPDGPLQVIVR  253
Sbjct:  236   RVVRFNPDGKLLGEIK  251
```

Figure 3-5. Individual protein sequence comparisons for the top three hits for the predicted OrfC protein

The top line of the alignment is the description of the subject sequence. Red letters - identical residues, blue letters - similar, nonidentical residues with positive alignment scores, dashes (-) - are gaps in the alignment, CD - length - refers to the number residues in the alignment, query - OrfC a. a. sequence, sbjct - database sequence with homology to query.

3.1.2.1 Strictosidine synthase

Strictosidine synthase enzymatically catalyzes the reaction between secologanin and tryptophan (Fig. 3-6), it has a 3α (S) stereochemistry which is needed for the formation of monoterpenoid indole alkaloids (Stockigt and Zenk, 1977). The product from this enzyme reaction is strictosidine, an alkaloidal glucoside intermediate in monoterpenoid indole alkaloid biosynthesis (Pfitzner and Zenk, 1989, Hemscheidt and Zenk, 1980, Hampp and Zenk, 1988). Indole alkaloids are medically the most important group of plant derived, nitrogen containing natural products, the vast majority of (1800 known) indole alkaloids structures are synthesized from the first intermediate, strictosidine.The original sources of these indole alkaloids come from the plants *Catharanthus roseus* G. Don and *Rauvolfia serpentina*. *C. roseus* G. Don, which is commonly known as Madagascar periwinkle, is a dicot shrub from the Apocynaceae family found in Southern United States (http://plants.usda.gov/).

Strictosidine synthase has been expressed in *E. coli* DH5 using *R. serpentina* cDNA. The expressed enzymatically active strictosidine synthase has an orf of 1032 bp and gives a 344 a. a. protein translation which has a consensus sequence (Asn-Ser-Thr) for N-linked carbohydrates (Kutchan, 1993).

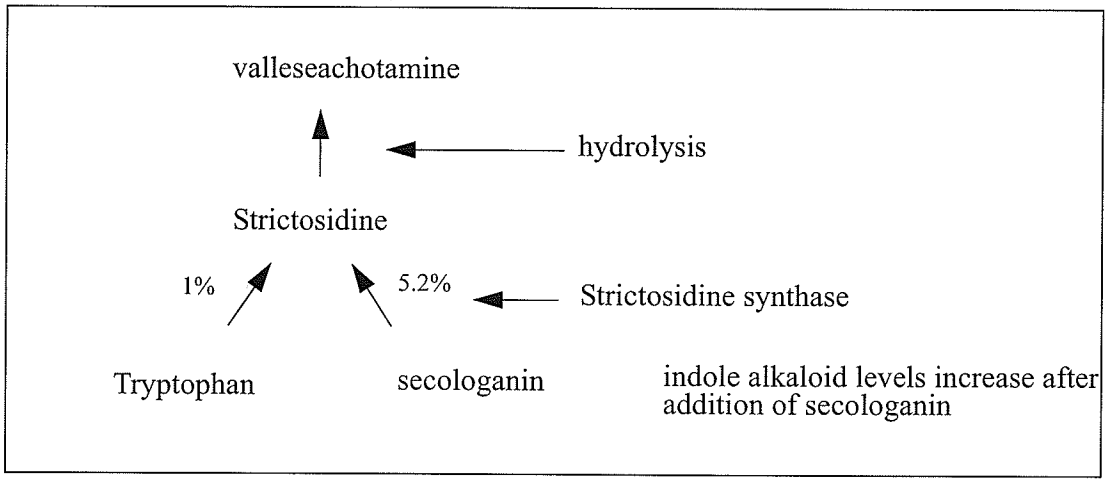

Figure 3-6. Pathway catalyzed by strictosidine synthase

The precursors tryptophan (1%) and secologanin (5.2%) are used by the enzyme strictosidine synthase to produce strictosidine which is further hydrolyzed to valleseachotamine. In the hydrolysis step D-δ-gluconolactone is an inhibitor of this reaction (Kutchan, 1993).

3.1.2.2 Gluconolactonase

Although gluconolactonase in the pBLAST search had only a 43.6% alignment, a score of 35.7 and an E value of 0.006 it is of interest to note that gluconolactonase product, D-δ-gluconolactone (Fig. 3-7), has been implicated in the strictosidine synthase pathway. D-δ-gluconolactone acts as a hydrolase reaction inhibitor (Fig. 3-6) causing a build up of strictosidine (Stockigt and Zenk, 1977). Gluconolactonase is an enzyme that catalyses the hydrolysis of D-glucose in the first stage of oxidative metabolism (Fig. 3-7) of *P. fluorescens* (Jermyn, 1960).

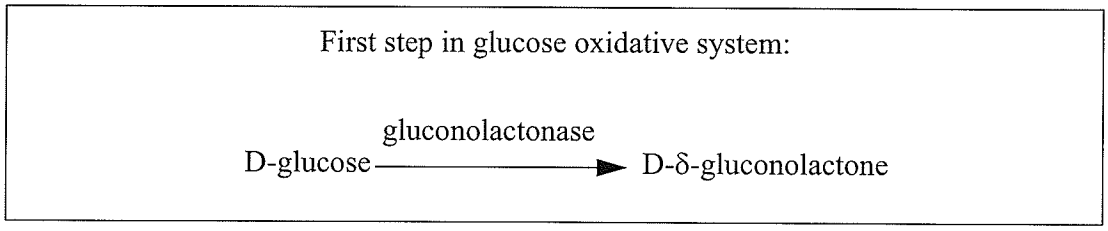

Figure 3-7. D-δ-gluconolactone production

The enzyme gluconolactonase plays a role in the first step of the glucose oxidative system of *P. fluorescens*. D-glucose is converted to D-δ-gluconolactone by the enzyme gluconolactonase (Jermyn, 1960).

3.1.3 pBLAST of orfD

The pBLAST search using the predicted OrfD protein sequence from the *P. aeruginosa* genome site resulted in 419 hits. Fig. 3-8 shows six significant alignments accompanied by each alignments score (bits) and an E value. Fig. 3-9 shows the amino acid comparisons of the query protein (OrfD) against the top three significant alignments. I have not included all six hits as the three last hits have a very low score and E values near 1. In the first comparison there is a 97.5% alignment with 233 residues of the total 288 residues of the OrfD query sequence. In the second comparison there is a 95.7% alignment with 271 residues of the total 288 residues of the OrfD query sequence. This sequence match is from *P. aeruginosa* strain UCBPP-PA14, derived from a human clinical isolate. In the final comparison there is a 49.4% alignment with 258 out of the total 288 residues of the OrfD query sequence. All three of the hits denoted describe spermidine synthase which gives strong support that OrfD protein may behave in a similar manner to this protein. A description of spermidine synthase is given in the following section.

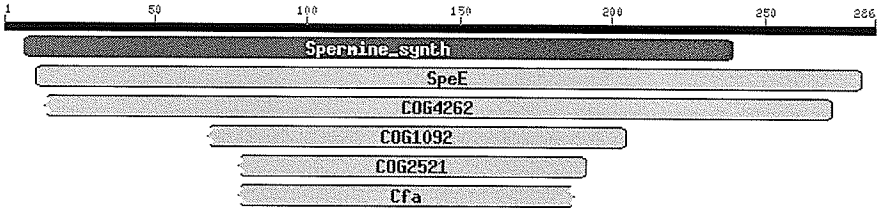

PSSMs producing significant alignments:	Score (bits)	E value
gnl|CDD|15373 pfam01564, Spermine_synth, Spermine/spermidine synthase. Sperm...	277	8e-76
gnl|CDD|10295 COG0421, SpeE, Spermidine synthase [Amino acid transport and m...	322	3e-89
gnl|CDD|13510 COG4262, COG4262, Predicted spermidine synthase with an N-term...	141	9e-35
gnl|CDD|10814 COG1092, COG1092, Predicted SAM-dependent methyltransferases [...	39.1	5e-04
gnl|CDD|12116 COG2521, COG2521, Predicted archaeal methyltransferase [Genera...	39.2	6e-04
gnl|CDD|11936 COG2230, Cfa, Cyclopropane fatty acid synthase and related met...	35.2	0.010

Figure 3-8. pBLAST showing significant alignments for the predicted OrfD protein Number line at top corresponds to the 286 a. a. of the putative OrfD protein. The bars below number line show the hits and where they are homologous in comparison to the 289 a. a. of putative OrfD protein. Red - denotes sequences with high homology, grey - denotes sequences with decreased homology. PSSM - position specific scoring matrix. Score (bits) - this value is derived by calculating the summing of scores for each letter-to-letter and letter-to-null position in the alignment. E value - represents the number of times this match or a better one would be expected to occur purely by chance in a search of the entire database. Blue letter number - locus identification.

gnl|CDD|15373, pfam01564, Spermine_synth, Spermine/spermidine synthase. Spermine and spermidine are polyamines. This family includes spermidine synthase that catalyses the fifth (last) step in the biosynthesis of spermidine from arginine, and spermine synthase.

```
              CD-Length = 239 residues,  97.5% aligned
              Score =  277 bits (711), Expect = 8e-76

Query:  7    TLYQGYGQRFSIDNMLHEVRTEHQHLVIFENARMGRVMALDGVIQTTEADEFIYHEMLTH  66
Sbjct:  6    DLWPGLAVEYKVEKVLYEEKSKYQDIEIFESKTFGRILVLDGRVQLTERDEFIYHEMIAH  65

Query:  67   VPILAHGAARRVLIIGGGDGGMLREVAKHKSVERITMVEIDGTVVDMCKEFLPNHSQGAF  126
Sbjct:  66   VPLCSHPNPKKVLIIGGGDGGVLREVVKHPSVEKITLVEIDEKVIDVSKKFLPSLA-GGF  124

Query:  127  DDPRLNLVIDDGMRFVATTEERFDVIISDSTDPIGPGEVLFSENFYQACRRCLNEGGILV  186
Sbjct:  125  DDPRVKVVIGDGFKFLKDYLVEFDVIIVDSTDPVGPAENLFSKEFYDLLKRALKEDGVFV  184

Query:  187  TQNGTPFMQLEEVRTTAARTDGLFADWHFYQAAVPTYIGGAMTFAWGSTHEGLR  240
Sbjct:  185  TQAESPWLHLELIINILKNGKKVFPVVMPYVVPVPTYPSGGWGFAVCSKKPSLK  238
```

gnl|CDD|10295, COG0421, SpeE, Spermidine synthase [Amino acid transport and metabolism]

```
              CD-Length = 282 residues,  95.7% aligned
              Score =  322 bits (827), Expect = 3e-89

Query:  11   GYGQRFSIDNMLHEVRTEHQHLVIFENARMGRVMALDGVIQTTEADEFIYHEMLTHVPIL  70
Sbjct:  13   GLRLMFRVERVLYEEKSEYQDIEIFESEDFGKVLVLDGVVQLTERDEFIYHEMLAHVPLL  72

Query:  71   AHGAARRVLIIGGGDGGMLREVAKHKSVERITMVEIDGTVVDMCKEFLPNHSQGAFDDPR  130
Sbjct:  73   AHPNPKRVLIIGGGDGGTLREVLKHLPVERITMVEIDPAVIELARKYLPEPSGGA-DDPR  131

Query:  131  LNLVIDDGMRFVATTEERFDVIISDSTDPIGPGEVLFSENFYQACRRCLNEGGILVTQNG  190
Sbjct:  132  VEIIIDDGVEFLRDCEEKFDVIIVDSTDPVGPAEALFTEEFYEGCRRALKEDGIFVAQAG  191

Query:  191  TPFMQLEEVRTTAARTDGLFADWHFYQAAVPTYIGGAMTFAWGSTHEGLRRLPLETLRQR  250
Sbjct:  192  SPFLQDEEIALAYRNVSRVFSIVPPYVAPIPTYPSGFWGFIVASFNKAHPLKSLDALQAR  251

Query:  251  FRDSGIATRYYNADIHLGAFALPQYVLQAIGK  282
Sbjct:  252  ALA-LLTLKYYNEDIHDAAFALPKNLQDELKE  282
```

gnl|CDD|13510, COG4262, COG4262, Predicted spermidine synthase with an N-terminal membrane domain [General function prediction only]

```
              CD-Length = 508 residues, only 49.4% aligned
              Score =  141 bits (357), Expect = 9e-35

Query:  14   QRFSIDNMLHEVRTEHQHLVIFENARMGRVMALDGVIQTTEADEFIYHEMLTHVPILAHG  73
Sbjct:  230  QQLYGDEIIHAIQSPYQRIVVTRRGDDLR-LYLDGGLQFSTRDEYRYHESLVYPALSSVR  288

Query:  74   AARRVLIIGGGDGGMLREVAKHKSVERITMVEIDGTVVDMCK--EFLPNHSQGAFDDPRL  131
Sbjct:  289  GARSVLVLGGGDGLALRELLKYPQVEQITLVDLDPRMIELASHATVLRALNQGSFSDPRV  348

Query:  132  NLVIDDGMRFVATTEERFDVIISDSTDPIGPGEV-LFSENFYQACRRCLNEGGILVTQNG  190
Sbjct:  349  TVVNDDAFQWLRTAADMFDVVIVDLPDPSTPSIGRLYSVEFYRLLSRHLAETGLMVVQAG  408

Query:  191  TPFMQLEEV-RTTAARTDGLFADWHFYQAAVPTYIGGAMTFAWGSTHEGLRRLPLETLRQ  249
Sbjct:  409  SPYFTPRVFWRIDATIKSAGYRVWP-YHVHVPTF------GEWGFILAAPGDADFEPPTE  461

Query:  250  RFRDSGIATRYYNADIHLGAFAL  272
Sbjct:  462  ----YRPPTRFLDAEVLHAAFVF  480
```

Figure 3-9. Individual protein sequence comparisons for the top six hits for the predicted OrfD protein

The top line of the alignment is the description of the subject sequence. Red letters - identical residues, blue letters - similar, nonidentical residues with positive alignment scores, dashes (-) - are gaps in the alignment, CD - length - refers to the number residues in the alignment, query - OrfD a. a. sequence, sbjct - is database sequence the query is aligned to.

3.1.3.1 Spermidine synthase

In *P. aeruginosa,* spermidine synthase is the enzyme which converts putrescine to spermidine (Fig. 3-10 and Table 3-1). The arginine decarboxylase (ADC) pathway produces succinate which is used in the TCA cycle. Biosynthesis of putresine and spermidine have been extensively studied in *E. coli*. In *P. aeruginosa,* homologues of all the *E. coli* ADC pathway genes have been identified, suggesting a common pathway between these two organisms. *P. aeruginosa* has an ABC transport system for spermidine uptake. (*spuDEFGH*, PA0297-PA0304, Lu *et al.*, 2002). Little is known about catabolism of spermidine in pseudomonads but it was seen that putrescine stabilizes ribosomes (Tabor and Tabor, 1985). It was found that exogenously added polyamines caused a response by a DNA binding protein which forms a nucleoprotein complex with the ADC pathway regulatory regions (Lu *et al.*, 2002).

Polyamines or lack thereof, have various effects on *E. coli* and other organisms such as *Saccharomyces cerevisiae*, *Neurospora crassa*, *Aspergillus nidulans*, *Physarum polycephalum*. Polyamines have been implicated in DNA, RNA and protein synthesis in *S. cerevisiae*, *N. crassa*, *A. nidulans*, membrane cell wall stability, ribosome stabilization in *E. coli* and *Pseudomonas* species (Tabor and Tabor, 1984), and signal transduction pathways in *A. nidulans* (Jin *et al.*, 2002). *E. coli* mutants in polyamine production demonstrate slow growth rates, 30% of that found with wildtype (Kallio and McCann, 1981, Tabor and Tabor, 1984, Jin *et al.*, 2002). The movement of DNA replication fork was affected in certain *E. coli* mutants (Tabor and Tabor, 1984). Also synthesis of RNA and thereby protein biosynthesis are affected in polyamine production impaired mutants (Tabor and Tabor, 1984).

In general, polyamines have a polybasic character (high affinity for acids), which is very important in determining their physiological action (Kallio and McCann, 1981, Tabor and Tabor, 1984). In particular, it has been shown that spermidine in *E. coli* is able to precipitate DNA and protect it from denaturation by heat or shearing (Tabor and Tabor, 1984). In the fungus *A. nidulans,* the deletion of spermidine synthase gene resulted in a strain which required exogenously supplied spermidine for growth plus it accumulated putrescine (Jin *et al.*, 2002).

Table 3-1. Abbreviation table for Fig. 3-10

Abbreviation	Full name
SAM	S-adenosyl methionine
dSAM	decarboxylated SSAM
speABCDE	genes for biosynthetic ADC
kauB	gene for 4-aminobutyraldehyde dehydrogenase
adcA	gene for guanidiobutyraldehyde dehydrogenase
speE	gene for spermidine synthase
aguA	gene for agmatine deiminase
aguB	gene for N-carbamoylputrescine aminotransferase
spuC	gene for putrescine-pyruvate aminotransferase

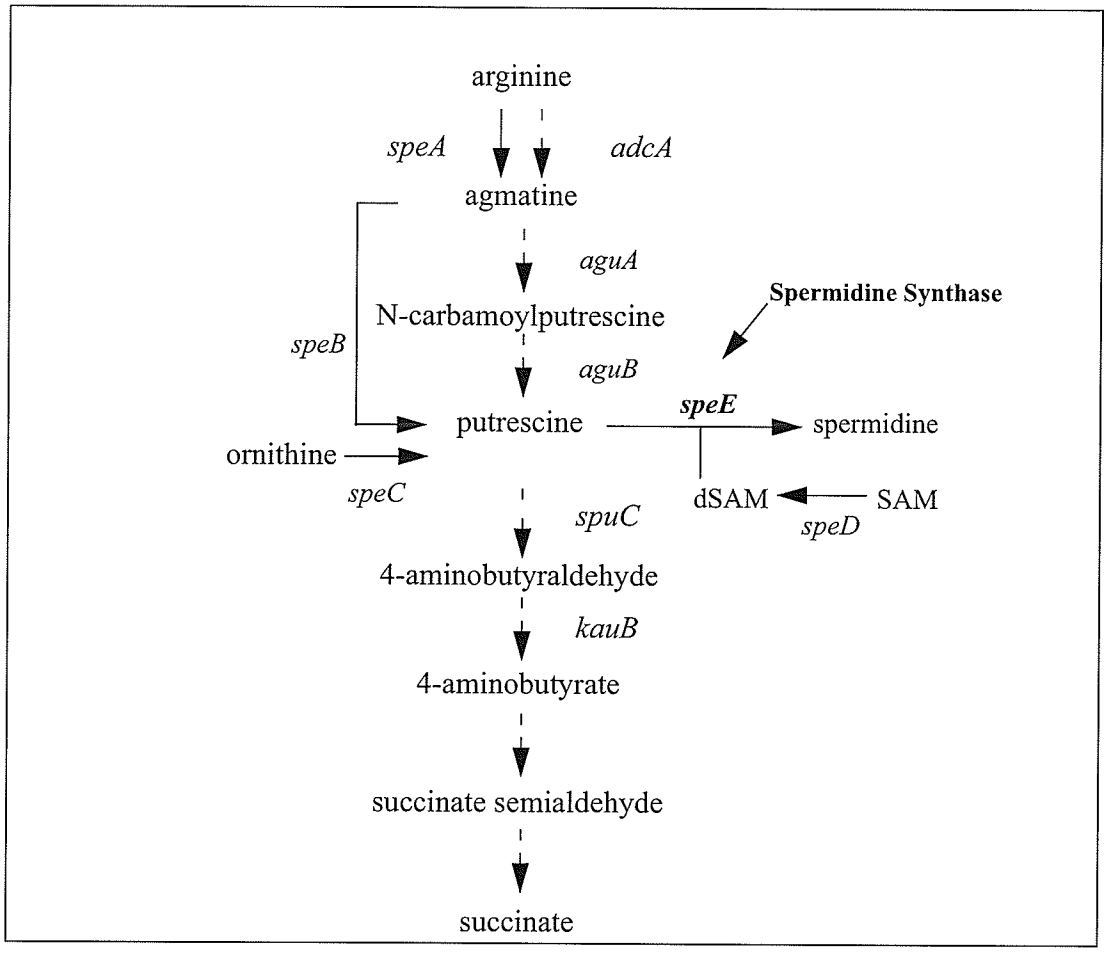

Figure 3-10. Schematic presentation of the ADC pathway and polyamine biosynthesis Solid and broken arrows represent biosynthetic and catabolic pathways, respectively. SAM, S-adenosyl methionine; dSAM, decarboxylated SAM. The *speABCDE* genes which encode biosynthetic ADC, agmatine uredihydrolase, ornithine decarboxylase, SAM decarboylase, and spermidine synthase, respectively, have been characterized in *E. coli*. *aguAB* encodes agmatine deminase and N-carbamoylputrescine-aminotransferase. *spuC* encodes putrescine-pyruvate aminotransferase. *kauB* and *adcA* code for the bifunctional 4-aminobutyaldehyde/guanidiobutyraldehyde dehydrogenase and arginine-inducible arginine decarboxylase (ADC) pathway (Lu *et al.*, 2002).

3.2 pBLAST search discussion

The pBLAST search showed for the predicted OrfB protein sequence a score (bits) of 307 and a 94.2% alignment with 647 residues of the total 700 residues. There is a high confidence in these results that *orfB* may be very similar to the MdoB protein of *E. coli*.

The pBLAST search showed for the predicted OrfC protein sequence a score (bits) of 43, 35.7 and a 36.5%, 43.6% alignment with strictosidine synthase and gluconolactonase, respectively. Both these alignments have a very low homology to the predicted OrfC protein. This fact is prominent and caution must be used when interpreting the results and aligning the OrfC protein with either of these predicted proteins.

The pBLAST search showed for the predicted OrfD protein sequence a score (bits) of 322 with 95.7% alignment with 282 residues of the total 286 residues. There is a high confidence in these results that the OrfD protein may be very similar to the spermidine synthase protein of *P. aeruginosa* UBCPP-PA14.

Although only OrfB and D appear to code for proteins with known functions, all three genes (*orfB*, *C* and *D*) were further analyzed for their putative role in the regulation of carbohydrate transport.

3.3 Insertion deletion mutants

The use of the deletion mutant is an important tool used in molecular biology. The ability to manipulate a gene which is understudy allows for the question to be asked, 'Does this gene play a role in growth and/or carbohydrate uptake for the organism?' The ability to have the wildtype organism directly compared in a particular assay with it's identical twin (less the gene in question) gives the scientist a firm starting point to build upon.

This project was initiated using the previously constructed *orfBCD* knock-out mutant strain of *P. aeruginosa* WMA200 (Adewoye, 1999). PCR was used to verify WMA200 as a knockout mutant using the forward and reverse primers (Table 2-3) for each *orf*. Each *orf* gave the expected PCR product seen in Fig. 3-11 (lanes 5-8 and 5-12), thus confirming WMA200 was **not** a mutant. The process to recreate the deletion mutant using pAK18Tc and pKK101 was unsuccessful (Appendix B). It was then decided to use the *P. aeruginosa* transposon insertion mutants (Jacobs *et al.*, 2003) to pursue this study.

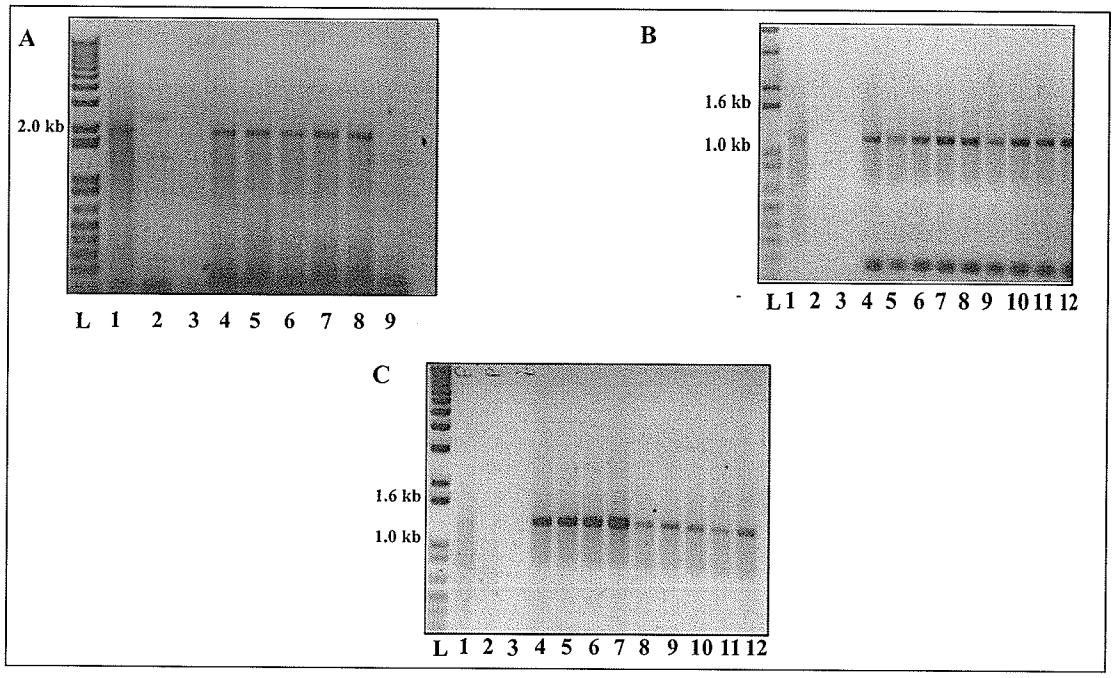

Figure 3-11. PCR of WMA200 with *orfB*, *orfC* and *orfD* primers

A: PCR using *orfB* primer set.

B: PCR using *orfC* primer set.

C: PCR using *orfD* primer set.

Lane 1 - pBL100 template DNA, Lane 2 - pUCP20 template DNA, Lane 3 - water, Lane 4 - wildtype template DNA, Lanes 5 to 12 - WMA200 template DNA (five - eight separate genomic boiling preparations).

L - 1 kb Plus DNA Ladder (Invitrogen) with the sizes corresponding to the appropriate band to the left of the gel.

3.3.1 Confirmation of insertion mutants

This section will detail the confirmation of the *P. aeruginosa* insertion mutants received from Washington State Genome Centre (Jacobs *et al.*, 2003).

Each of the *orf*s has a primer set (referred to as normal primer set), consisting of a forward and reverse primer (Table 2-3) for amplification. Using these primers it was possible to confirm the presence of the given *orf* by the appropriate size PCR product, or in the case of an insertion mutant, no PCR product. The genomic DNA of each of the insertion mutants was used as template to PCR the appropriate *orf* in question as well as wildtype, pBL100 and water as controls. In all cases using the *orfB*, *C* and *D* primer sets on each of the specific mutants produced an alternate PCR product, smaller than the orf in question. When using the *orfB*, *C* and *D* primer sets on each mutant and observing: no appropriate orf product, and secondary products, it was desirable to confirm the mutants by the production of a PCR product. This resulted in ordering of two separate primers which would amplify from the interior of the insertion site to the exterior of the interrupted orf site using either the forward or reverse primer of a particular orf.

In the case of mutants which had a *lacZ* insertion cassette, the reverse primer lacZ-211 was used and the mutants with the *phoA* insertion cassette the reverse Hah-166 primer was used to give the following PCR products: Mutant B = 780 bp, Mutant C = 964 bp, Mutant D = 922 bp (Fig. 3-12, A,B,C). See Material and Methods, Section 2.6 for insertion details, also note for mutant D (which is in the opposite direction of the gene) the *lacZ* forward primer was initially used with *orfD* reverse primer but no product was produced. The *phoA* reverse primer was tried with the *orfD* forward primer and a product was given at 922 bp. In all cases, vector pBL100 (Appendix B) was used as a positive control and water was used

as a negative control and depending on the case wildtype was used either as a positive or negative control.

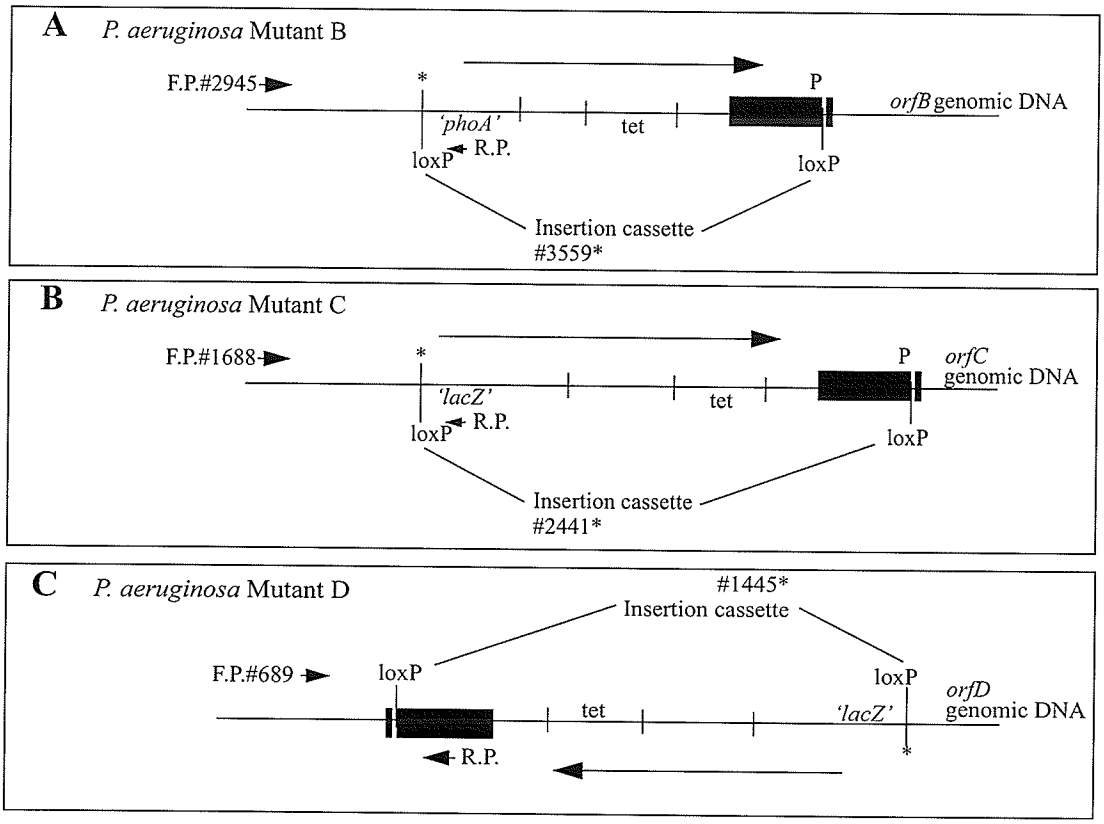

Figure 3-12. Diagrams of insertion cassettes in *P. aeruginosa* mutant B, C and D

A - F.P. - forward primer for *orfB* gene, R.P. - reverse primer for *phoA* insertion cassette which is 166 bases from insertion start point. **B** - F.P. - forward primer for *orfC* gene, R.P. - reverse primer for *lacZ* insertion cassette which is 211 bases from insertion start point. **C** - F.P. - forward primer for *orfD* gene, R.P. - reverse primer for *phoA* insertion cassette which is 166 bases from insertion start point. # = genome base pair number, * - genome base pair where insertion is located. loxP - Cre recognition sequence, P - neomycin phosphotransferase promoter, tet - tetracycline resistance cassette (Adapted from Jacobs *et al.*, 2003).

Fig. 3-13, A1-3 shows the initial results using the mutant B template DNA (lanes 1), wildtype template DNA (lanes 2), water as template (lanes 3) and pBL100 template DNA (Appendix B) in lanes 4 with *orfB*, *C* and *D* primer sets. Fig. 3-13, A-1 using *orfB* primer set in lane 1 there is no 2.0 kb product but an 850 bp band is seen. This band was later determined to be the *orfB* normal primer set producing PCR products from other parts of the genomic DNA (Fig. 3-14). Lane 2 shows the expected 2.0 kb sized product. There is no product observed in any Lane 3, regardless of the primer used. Lane 4 gives the expected 2.0 kb product as the template carries the *orfB* gene. Fig. 3-13, A-2 using *orfC* primer set in lane 1 there is the expected 1.1 kb product. Lane 2 gives the expected 1.1 kb product. Lane 4 gives the expected 1.1 kb product. Fig. 3-13, A-3 using *orfD* primer set in lane 1 there is the expected 1.3 kb product. Lane 2 gives the expected 1.3 kb product. Lane 4 gives the expected 1.3 kb product. Fig. 3-13B, shows the results using the insertion specific reverse primer (Hah-166) and *orfB* forward primer with the mutant B template DNA (lanes 1 and 2) giving the expected 780 bp product. Wildtype *P. aeruginosa* template DNA (lane 3) and water as template (lane 4) both show no product.

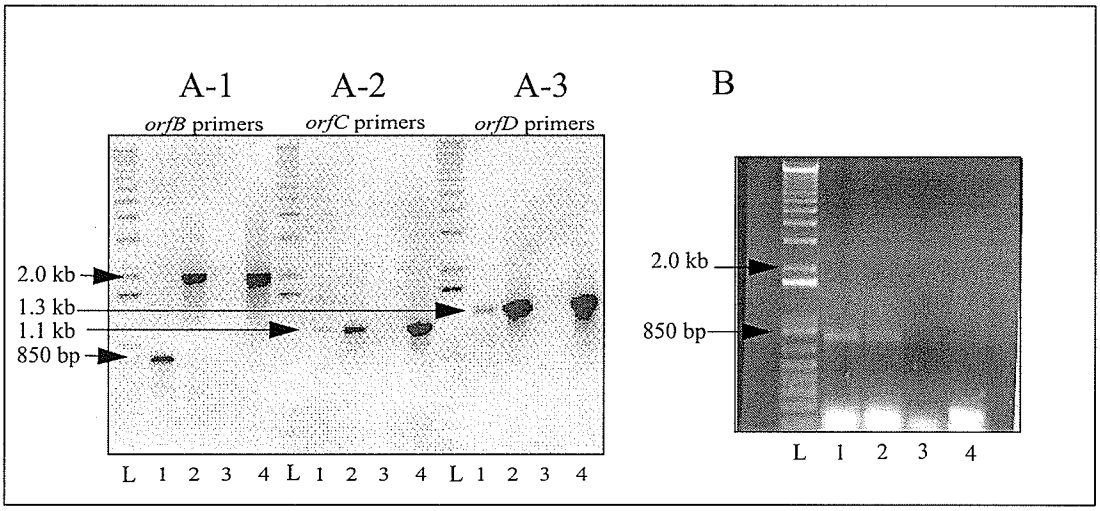

Figure 3-13. Mutant B PCR results

A-1: *orfB* primer set used with: lane 1 - mutant B template DNA, lane 2 - wildtype template DNA, lane 3 - water as template, lane 4 - pBL100 template DNA. **A-2:** *orfC* primer set used with same template DNA as in A-1. **A-3:** *orfD* primer set used with same template DNA as in A-1.

B: PCR using Hah-166 reverse primer and *orfB* forward primer with: lane 1 and 2 - mutant B template DNA, lane 3 - water as template, lane 4 - wildtype template DNA.

L - 1 kb Plus DNA Ladder (Invitrogen) with the sizes corresponding to the appropriate band to the left of the gel. Arrows are pointing to ladder sizes or PCR product bands.

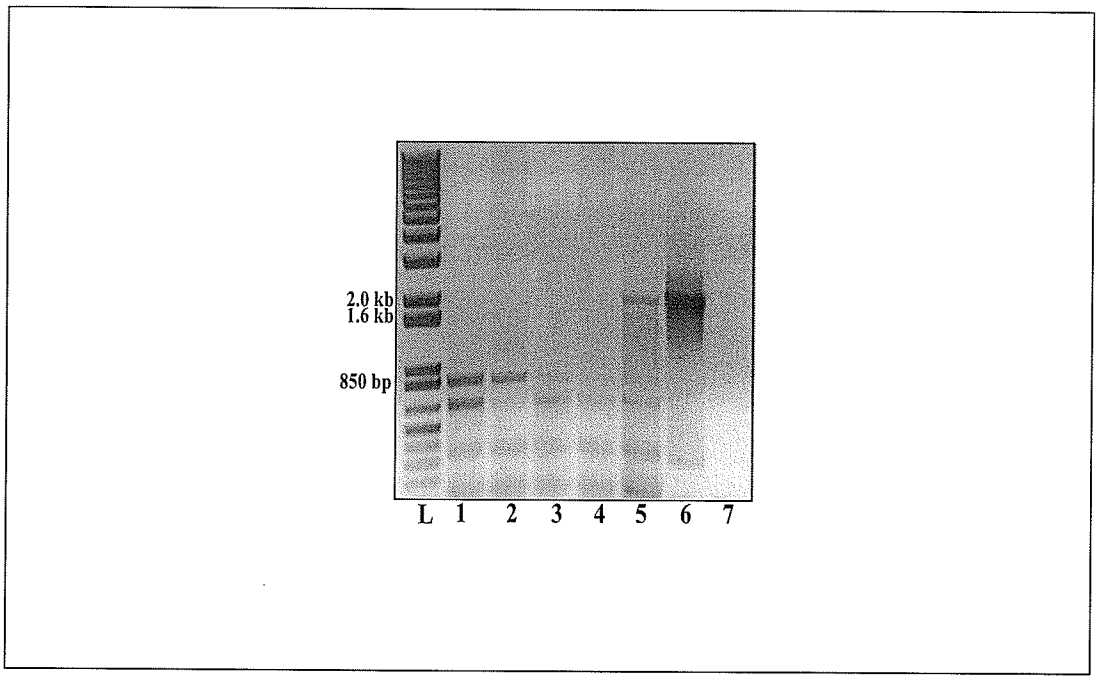

Figure 3-14. PCR results with *orfB* primer set using mutant B, transformed mutant B and wildtype DNA

Lane 1 and 2 - mutant B template DNA, lane 3 and 4 - transformed mutant B template DNA, lane 5 - wildtype template DNA, lane 6 - pBL100 template DNA, lane 7 - water as template.

L - 1 kb Plus DNA Ladder (Invitrogen) with the sizes corresponding to the appropriate band to the left of the gel.

Fig. 3-15, A1-3 shows the initial results using the mutant C template DNA (lanes 1), wildtype template DNA (lanes 2), water as template (lanes 3) and pBL100 template DNA (Appendix B) in lanes 4 with *orfB*, *C* and *D* primer sets. Fig. 3-15, A-1 using the *orfC* primer set there is no 1.1 kb product, but a 450 bp band is seen. This band was later determined to be the *orfC* normal primer set producing PCR products from other parts of the genomic DNA (Fig 3-16). Lane 2 gives the expected 1.1 kb product. There is no product observed in any Lane 3, regardless of the primer used. Lane 4 gives the expected 1.1 kb product as the template carries the intact *orfC* gene. Fig. 3-15, A-2 using the *orfD* primer set there is the expected 1.3 kb product. Lane 2 gives the expected 1.3 kb product. Lane 4 gives the expected 1.3 kb product. Fig. 3-15, A-3 using the *orfB* primer set there is the expected 1.4 kb product. Lane 2 gives the expected 1.4 kb product. Lane 4 gives the expected 1.4 kb product. An alternate set of *orfB* primers were used for this gel which accounts for the size difference between Fig. 3-13, A-1 and Fig. 3-15, A-3 and 3-17, A-3. The alternate set of primers was chosen so all the 3 *orf* primer sets could be run at the same time and annealing temperature in the PCR machine. Fig. 3-15B shows the results using the insertion specific reverse primer (lacZ-211) and *orfC* forward primer with mutant C template DNA (lane 1) giving the expected 964 bp product. Wildtype *P. aeruginosa* template DNA (lane 2) and water as template (lane 3) both show no product.

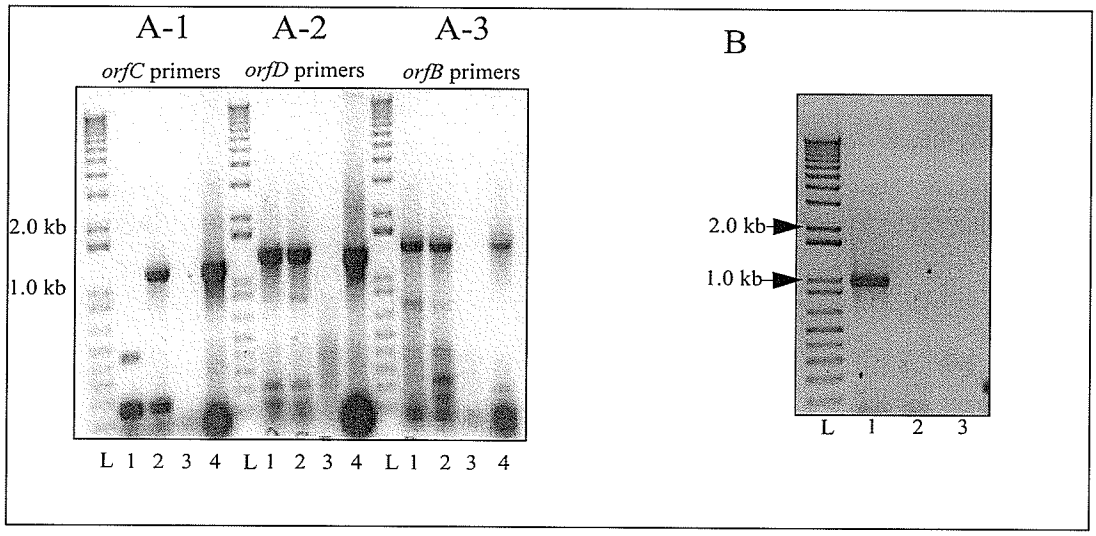

Figure 3-15. Mutant C PCR results

A-1: *orfC* primer set used with: lane 1 - mutant C template DNA, lane 2 - wildtype template DNA, lane 3 - water as template, lane 4 - pBL100 template DNA. **A-2:** *orfD* primer set used with same template DNA as A-1. **A-3:** *orfB* primer set used with same template DNA as A-1.

B: PCR using lacZ-211 reverse primer and *orfC* forward primer with: lane 1 - mutant C template DNA, lane 2 - wildtype template DNA, lane 3 - water as template.

L - 1 kb Plus DNA Ladder (Invitrogen) with the sizes corresponding to the appropriate band seen at left of the gel.

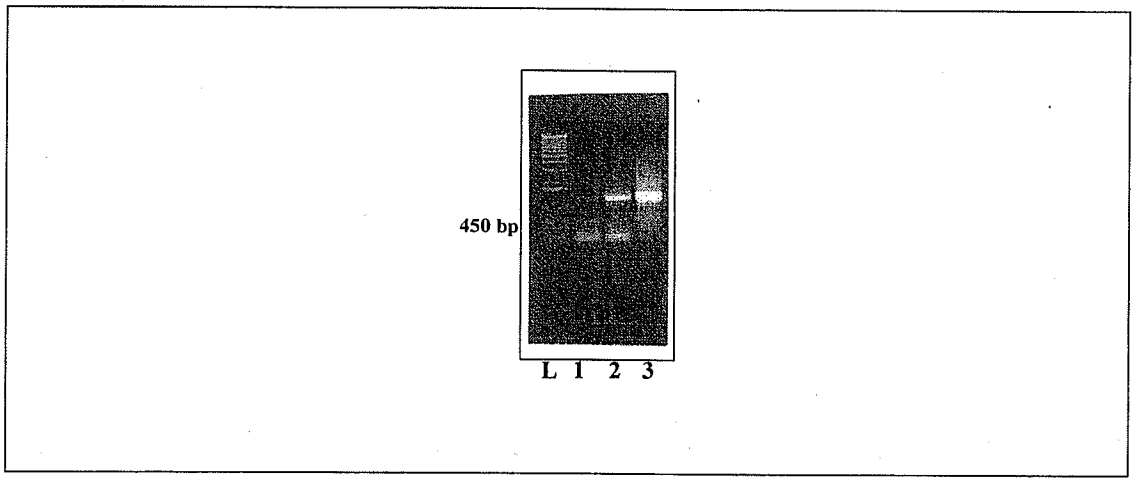

Figure 3-16. PCR results with *orfC* primer set using wildtype and pBL100 DNA
Lane 1 and 2 - wildtype template DNA, lane 3 - pBL100 template DNA.
L - 1 kb Plus DNA Ladder (Invitrogen) with the sizes corresponding to the appropriate band to the left of the gel.

Fig. 3-17, A1-3 shows the initial results using the mutant D template DNA (lanes 1), wildtype template DNA (lanes 2), water as template (lanes 3) and pBL100 template DNA (Appendix B) in lanes 4 with *orfB*, *C* and *D* primer sets. Fig. 3-17, A-1 using *orfD* primer set there is no 1.3 kb product but an 850 bp band is seen. This band is seen in both mutant D and wildtype PCR products due to the primer binding and amplifying an alternate site on the *P. aeruginosa* genome. Lane 2 the expected 1.3 kb sized product. There is no product observed in any Lane 3, regardless of the primer used. Lane 4 gives the expected 1.3 kb product as the template carries the intact *orfD* gene. Fig. 3-17, A-2 using *orfC* primers there is the expected 1.1 kb product. Lane 2 gives the expected 1.1 kb product. Lane 4 gives the expected 1.1 kb product. Fig. 3-17, A-3 using the *orfB* primers there is the expected 1.4 kb product. Lane 2 gives the expected 1.4 kb product. Lane 4 gives the expected 1.4 kb product. Fig. 3-17B shows the results using the insertion specific reverse primer (Hah-166) and the *orfD* forward primer with mutant D template DNA (lane 1) giving the expected 922 bp product. Wildtype *P. aeruginosa* template DNA (lane 2) and water as template (lane 3) both show no product.

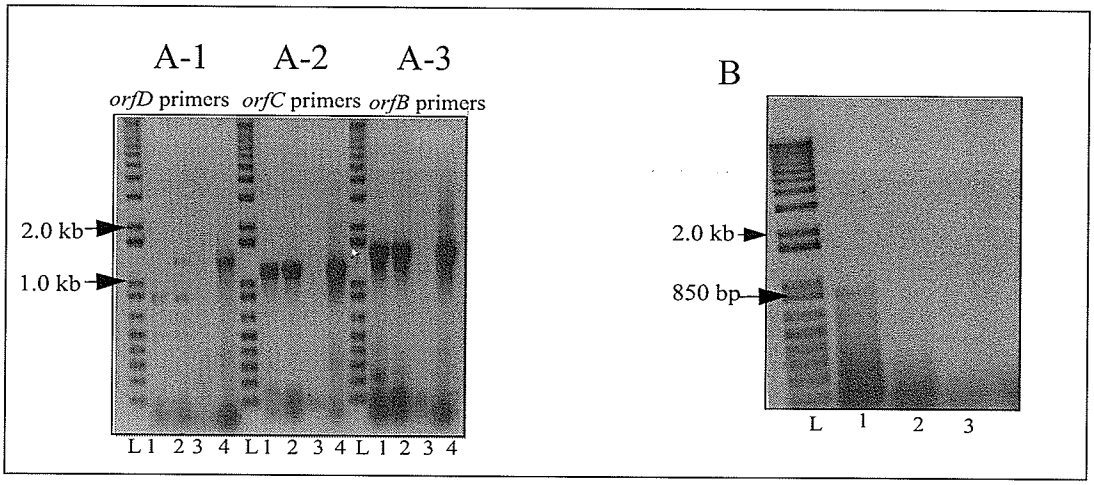

Figure 3-17. Mutant D PCR results

A-1: *orfD* primer set used with: lane 1 - mutant D template DNA, lane 2 - wildtype template DNA, lane 3 - water, lane 4 - pBL100 template DNA. **A-2:** *orfC* primer set used with same template DNA as in A-1. **A-3:** *orfB* primer set used with same template DNA as in A-1.

B: PCR using Hah-166 reverse primer and *orfD* forward primer with: lane 1 - mutant D template DNA, lane 2 - wildtype template DNA, lane 3 - water as template.

L - 1 kb Plus DNA Ladder (Invitrogen) with the sizes corresponding to the appropriate band to the left of the gel. Arrows are pointing to ladder sizes.

3.4 Discussion of insertion mutant confirmation results

In summary, each individual mutant was tested for the presence of an insertion in the gene of interest by using the specific *orf* primers for that gene. The results of the PCR reaction showed no product was made since the insertion in the gene would result in the gene being too large (insertions are either 4.83 kb or 6.16 kb in size) to give a PCR product under normal PCR conditions. In this case normal conditions refers specifically to the elongation time which is set according to the length of the PCR product being amplified. The general rule for elongation time is allowing 1 min/kb, thus in the case of *orfB* amplification, elongation time is 1.45 min, *orfC* and *orfD* amplification, elongation time is 1.30 min which is reflective of the size of band being amplified. In the case of the mutant with either a 4.83 kb or 6.16 kb size insertion, the normal elongation times would be insufficient to generate these large PCR products. During the same PCR reaction the mutant template DNA and PCR primers for the alternate two *orfs* were used to demonstrate that the other two genes were not affected by the insertion. The expected PCR products were produced for the non-mutated genes. The controls used for PCR reactions were wildtype and pBL100 as positive controls and water as the negative control.

A secondary PCR product was seen in Mutant B and C which were shown via PCR to be alternate products produced by the normal PCR primer set (Table 2-3) binding to alternate sites in the genome and producing the secondary product.

The PCR reaction using the primer specific for the insertion and the appropriate *orf* primer for each of the mutants gave an appropriately sized product. These positive product results confirmed the previous lack of product results, seen in Figs. 3-13A-1, 3-15A-1, and 3-17A-1 gels discussed previously. The primer specific for the insertion also eliminated any

concern there may of been in regards to the secondary products produced using the *orfB, orfC* and *orfD* normal primer sets in the cases of mutant B, C and D. In the insertion PCR reactions (B gels) there were two negative controls, wildtype and water.

3.5 Cloning of *orfB* into pUCP21

Insertion of *orfC* and *orfD* into pUCP20 was performed by Dr. R. Habibian as detailed in Appendix C. The insertion of *orfB* into pUCP21 is described in this thesis. *orfB* was initially removed from pBL100 using restriction enzymes *Msc*I (beginning of gene) and *Eco*RI (end of gene). The restriction fragment was purified and cloned into pUCP21 (Fig. 3-18).

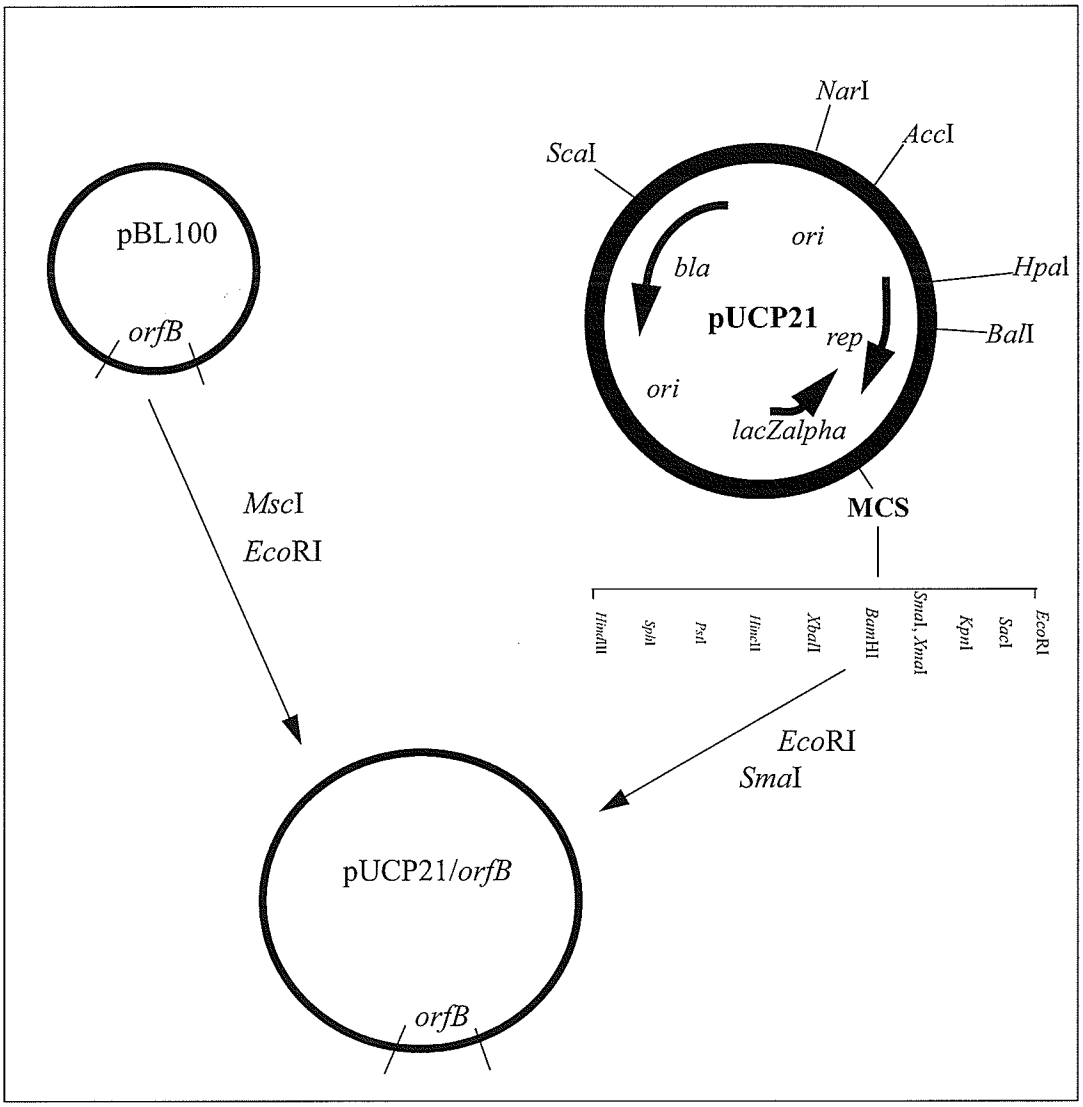

Figure 3-18. Cloning of *orfB* into pUCP21 vector

Fig. 3-19 is the sequence (lead strand only) of pUCP21/*orfB* vector generated using the OMIGA 2.0 (Oxford Moleculars) computer program. The pUCP21 sequence is from NCBI and *orfB* gene sequence is from PseudoCAP. The important points of the vector and insertion are noted in the legend of Fig. 3-19. The size of pUCP21/*orfB* cloning vector = 6497 bp [3898 bp (pUCP21) + 2599bp (*orfB* insertion sequence)].

1441	caccacggcc	cggcctgcct	ttcaggctgc	gcaactgttg	ggaagggcga	tcggtgcggg
1501	cctcttcgct	attacgccag	ctggcgaaag	ggggatgtgc	tgcaaggcga	ttaagttggg
1561	taacgccagg	gttttcccag	tcacgacgtt	gtaaaacgac	ggccagtgaa	ttccgctggc
1621	acgggcgctg	ctgcgcgacg	gcaatgtcga	ccagtacata	ccggcggacc	tgatccaggc
1681	caccgccgaa	gtcctgcgct	ggctggaaag	ccagcagacg	gatacgccct	gatcgctatc
1741	gggcagggca	gccgccgcgg	caccggcgac	gaaagacgct	gcgacctggc	gccgaaaaaa
1801	aggggcccga	aggccccttt	cacatgcttg	ctacgggtca	gtccttgtcc	gggatcccgt
1861	gtaccacgcc	cgcggtattc	tccagcaggc	tcttggtcgc	ggtctggatg	aacgactcca
1921	gcttcttctg	cagctcggcc	tggtccggca	cttccttggt	gatcaccgcc	ttggcatcgc
1981	cgcccagttg	gtaatcgtag	acgcgcacgt	caccgtcctt	cggccgcacc	aggatgcggt
	....	....	....	....	....	....
3061	ccaccagctt	gtcgttgggg	gtcagcaaca	tctgccgggt	ggtctccagg	gcgaccttgt
3121	cgtccagggt	ggccttccag	atgttcgcgc	ggtcttcgga	gaagcgctcc	ttggccgcct
3181	tgaccagggt	cagggtgccg	ttcaggccca	actggttggc	gaacatggac	tcggtggtga
3241	aggcatcgcc	ccagcgcagc	ggcgggccct	ggcgcagggt	gccgcgggcg	gcgaggacgc
3301	agaccagcac	gcagaggaac	agcaccacgc	cgcgcacgta	ccagggcgcg	gcagcgctcg
3361	gccgggcgat	cacgctgtct	tcgcgcggct	tgcgctggct	cgggcgggtc	accaggtcga
3421	tggccttgaa	cacccggtac	agcacccagg	tggcgaaggc	ccaggccagc	aggtagcgga
3481	ccaccgggaa	gccgtaccag	agcatgctca	tgacggtctt	cgggtcttcc	gacatgtact
3541	ggaagaccag	gctgttcagg	cgctggtgga	actcgcggta	gaagtccagt	tcgagtacgc
3601	cgaggaacag	ggtgatgctg	gcgaacagcg	tcaaccatgt	acggaacagg	ccgcgagcgg
3661	ccatcgcgcg	taccgcgaac	aacgacagca	ccagcggcgc	cacggcatag	acgacgaccc
3721	gcaggtcgaa	acgcacgccg	ttgccgaacg	cctcgaggaa	ggtgctcgcc	ggggtcgcgc
3781	cgatcagttc	gcggttgtag	atcagcaagg	ccaggcgcag	caggctgaac	atgaccagca
3841	gcaccagcgc	gctgagcgcg	gtgaacgcca	ggtggctgcg	gatggtgggc	tggaacagcc
3901	gtgggggcga	ttgggtggtt	cggacttccg	tttggtccat	gtttacaatt	cgctcttctg
3961	tcgttcgatt	tcgagaatgc	ggtcccgccc	ctgctcggcc	agcaggtagc	ggccgggccc
4021	gatgggcagt	agggactgtg	cggaacgcag	gcgccgtacg	atcacctgca	gcggcccgtc
4081	gggcggcagc	agcaaggctc	gcgcgttatg	cgtcgagtcc	tcggtgatcc	acaggccttc
4141	gctgtcgcac	agcaaaaagc	tcggtgcatt	cagtccgttc	agcaccacct	cgtcctcggc
4201	cccctcatgc	agacgcatga	cgtgggggga	tcctctagag	tcgacctgca	ggcatgcaag
4261	cttggcgtaa	tcatggtcat	agctgt**ttcc**	tgtgtgaaat	tgttatccgc	tcacaattcc

Figure 3-19. pUCP21/*orfB* leading strand sequence (bases 1441-4320)

*Eco*RI site (blue), sequencing data start using reverse primer (□), *orfB* insertion sequence (underlined) with *orfB* gene (**bold**), bases putative Rho-independent terminator (red, bases 1798-1820) (Adewoye, 1999), start of *orfB* gene (*green, base 3940*), putative RBS (*red, bases 3951 -3956*) (Adewoye, 1999), *Sma*I/*Msc*I hybrid site (magenta), sequencing data start using forward primer (□), . . . represents sequence not shown, all of the *orfB* gene is available on PseudoCAP [Adapted from OMIGA 2.0 (Oxford Moleculars) computer program].

Fig. 3-20 and 3-21 includes sequencing data (performed by NRC-DNA sequencing Lab, Saskatoon, Saskatchewan) using the pUCP reverse and forward primers. This sequence shows that the insertion was in the correct orientation for translation to occur.

AGATC**GAATTC***C*NGT□*C*GGG*N*GCTGCTGCGCGACGGCAATGTCGACCAGTACATACCGGCGGACCT
GATCCAGGCCACCGCCGAAGTCCTGCGCTGGCTGGAAAGCCAGCAGACGGATACGCCCTGATCGCT
ATCGGGCAGGGCAGCCGCCGCGGCACCGGCGACGAAAGACGCTGCGACCTGGCGCCGAAAAAAGG
GGCCCGAAGGCCCCTTTCACATGCTTGCTACGGGTCAGTCCTTGTCCGGGATCCCGTGTACCACGC
CCGCGGTATTCTCCAGCAGGCTCTTGGTCGCGGTCTGGATGAACGACTCCAGCTTCTTCTGCAGCT
CGGCCTGGTCCGGCACTTCCTTGGTGATCACCGCCTTGGCATCGCCGCCCAGTTGGTAATCGTAGA
CGCGCACGTCACCGTCCTTCGGCCGCACCAGGATGCGGTTGCCGGAGACGATGGCGACGTTCTGCT
CGCTGCCCGACGGCTTGATCACGCCGAAGCCCGTGTCGCCTTCCGGCAGGTTCAGCAGGTCGCGGC
CCCAGCACTGGTGGACGGTCTCGCCGCCGAGCAGGCCCATGATGGTCGGCACGATGTCGACCTGGG
TACCGACGGTCGGCAGGTGGGTACCGAACTTCTCCTGGATGCCGGGGGCGATCAGCAGCAGCGGCA
CGTTGAACGGTGCA*N*GTCCATCTCGGTGAGCTGCTCGGGGCTGCCGAA*N*CCATGGTCGCCGA*N*CAC
CACGAAAAAGGGTGTCC*N*TGTAGTAACGG*N*GACTTCTTCGCCTTCTCGAA*N*AA*N*TGGGCCAGCG*N*C
CAGTCGGAATA*N*CGCATGG*N*GGTCA*N*G*N*

Figure 3-20. Sequencing data for pUCP21/*orfB* using reverse primer

*Eco*RI site (**bold**), start of sequencing matching with insertion (**bold-*italic*,** □), mismatches with the known sequence (*italic*) of *orfB* from PseudoCAP. The sequencing data matches bases 1622 to 2424 lead strand of Fig. 3-19.

GCATC□*T*G*N*ATCCNGCAGGTCGACTCTAGAGGAT**CCCCCC**ACGTCATGCGTCTGCATGAGGGGCCG
AGGACGAGGTGGTGCTGAACGGACTGAATGCACCGAGCTTTTTGCTGTGCGACAGCGAAGGCCTGT
GGATCACCGAGGACTCGACGCATAACGCGCGAGCCTTGCTGCTGCCGCCCGACGGGCCGCTGCAGG
TGATCGTACGGCGCCTGCGTTCCGCACAGTCCCTACTGCCCATCGGGCCCGGCCGCTACCTGCTGG
CCGAGCAGGGGCGGGACCGCATTCTCGAAATCGAACGACAGAAGAGCGAATTGTAAACATGGACCA
AACGGAAGTCCGAACCACCCAATCGCCCCCACGGCTGTTCCAGCCCACCATCCGCAGCCACCTGGC
GTTCACCGCGCTCAGCGCGCTGGTGCTGCTGGTCATGTTCAGCCTGCTGCGCCTGGCCTTGCTGAT
CTACAACCGCGAACTGATCGGCGCGACCCCGGCGAGCACCTTCCTCGAGGCGTTCGGCAACGGCGT
GCGTTTCGACCTGCGGGTCGTCGTCTATGCCGTGGCGCCGCTGGTGCTGTCGTTGTTCGCGGTACG
CGCGATGGCCGCTCGCGGCCTGTTCCGTACATGGTTGACGCTGTTCGCCAGCATCACCCTGTTCCT
CGGCGTACTCGAACTGGACTTCTACCGCGAGTTCCACCAGCGCCTGAACAGCCTGGTCTTCCAGTA
CATGTCGGAAGACCGAA*N*ACCGTCATGAGCATGCTCTGGTACGGCTTCCCG*N*GGTCCGCTACCTGC
TGG*N*CTGGG*N*CTTC*N*CC*N*CCT

Figure 3-21. Sequencing data for pUCP21/*orfB* using forward primer

*Sma*I/*Msc*I hybrid site (**bold**), start of sequence matching with insertion (**bold-*italic*,** □), mismatches with the known sequence (*italic*) of *orfB* from PseudoCAP. The sequencing data matches bases 4258 to 3447 lagging strand of Fig. 3-19, note only lead strand of sequence is shown.

3.6 Lead strand and sequencing data for *orfC and orfD* into pUCP20

Fig. 3-22 is the partial sequence (lead strand only) of pUCP20/*orfC* gene. The pUCP20 vector sequence was retrieved from NCBI and the *orfC* sequence is from PseudoCAP. The important points of the vector and insertion are noted in the figure legend. The size of pUCP20/*orfC* cloning vector is 4991 bp [3898 bp (pUCP20) + 1093bp (*orfC* insertion sequence)].

1501	cctcttcgct	attacgccag	ctggcgaaag	ggggatgtgc	tgcaaggcga	ttaagttggg
1561	taacgccagg	gttttcccag	tcacgacgtt	gtaaaacgac	ggccagtgcc	aagcttgcat
1621	gcctgcaggt	cgactctaga	gatccacctg	ggcgcgtttg	ctctgccgca	gtacgtgctg
1681	caggccatcg	gcaagcagga	caacgactga	cgcttcacca	agaagggccg	caaggccctt
1741	tttcatgcgt	cgctccgaca	tcccctgtta	ctgccagcta	acatttttt	cacaatcgat
1801	ccgggaaaat	ctgcgcgctt	ttttccgttg	ccatggctat	aaatggcagt	tttgtccttg
1861	agtgcatcga	atgctgacca	aacgattgcg	ccagagcggc	gtagtagtct	cctgcctgct
1921	cggtagcgtc	ctcttcatcg	ccctggcctt	cctcggctgg	cagcgtttcg	ccccggcagc
1981	caccgtatcc	ggctggacct	accgggtagt	gctcgaggac	attccccacg	tcagcgccct
2041	ggcccgcgac	ccggacggcc	tgctctacgt	gagccaggag	ttgcaggacg	gcaagggcct
2101	ggtgttccgc	atcgccgccg	atggcagccg	cgatacggtg	ctcgacgggc	tgtccaaacc
2161	cgacggcatg	gccagcttcc	gcgacggcat	cgcgatcagc	caggagcagg	gcgcctcgcc
2221	ggtgttctgg	tggcatgccc	agcaggcccg	gccgctgttc	gacggcatcc	aggtggaggg
2281	cgtcgccagc	gacggccgct	acctgtacgc	cgccgaggat	cgcgacctgg	acgggcggat
2341	tctccgctac	gacccggaga	ccggcggact	gacggtactg	cgcgagggat	tgcagcgctc
2401	cgaaggggtg	gccgcctgcc	cggacggaag	cgtcttctac	acggaaaaga	aacgtggcca
2461	cgtcatgcgt	ctgcatgagg	gggccgagga	cgaggtggtg	ctgaacggac	tgaatgcacc
2521	gagctttttg	ctgtgcgaca	gcgaaggcct	gtggatcacc	gaggactcga	cgcataacgc
2581	gcgagccttg	ctgctgccgc	ccgacgggcc	gctgcaggtg	atcgtacggc	gcctgcgttc
2641	cgcacagtcc	ctactgccca	tcgggcccgg	ccgctacctg	ctggccgagc	aggggcggga
2701	ccgcattctc	gaaatcgaac	gacagaagag	cgaattgtaa	acatggacca	aacggaattc
2761	gtaatcatgg	tcatagctgt	ttcctgtgtg	aaattgttat	ccgctcacaa	ttccacacaa
2821	catacgagcc	ggaagcataa	agtgtaaagc	ctggggtgcc	taatgagtga	gctaactcac
2881	attaattgcg	ttgcgctcac	tgcccgcttt	ccagtcggga	aacctgtcgt	gccagctgca
2941	ttaatgaatc	ggccaacgcg	cggggagagg	cggtttgcgt	attgggcgct	cttccgcttc

Figure 3-22. pUCP20/*orfC* leading strand sequence (bases 1501-3000)

*Bam*HI site (blue), sequencing data start using forward primer (□), insertion sequence (underlined) with *orfC* gene (**bold**), start of *orfC* gene (green, base 1871), end of *orfC* gene (green, base 2740), putative RBS (red, bases 1858 - 1862) (Adewoye, 1999), *Eco*RI site (magenta), sequencing data start using reverse primer (□).

Fig. 3-23 and 3-24 are sequences of both strands of pUCP20/*orfC* (NRC - DNA Sequencing Lab, Saskatoon, Saskatchewan).

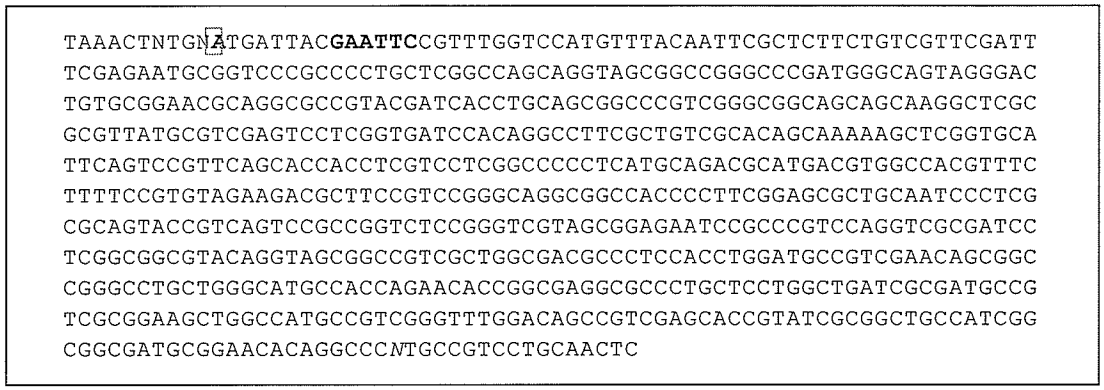

Figure 3-23. Sequencing data for pUCP20/*orfC* using reverse primer

*Eco*RI site (**bold**), start of sequencing match with insertion (**bold**-*italic*, □), mismatches with the known sequence (*italic*) of *orfC* from PseudoCAP. The sequencing data matches bases 2768 to 2078 lagging strand of Fig. 3-22, note only lead strand of sequence is shown.

Figure 3-24. Sequencing data for pUCP20/*orfC* using forward primer

*Bam*HI site (**bold**), letter is start of sequencing match with insertion (**bold**-*italic*, □), mismatches with the known sequence (*italic*) of *orfC* from PseudoCAP. The sequencing data matches bases 1628 to 2320 lead strand of Fig. 3-22.

Fig 3-25 is the sequence (lead strand only) of pUCP20/*orfD* gene generated using the OMIGA 2.0 (Oxford Moleculars) computer program. The sequence of pUPC20 was retrieved from NCBI and the sequence for *orfD* is from PseudoCAP. The important points of the vector and insertion sequence are noted in the figure legend. The size of pUCP20/ *orfD* cloning vector = 5155 bp [3898 bp (pUCP20) + 1257 bp (*orfD* insertion sequence)].

1501 cctcttcgct attacgccag ctggcgaaag ggggatgtgc tgcaaggcga ttaagttggg
1561 taacgccagg gttttcccag tcacgacgtt gtaaaacgac ggccagtgcc aagcttgcat
1621 gcctgcaggt cgactctaga ggatcctact acgccgctct ggcgcaatcg tttggtcagc
1681 attcgatgca ctcaaggaca aaactgccat ttatagccat ggcaacggaa aaaagcgcgc
1741 agattttccc ggatcgattg tgaaaaaaat gttagctggc agtaacaggg gatgtcggag
1801 cgacgcatga aaaagggcct tgcggcgctt cttggtgaag cgtcagtcgt tgtcctgctt
1861 gccgatggcc tgcagcacgt actgcggcag agcaaacgcg cccaggtgga tatcggcgtt
1921 gtagtagcgg gtggcgatgc cgctgtcgcg gaagcgctgg cgcagcgttt ccagcggaag
1981 gcgacgcagg ccttcgtggg tcgaacccca ggcgaaggtc atggcgccgc cgatataggt
2041 cggcaccgcc gcctggtaga aatgccagtc ggcaaacagc ccgtcggtac gtgcggcggt
2101 ggtgcgcact tcctccagtt gcatgaacgg cgtgccgttc tgggtgacca ggatgccacc
2161 ctcgttcagg cagcgccggc aggcctggta gaagttctcg gagaacagca cctcgccagg
2221 gccgatcggg tcggtggagt cggagatgat cacgtcgaag cgttcttccg tggtagccac
2281 gaagcgcatg ccgtcgtcga tcaccaggtt cagccgcggg tcgtcgaagg cgccctggga
2341 gtggttgggc aggaactcct tgcacatgtc gaccacggtg ccgtcgatct cgaccatggt
2401 gatccgctcg acgctcttgt gcttggccac ctcgcgcagc atgccaccgt cgccgccgcc
2461 gatgatcagc acgcgccggg ccgcgccgtg ggcgaggatc ggcacgtggg tgagcatctc
2521 gtggtagatg aactcgtcgg cctcggtggt ctggatcact ccatcgagcg ccatcacccg
2581 gcccatccgg gcgttttcga aaatcaccag gtgctggtgc tcggtgcgca cctcatgcag
2641 catgttgtcg atgctgaagc gctggccgta gccctggtac agagtttcct gataatcgct
2701 catgggccgg gatctcctg gtaaggctgc aatctggcag cgggacttgc ccgcgccgcg
2761 aagaaaggcg cgcattctac gctggcggca atgacaggtc gaaccccgcc ggcggatggc
2821 gccggctgcg ccggacaggt atcgtctgcc catgagccag cctacctctc ccctcgtcct
2881 gcacctgccc taccagtcac cctgggaatg gcgcgaatta attcgtaatc atggtcatag
2941 ctgtttcctg tgtgaaattg ttatccgctc acaattccac acaacatacg agccggaagc
3001 ataaagtgta aagcctgggg tgcctaatga gtgagctaac tcacattaat tgcgttgcgc
3061 tcactgcccg ctttccagtc gggaaacctg tcgtgccagc tgcattaatg aatcggccaa
3121 cgcgcgggga gaggcggttt gcgtattggg cgctcttccg cttcctcgct cactgactcg
3181 ctgcgctcgg tcgttcggct gcggcgagcg gtatcagctc actcaaaggc ggtaatacgg
3241 ttatccacag aatcagggga taacgcagga aagaacatgt gagcaaaagg ccagcaaaag

Figure 3-25. pUCP20/*orfD* leading strand sequence (bases 1501 -3300)

*Bam*HI site (blue), sequencing data start using forward primer (□), insertion sequence (underlined) with *orfD* gene (**bold**), start of *orfD* gene (green, base 1843), end of *orfD* gene (green, base 2703), putative RBS (red, bases 2723-2727) (Adewoye, 1999), *Eco*RI site (magenta), and sequencing data start site using reverse primer (□).

Fig. 3-26 and 3-27 are sequences of both strands of pUCP20/*orfD* (NRC - DNA Sequencing Lab, Saskatoon, Saskatchewan).

Figure 3-26. Sequencing data for pUCP20/*orfD* using reverse primer

*Eco*RI site (**bold**), start of sequencing matching with insertion (**bold**-*italic*,□), mismatches with the known sequence (*italic*) of *orfD* from PseudoCAP. The sequencing data matches bases 2919 to 2040 lagging strand of Fig. 3-25, note only lead strand of sequence is shown.

Figure 3-27. Sequencing data for pUCP20/*orfD* using forward primer

*Bam*HI site (**bold**), start of sequencing matching with insertion (**bold**-*italic*,□), mismatches with the known sequence (*italic*) of *orfD* from PseudoCAP. The sequencing data matches bases 1623 to 2090 lead strand of Fig. 3-25.

3.7 Transformation/complementation of insertion deletion mutant strains of *P. aeruginosa* with cloned *orf's B, C and D*

The pUCP21/*orfB*, pUCP20/*orfC* and pUCP20/*orfD* plasmids were each used to transform the respective mutant as detailed in Section 2.7 (*e.g.* Mutant B complemented with pUCP21/*orfB*). The transformants were selected via growth on tetracycline and carbenicillin selective plates. The transformed colonies were confirmed by performing a plasmid preparation which was subjected to restriction digest and PCR for the appropriate sized products in the cases of pUCP21/*orfB*, pUCP20/*orfC* and pUCP20/*orfD* (Fig. 3-28). A restriction digest of pUCP21/*orfB* with *Eco*RI and *Bam*HI should yield a 2.6 kb and a 3.9 kb product. The predicted PCR product using *orfB* primers (Table 2-3) should yield a 2.0 kb sized product. A restriction digest of pUCP20/*orfD* with *Eco*RI and *Bam*HI should yield a 1.2 kb and a 3.9 kb product. The predicted PCR product using *orfD* primers (Table 2-3) yields a 1.3 kb sized product. A restriction digest of pUCP20/*orfC* with *Eco*RI and *Bam*HI should yield a 1.1 kb and a 3.9 kb product. There should be no PCR product using *orfC* primers (Table 2-3) since *orfC* was cloned via PCR using the *orfC* primer set (Table 2-3) with pBL100 as template DNA. The PCR product was digested to produce the appropriate ends needed to ligate the gene with vector pUCP20. The digestion eliminates parts of the forward and reverse primer binding regions which disrupts PCR using the plasmid preparation pUCP20/*orfC* as template DNA. It would have been possible to PCR *orfC* by using internal primers, this would entail ordering an alternate set of *orfC* primers which was not done.

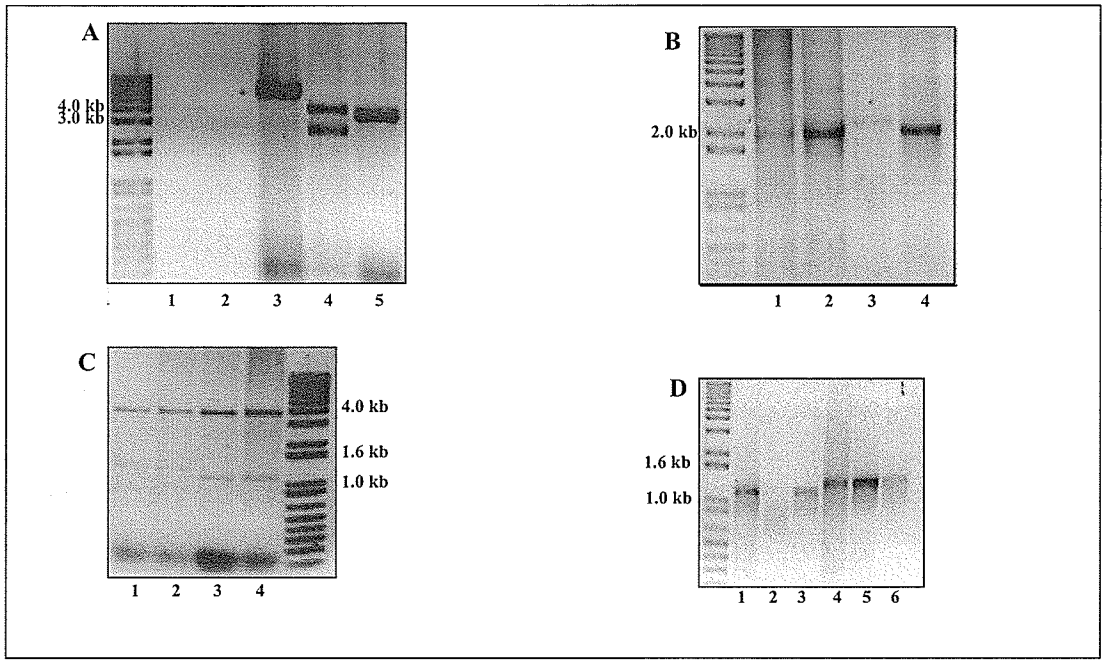

Figure 3-28. Restriction digest and PCR verifying transformation of insertion mutants B, C & D with the corresponding cloned *orf*.

Gel A: Verification of *orfB* via restriction digest, Lane 1 - pUCP21 vector (3.9 kb) double digest using *Sma*I and *Eco*RI, Lane 2 - *orfB* insertion (2.6 kb), Lane 3 - plasmid preparation of mutantB/pUCP21/*orfB* with pUCP21/*orfB,* single digest using *Bam*HI (6.5 kb), Lane 4 - plasmid preparation of mutantB/pUCP21/*orfB* with pUCP21/*orfB,* double digestion using *Eco*RI and *Bam*HI (2.6 and 3.9 kb), Lane 5 - pUCP21 vector, single digest using *Eco*RI (3.9 kb). **Gel B:** PCR with *orfB* primers (Table 2-3), Lane 1-3 - three different plasmid preparations of mutantB/pUCP21/*orfB* template DNA (note Lane 3 size was incorrect and this transformed mutant B was discarded), Lane 4 - plasmid preparation of pBL100 template DNA. **Gel C:** Verification of *orfC* and *orfD* via restriction digest, Lane 1 & 2 - plasmid preparation from mutant D/pUCP20/*orfD* with pUCP20/*orfD,* double digest (1.2 and 3.9 kb) using *Eco*RI and *Bam*HI, Lane 3 & 4 - plasmid preparation from mutantC/pUCP20/*orfC* with pUCP20/*orfC,* double digest (1.1 and 3.9 kb) using *Eco*RI and *Bam*HI. **Gel D:** PCR with *orfC* (lanes 1-3) and *orfD* (lanes 4-6) primers (Table 2-3), Lane 1, 3 & 4 - plasmid preparation of pBL100 template DNA, Lane 2 - plasmid preparation from mutantC/pUCP20/*orfC* template DNA, Lane 5 & 6 - plasmid preparation from mutantD/pUCP20/*orfD* template DNA.

SDS-PAGE was performed using whole cell lysis preparations of the wildtype, mutant and transformed mutant (Fig. 3-29). Expected protein products were mutant B - 77 kDa, mutant C and D - 32 kDa. All gels showed no evidence of protein expression or lack of expression as may be the case in wildtype, mutants and the transformed mutants.

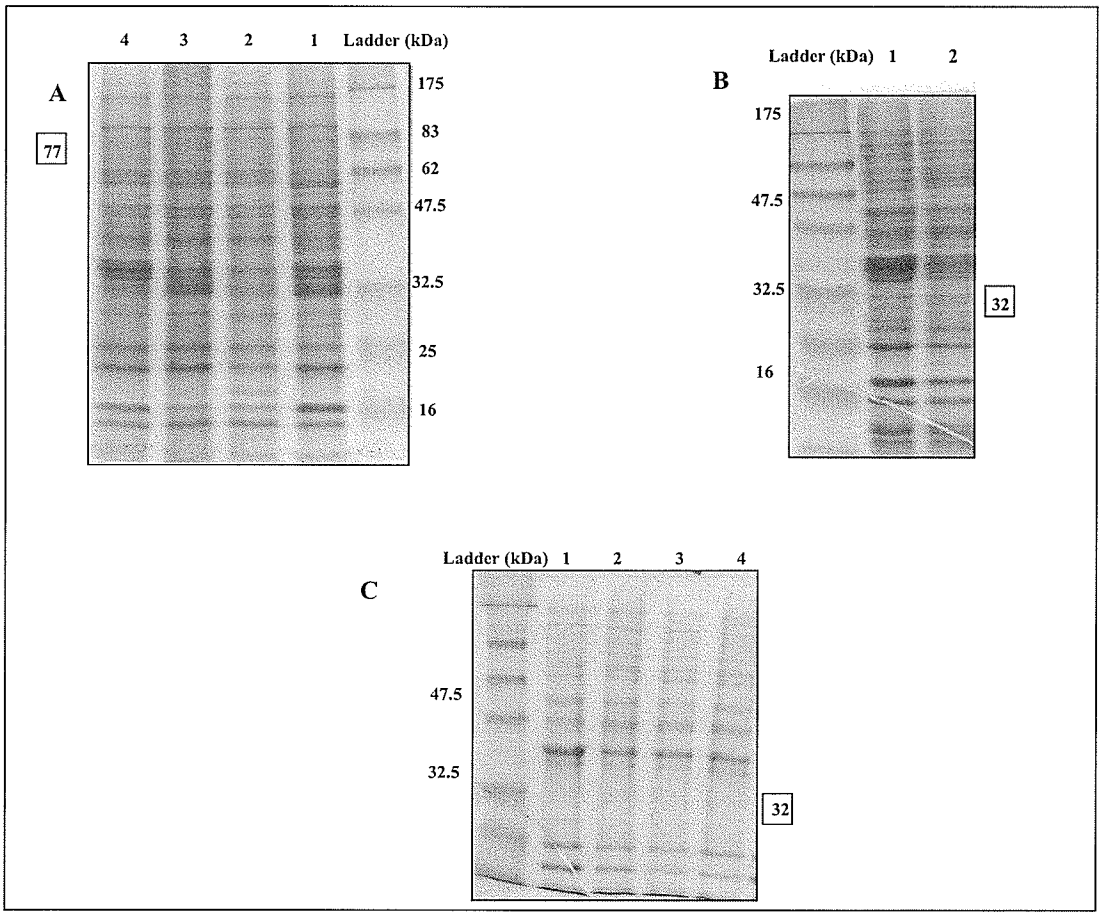

Figure 3-29. SDS-PAGE gel electrophoresis of whole cell lysis of wildtype, mutants and transformed mutants

Gel A: Lane 1 - *P. aeruginosa* wildtype, Lane 2 - mutant B, Lane 3 - mutantB/pUCP21, Lane 4 - mutantB/pUCP21/*orfB*. **Gel B:** Lane 1 - *P. aeruginosa* wildtype, Lane 2 - mutant C. **Gel C:** Lane 1 - *P. aeruginosa* wildtype, Lane 2 - mutantD/pUCP20, Lanes 3 & 4 - mutantD/pUCP20/*orfD*. Note numbers in squares denote sizes of expected proteins and area where the predicted protein would run.

3.7.1 Discussion

In section 3.5, Figs. 3.19 - 3.27 clearly shows that the sequencing data in both directions (forward and reverse) from the vectors pUCP21/*orfB*, pUCP20/*orfC* and pUCP20/*orfD* match to there appropriate sequence (PseudoCAP) and also show directionality of the gene in the vector. This data shows that the pUCP21/20/*orf* vectors were correct and this leads to the following step of transforming the *P. aeruginosa* mutant with the appropriate vector to complement the insertion deletion. The verification of the transformation of the insertion mutants was carried out by restriction digest and PCR of plasmid preparations. The predicted pUCP21/*orfB* restriction products of 2.6 and 3.9 kb coincided with the restriction gels (Fig. 3-28, A). The *orfB* gene was also verified via PCR using *orfB* primers (Table 2-3) with plasmid preparation from mutantB/pUCP21/*orfB* as well as the control plasmid preparation from pBL100. Both template DNAs yielded the expected 2.0 kb size band (Fig. 3-28, B). The predicted pUCP20/*orfC* restriction products of 1.1 and 3.9 kb coincide with the restriction gels (Fig. 3-28, C). The *orfC* gene was not verified via PCR using *orfC* primers (Table 2-3) with template pUCP20/*orfC* (Fig. 3-28, D). The lack of PCR product is explained by the fact that when constructing pUCP20/*orfC*, the *orfC* gene was amplified by PCR using the *orfC* primers (Table 2-3) with pBL100 template DNA. The *orfC* PCR product was subjected to restriction digest to prepare the *orfC* gene for ligation into the pUCP20 vector. The restriction digest caused the removal of a significant portion of the primer binding sites. The lack of the whole PCR primer binding sites does not allow the PCR process to produce a product from the pUCP20/*orfC* template DNA. The predicted pUCP20/*orfD* restriction products of 1.2 and 3.9 kb coincide with the restriction gel (Fig. 3-28, C). The *orfD* gene was also verified via PCR using *orfD* primers (Table 2-3) with

plasmid preparation from mutantD/pUCP20/*orfD* as well as plasmid preparation of pBL100 (Fig. 3-28, D). pBL100 template DNA yielded the expected 1.3 and 1.1 kb products with *orfD* and *orfC* primer sets, respectively. The restriction digest and PCR data show that the mutants were transformed with the correct vector/gene plasmid.

The expected protein band in the SDS-PAGE gel for the OrfB protein in the cases of *P. aeruginosa* wildtype and mutantB/pUCP21/*orfB* was 77 kDa in size. In the case of samples from mutant B and mutant B with empty plasmid (pUCP21) no band is expected. Fig. 3-29, A it is impossible to see the lack of a band at 77 kDa in lanes 2 and 3.

The expected protein band in the SDS-PAGE gel for the OrfC protein in the case of *P. aeruginosa* wildtype was 32 kDa in size. In the case of mutant C no band is expected. In Fig. 3.29, B it is impossible to see a lack of a band in the case of mutant C compared to wildtype.

The expected protein band in the SDS-PAGE gel for OrfD protein in the case of *P. aeruginosa* wildtype and mutantD/pUCP20/*orfD* is 32 kDa in size. In the case of mutant D and mutant D with the empty vector (pUCP20) no band is expected. Fig. 3.29, C shows no difference in banding pattern between wildtype, mutant D/pUCP20/*orfD*, mutant D and mutant D with empty vector (pUCP20).

Thus in looking at all the SDS-PAGE gels there was no protein expression detected. In all cases this data does not support the idea that the transformed mutants were functionally complemented. It is possible that the amount of protein made is not detectable by the SDS-PAGE system or alternatively the size ranges of interest may be common sizes and the lack of the *orf* encoded protein is negligible in comparison to all the other proteins of the same

size. This data shows that the transformed mutants did not show detectable complementation via SDS-PAGE. All the three *orf*s have a putative ribosome binding site (RBS) before each appropriate gene in the vector (Figs. 3-19, 3-22 and 3-25). The identification of a RBS shows that it is possible for the gene to be translated in the *P. aeruginosa* mutant.

3.8 Growth curves of *P. aeruginosa* wildtype and mutants

Growth curves were produced using each of the insertion mutants (mutant B, C, D) and wildtype *P. aeruginosa* grown on carbohydrates glucose, fructose, mannitol or glycerol. (Fig. 3-30) The doubling times for each mutant and wildtype with each carbohydrate were also calculated and are found in Table 3-2. In Table 3-2 wildtype doubling time is considered normal under each of the induced carbohydrate conditions. Any mutant which has a doubling time that is more or less than 1.5 of wildtype is considered significantly different because the increase/decrease in doubling time reflects the health of the cells in culture. If a cell is taking longer to double it is most likely experiencing problems in attaining the nutrients, metabolic signals, *etc.* required for growth, in turn, if a cell has a short doubling time the cell is attaining adequate nutrients, metabolic signals, *etc.*

Table 3-2. Bacterial doubling times (min) under various growth conditions

P. aeruginosa strain	Doubling time in glucose (min)	Doubling time in fructose (min)	Doubling time in mannitol (min)	Doubling time in glycerol (min)
Wildtype	77 (+/- 0)	204(+/- 4)	130 (+/- 3)	227 (+/- 5)
Mutant B	154 (+/- 2)	114 (+/- 3)	116 (+/- 0)	112 (+/- 1)
Mutant C	77 (+/- 0)	204(+/- 8)	100 (+/- 0)	122 (+/- 3)
Mutant D	91 (+/- 0)	145 (+/- 7)	105 (+/- 3)	128 (+/- 5)
The doubling time was determined from a minimum of three replications. The significant difference is given in brackets after the doubling time.				

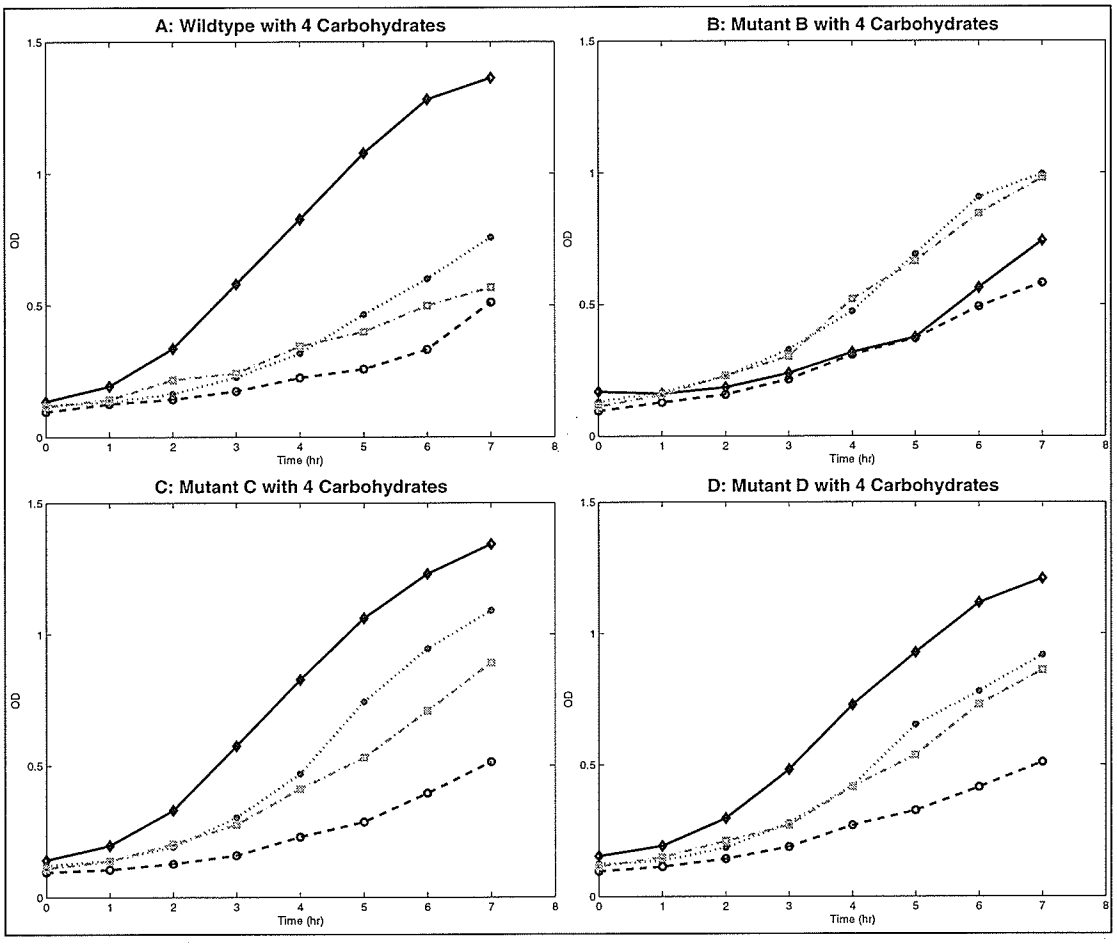

Figure 3-30. *P. aeruginosa* strains grown in various carbohydrates

Graph **A**: wildtype, **B**: mutant B, **C**: mutant C, **D**: mutant D and the carbohydrates in each graph are: glucose (♦), fructose (○), mannitol (●) and glycerol (□). Overnight cultures (1 ml) in LB were subcultured into 50 ml of minimal media supplemented with 20 mM of appropriate carbohydrate. No error bars were used because data generated for the curves was observed from the minimum of 3 trials and error was negligible.

P. aeruginosa wildtype and mutants were grown under conditions which would induce the high affinity uptake systems. In the case of glucose these conditions include growing in minimal media supplemented with 20 mM glucose (Eagon and Phibbs, 1971, Midgley and Dawes, 1973, Guymon and Eagon, 1974). The fructose PTS uptake system required minimal media supplemented with 20 mM fructose (Durham and Phibbs, 1982, Eagon and Phibbs, 1971, Phibbs and Eagon, 1970, Phibbs *et al.*, 1978, Eagon and Williams, 1960). Induction of the high affinity uptake systems for mannitol and glycerol required growth in either 20 mM mannitol (Phibbs and Eagon, 1970, Eagon and Phibbs, 1971) or 20 mM glycerol, respectively (Tsay *et al.*, 1971, Seigel and Phibbs, 1979, Schweizer, 1991, Williams *et al.*, 1994).

As seen in Fig. 3-32, **A** *P. aeruginosa* wildtype is best suited to grow under induced glucose conditions, with a doubling time of 77 mins (Table 3-2). In the presence of the other carbohydrates doubling time increases by 2.0 to 3.0 fold. Fig. 3-32, **B** shows mutant B growth curves with the four carbohydrates. Mutant B is able to grow in all carbohydrates with not much difference in doubling times which vary from 154 mins under induced glucose conditions, 114 mins under induced fructose conditions, 116 mins under induced mannitol conditions to 116 mins under induced glycerol conditions (Table 3-2). Fig 3-32, **C** shows mutant C growth curves with the four carbohydrates. Mutant C is best suited to grow under induced glucose conditions with a doubling time of 77 mins (Table 3-2). It is least suited to grow under induced fructose conditions with a doubling time of 204 mins, while doubling times of 100 and 112 mins were calculated for mutant D under induced mannitol and induced glycerol conditions, respectively. Fig. 3-32, **D** shows mutant D growth curve with the four carbohydrates. Mutant D is best suited to grow under induced

glucose conditions with a doubling time of 91 mins (Table 3-2). It is the least suited to grow under induced fructose conditions with a doubling time of 145 mins. Growth in mannitol or glycerol was intermediate.

Upon examination of the four curves in Fig. 3-32 and doubling times in Table 3-2, it is obvious that wildtype, mutant C and mutant D are each portraying the same growth patterns in all four carbohydrates. Mutant B growth curves stand out from the rest in that mutant B grows the best in mannitol (116 min) followed by glycerol (112 min) and it grows about the same in both glucose (154 min) and fructose (114 min).

3.8.1 Summary of growth curve results

When looking at doubling times (Table 3-2) and growth curves (Fig. 3-32) it is clear there is a different growth profile seen for mutant B when compared to wildtype, mutant C and mutant D. In glucose, mutant B shows a 2.0 fold increase in doubling time compared to wildtype but in the case of fructose and glycerol has better growth than wildtype (1.8 and 2.0 fold, respectively). In Fig. 3-32 it shows that for wildtype, mutant C and mutant D the growth pattern in the four carbohydrates are generally the same which is best in glucose followed by mannitol then glycerol. The slowest growth is observed under fructose conditions.

Results seen by Adewoye (1999), Fig. 1-4, A show that in the case of glucose uptake assay that *orfBCD* mutant has a 5-fold less uptake than wildtype. In the case of growth curves for mutant B in glucose, growth is severely challenged compared to wildtype and mutant C and D. It may be possible that *orfB* and *orfD* (partially) may be contributing to the lower glucose uptake seen in Fig. 1-4, A. Whereas in the case of *orfC* it doesn't seem

to be playing a role in the carbohydrates glucose and fructose uptake phenotype. This seems like a plausible explanation for all carbohydrates with the exception of glycerol where this trend is not seen. The putative *orfB* gene product MdoB has been implicated in slow growth rates in mutants void of MdoB (Jackson, *et al.*, 1986). The putative *orfC* gene product strictosidine synthase has no role in growth and thus does not contribute to the uptake assay phenotype. In the case of *orfD* with the putative gene product spermidine synthase, it has been shown the lack of this protein contributes to slow growth rates in *E. coli* (Kallio and McCann, 1981, Tabor and Tabor, 1984, Jin *et al.*, 2002).

3.9 Uptake of radiolabelled carbohydrates

This section will look at the results obtained from the carbohydrate uptake assays over a 60 s and 24 min time intervals, using each specific mutant, wildtype and transformed mutant (the 24 min graphs were generated for interest only). The results compare each mutant to wildtype and transformed mutant with the four carbohydrates (glucose, fructose, mannitol and glycerol). No error bars are used due to the conditions of the assay. To put this in perspective it must be realized that 0.5 µl of 100 fold dilution of [^{14}C] carbohydrate into 10 mls of scintillation fluid resulted in the following counts per minute (cpm): Glucose - 6277, fructose - 3798, mannitol - 2917 and glycerol - 3392. When performing the assay, the samples are diluted to an OD_{600} = 0.04, at this low OD variation can be introduced just by the accuracy of the spectrophotometer. The assay is performed by adding volumes ranging from 1.4 µl to 13.5 µl of the stock [^{14}C] carbohydrate (as dependent on carbohydrate concentration in the given manufacturers solution) into 10 mls of cells. Due to the variability of the assay error between replicates is not as important as the

reproducibility of the trends of uptake seen between wildtype, mutant and transformed mutant.

The carbohydrate uptake results for up to 60 s after the addition of [^{14}C] carbohydrate for mutant B is found in Fig. 3-31. In order to compare the rate of uptake the slope of linear portion of the curve is calculated. The 20 s slopes were calculated by the MATLAB 6.5 computer program and values are presented in Table 3-3. From these results it can be concluded that mutant B has an impaired uptake of all carbohydrates tested when compared to wildtype. In the case of fructose uptake for mutant B the results are too low and will not be discussed. The transformed mutant has an identical or decreased slope compared to mutant B in the case of glucose and mannitol. However, in the case of glycerol, the transformed mutant regains some uptake function however it does not reach that seen with the wildtype. Particularly in glycerol transformed mutant B has a slope increase of 3.5 compared to mutant B and a slope decrease of 6.5 compared to wildtype (Table 3-3). In the case of glycerol there is evidence of complementation.

When the uptake assays were run for 24 mins (Fig. 3-32) mutant B is taking up less carbohydrate than wildtype. Due to low uptake by mutant B in fructose these results will not be discussed. The complemented mutant B does not complement glucose or mannitol uptake. In the case of glycerol a partial complementation of uptake is observed, but is not equal to wildtype uptake.

Table 3-3. Slopes obtained from 0 - 20 s carbohydrate uptake data for wildtype, mutant B and transformed mutant B

Carbohydrate	*P. aeruginosa* strain	20 s slope[1]
Glucose	wildtype	8.0
	mutant B	7.2
	transformed mutant B	5.0
Fructose	wildtype	4.4
	mutant B	0.1
	transformed mutant B	1.1
Mannitol	wildtype	5.0
	mutant B	0.9
	transformed mutant B	0.9
Glycerol	wildtype	16.1
	mutant B	6.1
	transformed mutant B	9.6

[1] - 20 s slope was calculated by dividing the counts per minute by 20 using MATLAB 6.5 computer program (data not shown).

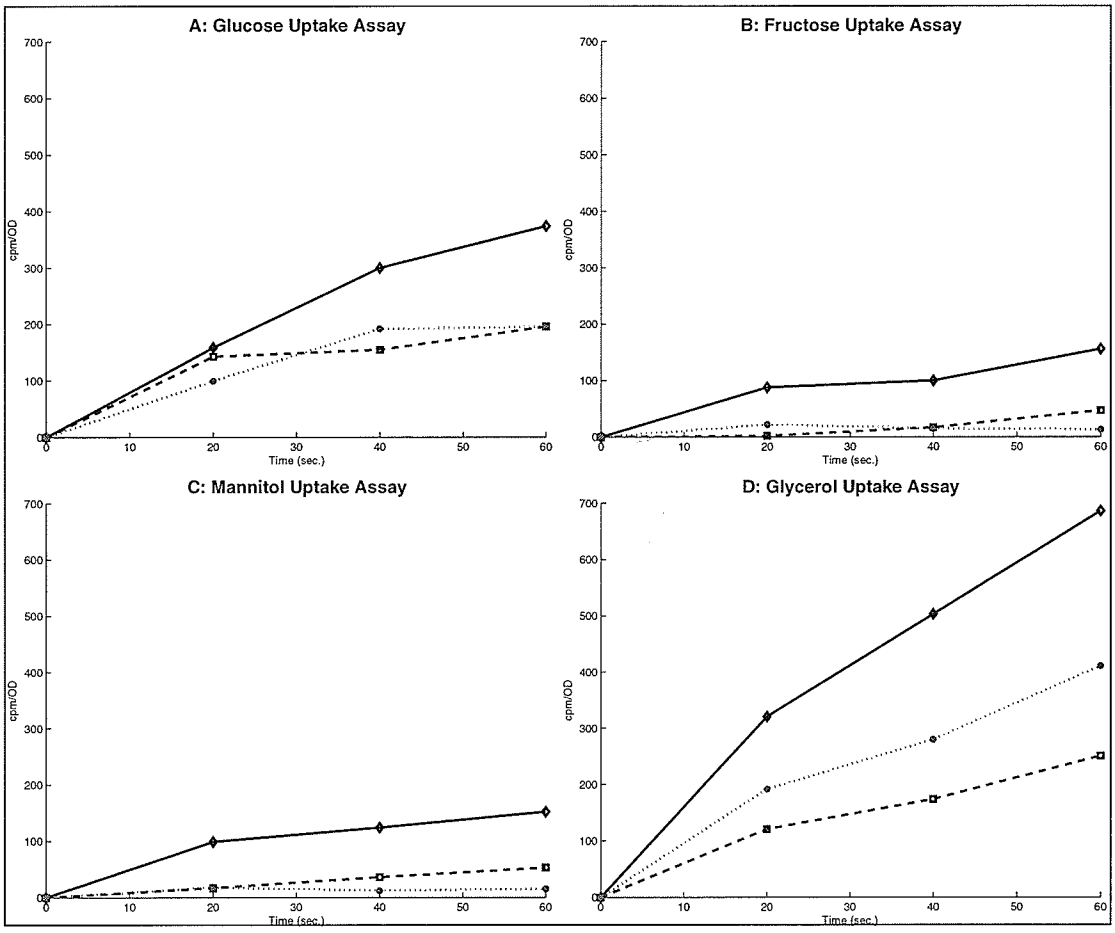

Figure 3-31. Carbohydrate uptake assays using *P. aeruginosa* wildtype, mutant B and transformed mutant B

Panel **A**: Glucose, Panel **B**: Fructose, Panel **C**: Mannitol, Panel **D**: Glycerol. *P. aeruginosa* wildtype (◇), mutant B (□), transformed mutant B (●). Uptake of 0.33 μM of [^{14}C] glucose or 2.4 μM of [^{14}C] fructose, mannitol or glycerol was studied at a cell density, OD_{600}= 0.04, in order to ensure a linear initial uptake of radiolabelled sugar by starved cells of *P. aeruginosa* strains. Aliquots (0.5 ml) were withdrawn at 20, 40 and 60 s after addition of [^{14}C] sugars. Data is representative of at least three independent assays.

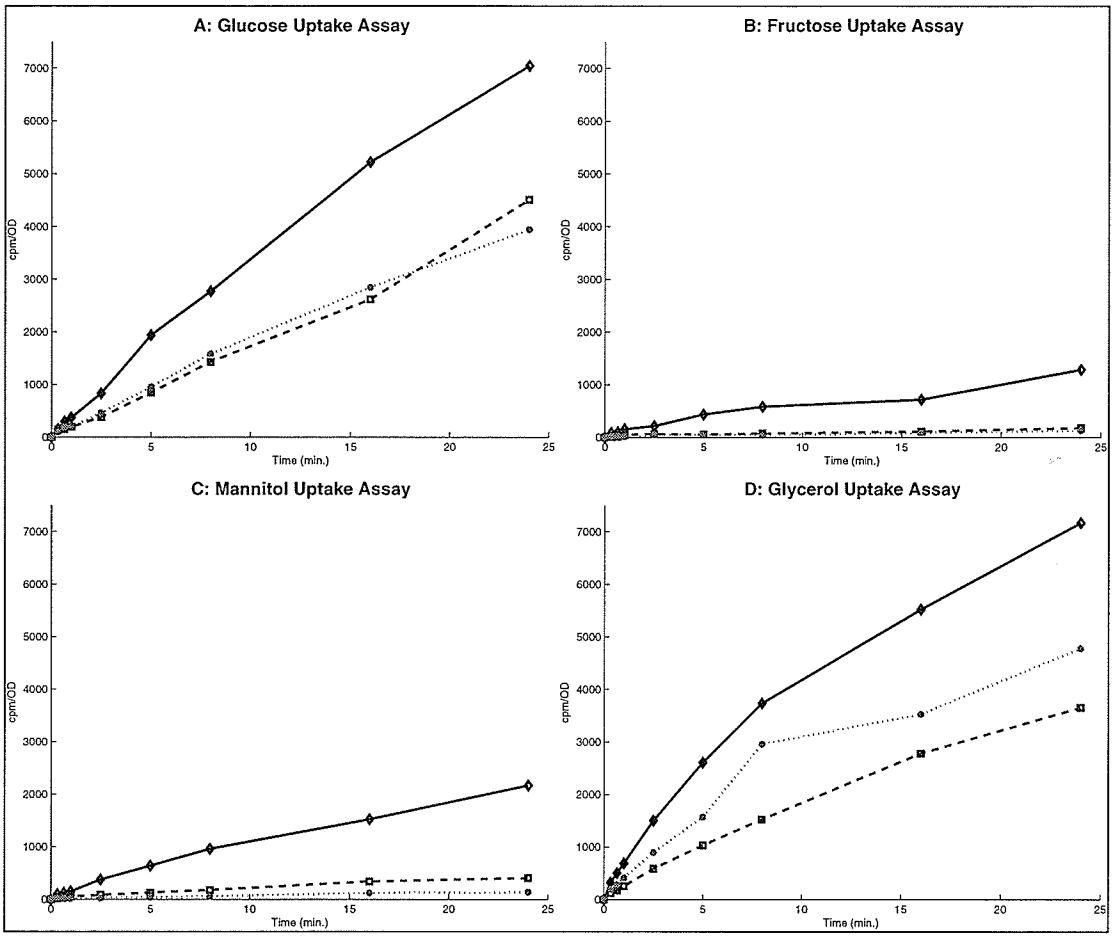

Figure 3-32. Carbohydrate uptake assays of *P. aeruginosa* wildtype, mutant B, transformed mutant B

Panel **A**: Glucose, **B**: Fructose, **C**: Mannitol, **D**: Glycerol. *P. aeruginosa* wildtype (◇), mutant B (□), transformed mutant B (●). Uptake of 0.33 μM of [^{14}C] glucose and 2.4 μM of [^{14}C] fructose, mannitol or glycerol was studied at a cell density, OD_{600} = 0.04, in order to ensure a linear initial uptake of radiolabelled sugar by starved cells of *P. aeruginosa* strains. Aliquots (0.5 ml) were withdrawn at 0.33, 0.66, 1.0, 2.5, 5.0, 8.0, 16.0 and 24.0 mins after addition of [^{14}C] sugars. Data are representative of at least three independent assays no error bars are used.

The carbohydrate uptake results for 60 s after the addition of [^{14}C] carbohydrate for mutant C are presented in Fig. 3-33. In order to compare the rate of uptake the slope of the linear portion of the curve is calculated. The 20 s slopes were calculated by the MATLAB 6.5 computer program and values are presented in Table 3-4. These results show mutant C has an impaired uptake of all carbohydrates tested, as compared to wildtype. The uptake data for fructose and mannitol in the case of mutant C will not be used due to non linear uptake as seen in Fig. 3-33, panels B and C. The transformed mutant has the same slope as mutant C in the case of glucose. In the case glycerol uptake transformed mutant shows complementation yielding better uptake than wildtype, with a slope increase of 5.0 compared to wildtype.

When the uptake assays were run for 24 mins (Fig. 3-34) in all carbohydrates tested mutant C is taking up less than wildtype. Due to low uptake of mutant C in fructose and mannitol these results will not be discussed. The transformed mutant C shows full complementation in the case of glycerol.

Table 3-4. Slopes obtained from 0 - 20 s carbohydrate uptake data for wildtype, mutant C and transformed mutant C

Carbohydrate	*P. aeruginosa* strain	20s slope[1]
Glucose	wildtype	20.2
	mutant C	7.3
	transformed mutant C	7.2
Fructose	wildtype	1.7
	mutant C	0.7
	transformed mutant C	1.8
Mannitol	wildtype	4.2
	mutant C	1.9
	transformed mutant C	2.3
Glycerol	wildtype	29.7
	mutant C	19.3
	transformed mutant C	34.7

[1] - 20 s slope was calculated by dividing the counts per minute by 20 using MATLAB 6.5 computer program (data not shown),

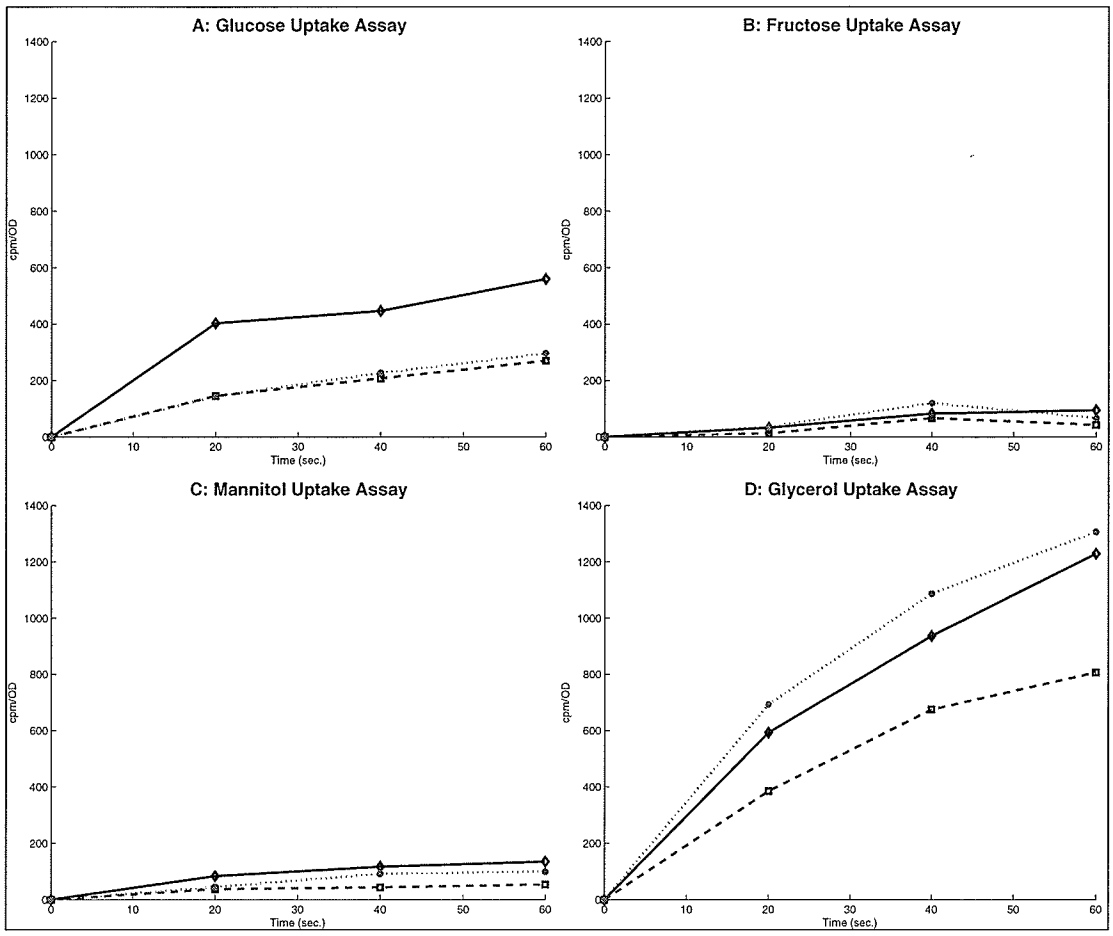

Figure 3-33. Carbohydrate uptake assays using *P. aeruginosa* wildtype, mutant C and transformed mutant C

Panel **A**: Glucose, Panel **B**: Fructose, Panel **C**: Mannitol, Panel **D**: Glycerol. *P. aeruginosa* wildtype (◊), mutant C (□), transformed mutant C (●). Uptake of 0.33 μM of [^{14}C] glucose or 2.4 μM of [^{14}C] fructose, mannitol or glycerol was studied at a cell density, OD_{600}= 0.04, in order to ensure a linear initial uptake of radiolabelled sugar by starved cells of *P. aeruginosa* strains. Aliquots (0.5 ml) were withdrawn at 20, 40 and 60 s after addition of [^{14}C] sugars. Data is representative of at least three independent assays.

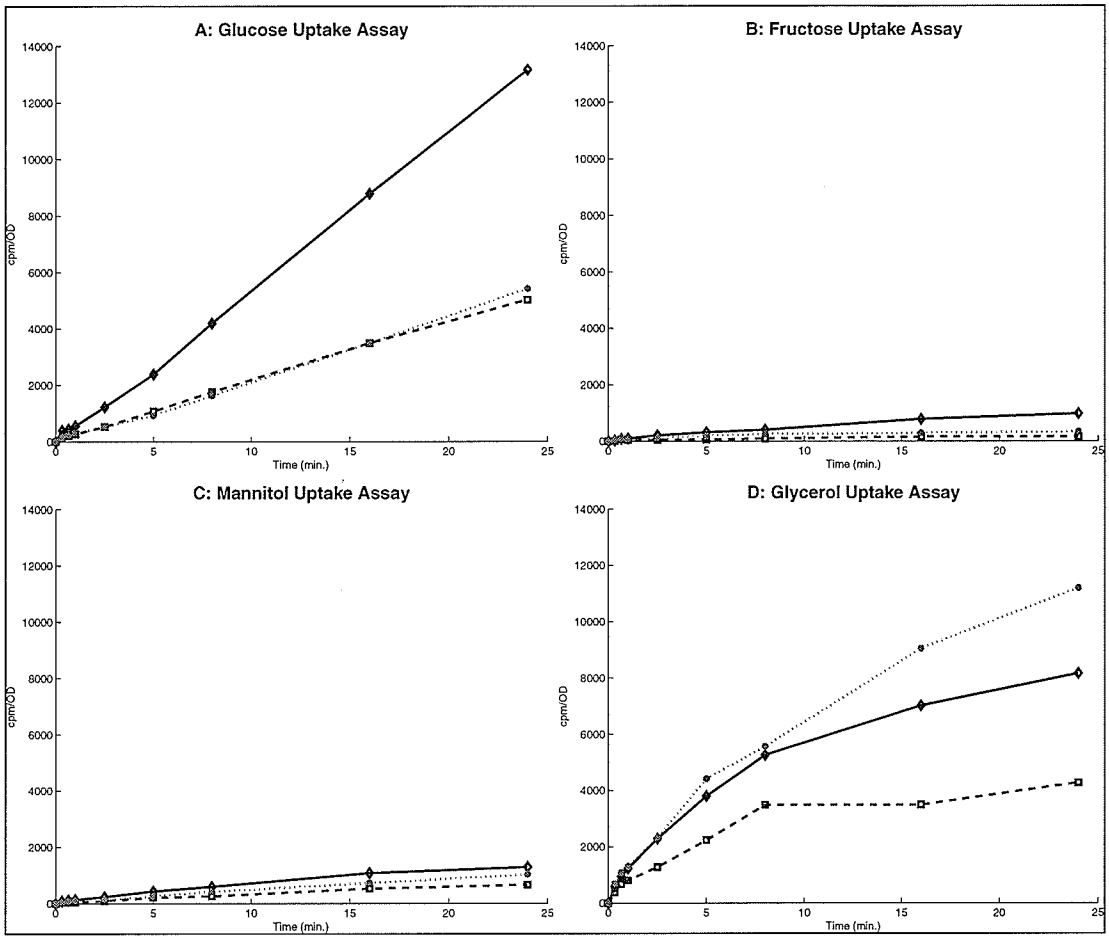

Figure 3-34. Carbohydrate uptake assays of *P. aeruginosa* wildtype, mutant C, transformed mutant C

Panel **A**, Glucose, Panel **B**, Fructose, Panel **C**, Mannitol, Panel **D**, Glycerol. *P. aeruginosa* wildtype (◇), mutant C (□), transformed mutant C (●) . Uptake of 0.33 μM of [^{14}C] glucose and 2.4 μM of [^{14}C] fructose, mannitol or glycerol was studied at a cell density, OD_{600} = 0.04, in order to ensure a linear initial uptake of radiolabelled sugar by starved cells of *P. aeruginosa* strains. Aliquots (0.5 ml) were withdrawn at 0.33, 0.66, 1.0, 2.5, 5.0, 8.0, 16.0 and 24.0 mins after addition of [^{14}C] sugars. Data are representative of at least three independent assays no error bars are used.

The carbohydrate uptake results for 60 s after the addition of [^{14}C] carbohydrate for mutant D are presented in Fig. 3-35. In order to compare the rate of uptake the slope of the linear portion of the curve is calculated. The 20 s slopes were calculated by the MATLAB 6.5 computer program and values are presented in Table 3-5. From this data it is concluded that mutant D has an impaired uptake of all carbohydrates tested. Due to the low uptake in fructose the results will not be included in the discussion. In the case of transformed mutant D a slope increase of 2.0 and 0.3 compared to wildtype in mannitol and glycerol respectively, show complementation in these two cases has occurred.

When the uptake assays were run for 24 mins (Fig. 3-36) in all carbohydrates tested mutant D is taking up less than wildtype. Due to low uptake by mutant D in the case of fructose these results will not be discussed. The transformed mutant D shows no complementation for glucose. In the case of mannitol and glycerol, full complementation is observed.

Table 3-5. Slopes obtained from 0 - 20 s carbohydrate uptake data for wildtype, mutant D and transformed mutant D

Carbohydrate	*P. aeruginosa* strain	20s slope[1]
Glucose	wildtype	16.0
	mutant D	8.5
	transformed mutant D	7.7
Fructose	wildtype	5.8
	mutant D	0.4
	transformed mutant D	0.8
Mannitol	wildtype	3.4
	mutant D	1.9
	transformed mutant D	5.4
Glycerol	wildtype	11.8
	mutant D	6.6
	transformed mutant D	11.5

[1] - 20 s slope was calculated by dividing the counts per minute by 20 using MATLAB 6.5 computer program (data not shown).

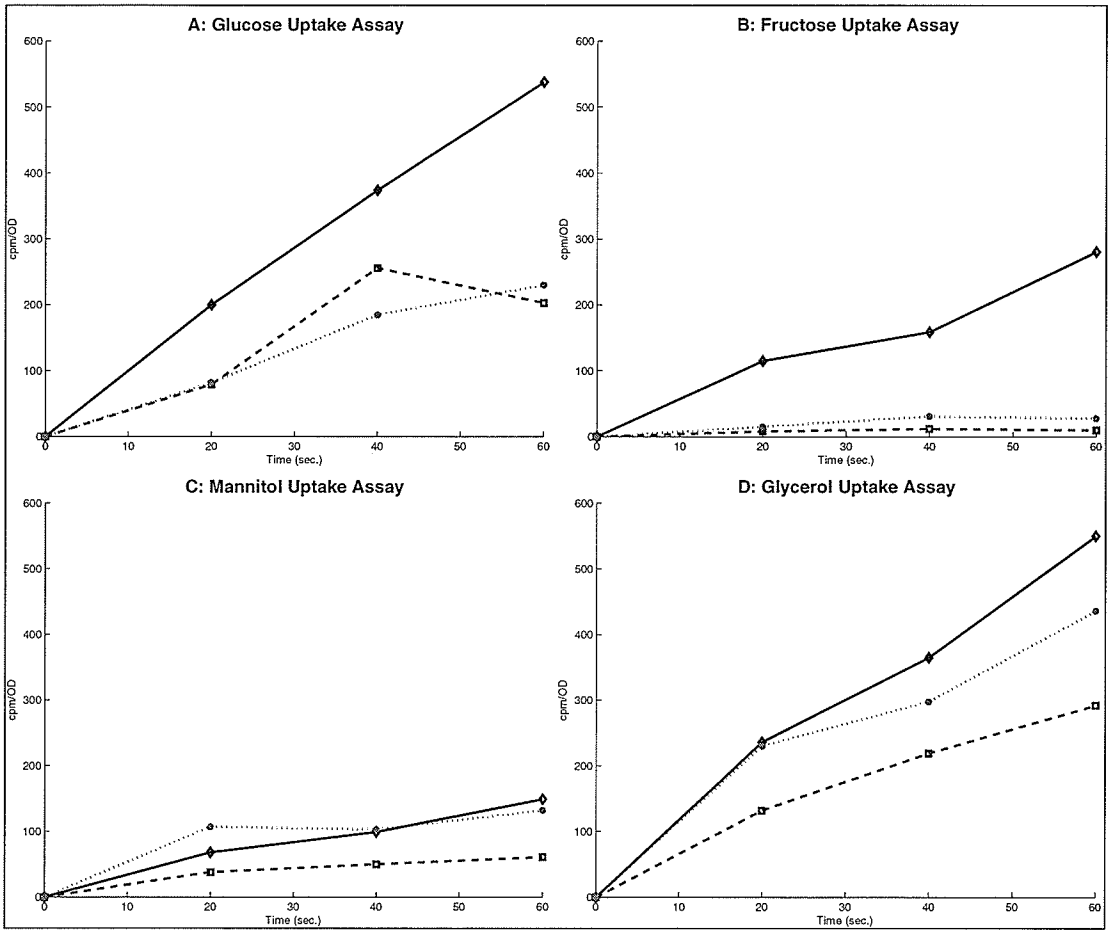

Figure 3-35. Carbohydrate uptake assays using *P. aeruginosa* wildtype, mutant D and transformed mutant D

Panel **A**: Glucose, Panel **B**: Fructose, Panel **C**: Mannitol, Panel **D**: Glycerol. *P. aeruginosa* wildtype (◇), mutant D (□), transformed mutant D (●). Uptake of 0.33 μM of [^{14}C] glucose or 2.4 μM of [^{14}C] fructose, mannitol or glycerol was studied at a cell density, OD_{600}= 0.04, in order to ensure a linear initial uptake of radiolabelled sugar by starved cells of *P. aeruginosa* strains. Aliquots (0.5 ml) were withdrawn at 20, 40 and 60 s after addition of [^{14}C] sugars. Data is representative of at least three independent assays.

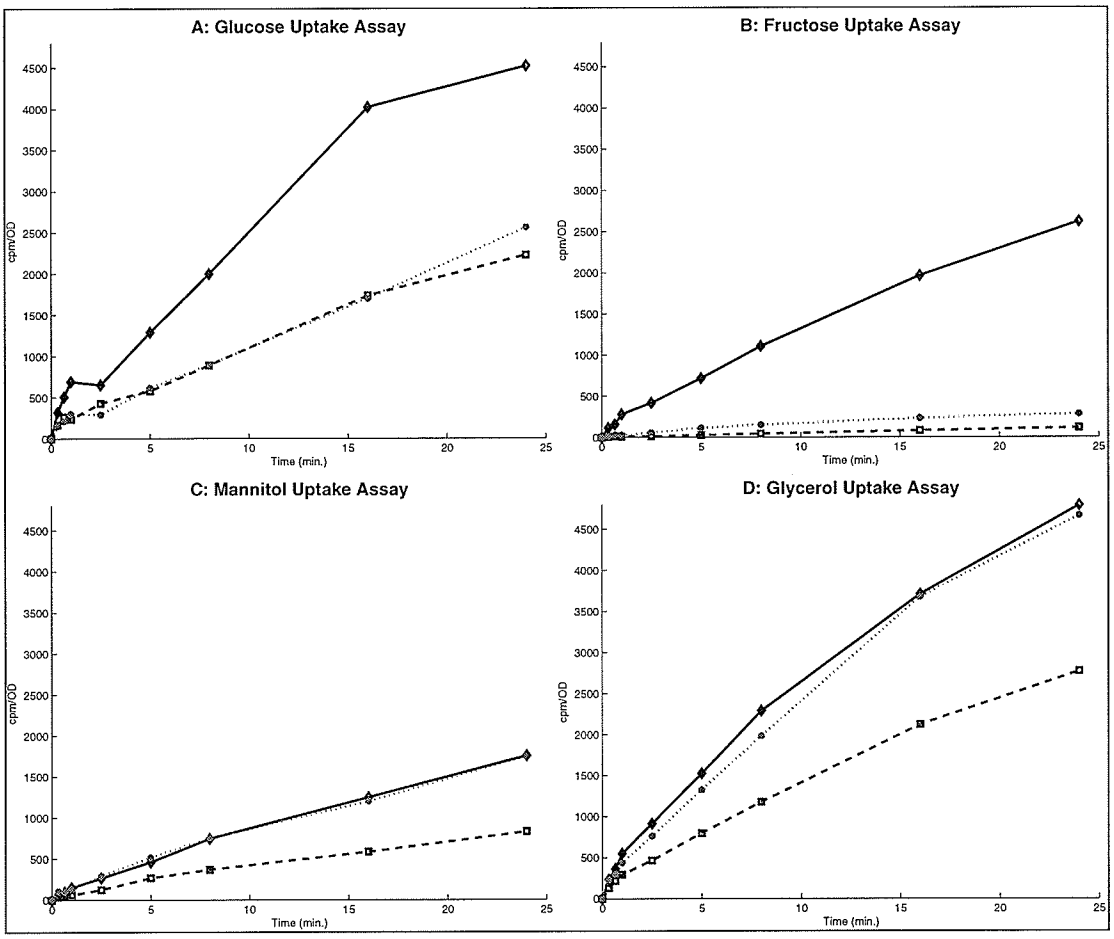

Figure 3-36. Carbohydrate uptake assays of *P. aeruginosa* wildtype, mutant D, transformed mutant D

Panel **A**, Glucose, Panel **B**, Fructose, Panel **C**, Mannitol, Panel **D**, Glycerol. *P. aeruginosa* wildtype (◊), mutant D (□), transformed mutant D (●). Uptake of 0.33 μM of [^{14}C] glucose and 2.4 μM of [^{14}C] fructose, mannitol or glycerol was studied at a cell density, OD_{600} = 0.04, in order to ensure a linear initial uptake of radiolabelled sugar by starved cells of *P. aeruginosa* strains. Aliquots (0.5 ml) were withdrawn at 0.33, 0.66, 1.0, 2.5, 5.0, 8.0, 16.0 and 24.0 mins after addition of [^{14}C] sugars. Data are representative of at least three independent assays no error bars are used.

3.9.1 Summary of uptake assay results

In the case of mutants B, C and D under all carbohydrate conditions the calculated slope for uptake was lower than wildtype. In the case of mutant B, complementation evidence was only observed when monitoring glycerol uptake. Complemented mutant C also demonstrated near wildtype levels of glycerol uptake. One could also argue the same for mannitol but with some reservations as the overall uptake levels for all 3 strains was very low. Complementation of mutant D was clearly evident for mannitol and glycerol uptake.

3.10 *OrfB* discussion

This section will look at the facts and data generated as set out in the objectives section and discuss the possible function *orfB* may play in the high affinity glucose uptake system as well as the three other uptake systems.

The pBLAST showed that the predicted OrfB protein sequence had a 94.2% alignment to *E. coli* MdoB (phosphoglycerol transferase I) protein. Mutant B had a different growth profile than wildtype (Fig. 3-30) with a significantly slower doubling time in glucose (152 min, Table 3-2) compared to wildtype (77 min). Mutant B had a significantly faster growth rate in fructose (114 min) and glycerol (112 min) compared to wildtype (204 and 227 min, respectively). The uptake data for mutant B showed a decrease in uptake in all carbohydrates compared to wildtype. One could say that in general mutant B shows an inverse relationship between growth and uptake rates. The examination of how MDO's and the specific function of MdoB particularly may fostering some understanding as to what is occurring in mutant B.

MDO's are responsible for many functions in the cell such as cell to cell signalling, chemotaxis, lysis induction by bacteriophage, regulation of polysaccharide synthesis, osmoregulation of outer membrane protein expression (Geiger *et al.*, 1991). The lack of MdoB leads to abnormal production of MDO's in the cytoplasm which could be triggering one or all of the functions mentioned above. The lack of MdoB in mutant B could cause an imbalance in the precursor UDP-glucose (Fig. 3-3). The imbalance of UDP-glucose in the cytoplasm may disrupt other pathways which use this precursor, such as lipopolysaccaride formation (Schulman and Kennedy, 1977, Bohin and Kennedy, 1996, Rajagopal *et al.*, 2003) which has implications in the cell wall formation.

If Mutant B has a non-functional MdoB protein, as predicted by the pBLAST results, this could cause a build up of UDP-glucose in the cytoplasm of the cell. UDP-glucose is the precursor of the glucose residues for MDOs and is also required for the synthesis of the core oligosaccaride region of the lipopolysaccharide involved in cell wall synthesis (Osborn, *et al.*, 1964, Schulman and Kennedy, 1977, Bohin and Kennedy, 1996). The enzyme phosphoglucoisomerase (Pgi) is involved in the EDP cycle and catalyzes the reversible process between fructose-6-phosphate and glucose-6-phosphate (Fig. 1-1). The enzyme Pgi has been implicated as an important enzyme needed for proper core oligosaccaride regions of lipopolysaccharides which are important in cell wall synthesis (Osborn, *et al.*, 1964, Schulman and Kennedy, 1977). The build up of UDP-glucose in the mutant may cause inhibition feedback regulation of Pgi and thus its activity is decreased. This decrease in Pgi in turn could cause the enzymes of the EDP system to be repressed, resulting in a decrease in glucose uptake. Down regulation of EDP, could cause the intermediate glyceraldehyde-3-phosphate, which is normally recycled through the EDP, to be used in the lower EMP

pathway which drives the production of pyruvate which is then used by the TCA cycle (Temple *et al.*, 1998). This change in pathways allows mutant B to grow more efficiently in fructose, mannitol and glycerol than wildtype, under these induced conditions plus the increase in TCA cycle intermediates in turn causes CRC (catabolic repression control). It has been shown by O'Toole (2000) that the catabolic repression control (crc) gene (PA5332) in *P. aeruginosa* is found not only to play a role in carbohydrate utilization but seems to be involved in a signal transduction pathway that can sense and respond to nutritional signals which has consequences in the bacteria growth transition from planktonic to biofilm growth. This, compounded with the role that Pgi has in the formation of lipopolysaccarides, may be responsible for the slow growth in glucose seen in this study. This has also been seen to occur with *E. coli* MdoB mutants (Jackson *et al.*, 1986). The importance of the Pgi enzyme in cell wall synthesis and the role CRC has in signal transduction and growth transition may be factors associated with the slow growth rate in mutant B under the induced glucose conditions. MdoB mutants have also been seen to have a decrease or loss of virulence as has been shown in *Salmonella typhimurium* and *Erwinia chrysanthemi* respectfully coupled with the inability of these mutants to grow in anionic detergent such as SDS (Valentine, *et al.*, 1998, Page *et al.*, 2001, Rajagopal *et al.*, 2003). These incidents support the idea that the build up of UDP-glucose in the cytoplasm may be the cause of decreased cell wall synthesis and the increase in the CRC which plays a role in signal transduction which induces growth transition from planktonic to biofilm growth to cause the decreased growth phenotype seen in mutant B.

In the case of glycerol, partial complementation may be due to the fact that glycerol is the only carbohydrate which has the option of using the EDP or the EMP pathway for

catabolism. Complementation may be occurring because of the cell using the EMP pathway. The ability to use this pathway may allow for the products needed by the plasmid to be operational. In the case of the other three carbohydrate conditions there is no complementation due to the lack of another pathway to allow for the necessary products which in turn would allow the plasmid to function.

3.11 *OrfC* discussion

This section will look at the facts and data generated as set out in the objectives section and discuss the possible function *orfC* may play in the high affinity glucose uptake system.

The pBLAST showed that predicted OrfC protein sequence had a 36.5% and 43.6% alignment to strictosidine synthase and gluconolactonase proteins, respectively. Mutant C grew at the same rate as wildtype in glucose, fructose and grew better then wildtype in mannitol and glycerol (Table 3-2). The uptake data for mutant C showed a decrease in uptake in all carbohydrates compared to wildtype. The uptake assay data showed complementation in the case of fructose, mannitol and glycerol conditions, however uptake of fructose and mannitol was too low to be considered significant at this time. In the case of mutant C relating this data to the pBLAST is not possible due to the very low homology seen in the two predicted proteins.

3.12 *OrfD* discussion

This section will look at the facts and data generated as set out in the objectives section and discuss the possible function *orfD* may play in the high affinity glucose uptake system.

The pBLAST showed that predicted OrfD protein sequence had a 95.7% alignment to *E. coli* spermidine synthase protein. The uptake assay data showed complementation in the case of mannitol and glycerol conditions. Growth curve data showed that mutant D had a similar growth profile to wildtype in the four carbohydrates. Mutant D was most hindered in growth compared to wildtype in glucose but grew better than wildtype in the other two carbohydrate conditions and significantly better than wildtype in glycerol. In general mutant D shows some discrepancy between uptake and growth doubling time. The uptake data for mutant D showed a decrease in uptake in all carbohydrates compared to wildtype. Under high affinity glucose conditions mutant D grew about the same rate as wildtype.

The discussion in this section will be focussed on the effects of *orfD* mutation on the uptake of carbohydrates and how the putative OrfD protein, spermidine synthase, could cause the effects seen in both the uptake assays and the growth curves.

In mutant D complementation occurred for only mannitol and glycerol uptake. In the case of glycerol the complementation may be explained by the fact that glycerol has the option of using the EDP or the EMP pathway for catabolism. As in the case of mutant B complementation the ability to use the EMP pathway allows for production of components to aid the replication of the orf from the plasmid. In the case of mannitol complementation a possible explanation for the ability of the transformed mutant to complement may be due to the fact that growth under induced mannitol conditions is not as demanding on mutant D and the cell is still able to make components which are needed to aid in the replication of the orf from the plasmid.

In the case of mutant D one could speculate that no spermidine synthase would be produced. The lack of this enzyme in the cell would cause no spermidine to be synthesized

coincident with a build up of putresine, which is the substrate of spermidine synthase. Fig. 3-10 shows that the ADC pathway has an alternate route if spermidine synthase is not available. Increased amounts of putresine would be available and then be catabolized to the end product succinate. In this case succinate is the preferred energy source over carbohydrates in *P. aeruginosa* (Temple *et al.*, 1998). Succinate is catabolized via the TCA cycle and the intermediates of the TCA cycle cause catabolite repression control (Tiwara and Campbell 1969, MacGregor *et al.*, 1991). The CRC is the major inhibitor of the catabolic enzymes in the EDP thus decreasing the uptake of all the carbohydrates by *P. aeruginosa.*

The growth curve results therefore may not be a reflection of the mutants growth caused by the particular carbohydrate being used but are growth rates which are a result of the increased succinate, a preferred energy source which is now available to the TCA cycle complements of mutant D.

3.13 Summary of results

The objective of this thesis was to offer alternate explanations of how each putative gene (*orfB, C, D*) is affecting high affinity carbohydrate uptake in *P. aeruginosa*. The use of insertion mutants to follow growth and carbohydrate uptake when combined allow for the following explanations.

In the case of *orfC* no further interpretation can be provided other than the results of the growth curves and uptake data since the pBLAST did not provide protein matches with high enough homology to comfortably identify *orfC*.

The *orfD* mutation could cause an increase in the preferred energy source product, succinate, which due to the mutations are available to be used by the TCA cycle. The use of the TCA cycle causes the mutant to grow the same or better than wildtype under the same induced carbohydrate conditions even though the high affinity uptake system is suppressed by CRC. The use of the TCA cycle up regulates the CRC which in turn down regulates the enzymes used in the EDP and thus causes the reduced high affinity uptake of carbohydrates seen in the uptake experiments.

In the case of *orfB* the lack of the putative protein MdoB causes an increase of UDP-glucose in the cytoplasm of the cell which in turn may lead to the inhibition of the enzyme Pgi which is involved in the EDP of the carbohydrate catabolism for all the carbohydrates tested. It is possible that the decrease in this enzyme also causes a problem in the use of UDP-glucose in cell wall synthesis which in turn may be linked to MdoB mutants that have a decrease or loss of virulence as well as susceptibility to anionic detergent (SDS) (Rajagopal *et al.*, 2003, Page *et al.*, 2001, Valentine *et al.*, 1998). The growth curve results reflect a possible lack of Pgi forcing the glyceraldehyde 3-phosphate to be no longer cycled by the EDP but to be used by the EMP pathway for growth of the mutant in this case. The use of the EDP pathway produces pyruvate which is used by the TCA cycle. The TCA cycle in turn produces CRC which is used to further suppress the EDP. Through the use of the TCA cycle the mutant is able to grow at a better rate than wildtype in all carbohydrates tested except for glucose. In the case of glucose growth curves the CRC may be involved in down regulating the EDP, as well as a possible role in the signal transduction pathway (O'Toole *et al.*, 2000) which senses and responds to the nutritional signals in the case of glucose (very low external glucose concentrations and high cytoplasmic UDP-glucose) and

responds by lowering the cells growth in glucose. This CRC signal transduction pathway may not be involved in the cases of mannitol, fructose and glycerol which is why we see the increase in growth over wildtype under these conditions. This is only speculation as only recently has CRC been implicated in signal transduction in *P. aeruginosa*, besides its known effect as a carbohydrate regulator. The increase in UDP-glucose causes the down regulation of Pgi, forcing the use of EMP pathway to produce pyruvate which is used by the TCA cycle that in turn produces CRC.

The introduction of a polar mutation by the insertion deletion is possible in the case of mutant D as the insertion is in the opposite orientation to the direction of gene transcription. This difference results in the *Pseudomonas*-specific promoter to be non-operational for the downstream *orfs C* and *B*. In this case the results seen with mutant D are possibly representing a deletion in all three *orfs* (*D, C* and *B)*. If this is the case then it would be expected that the results in the uptake assay would mimic those seen by Adewoye (1999) shown in Fig. 1-4. However, the only similarity is found in the case of glucose uptake where wildtype is uptaking better than mutant. Mannitol and glycerol uptake results are opposite to those seen by Adewoye thereby showing evidence that *orfB*, *C* and *D* are not functioning as an operon, since each orf has its own start codon.

The results, specifically those seen in the case of mutant B, indicates that *orfB* may be a gene to target using an inhibitor which could cause a decreased growth rate possibly making antibiotics more effective at eliminating *P. aeruginosa* in nosocomial situations.

Finally in the cases of Mutant D and B the end results of these mutations do not directly impact the carbohydrate transport system but may still play a role in leading to better control of *P. aeruginosa* in nosocomial situations.

Chapter 4

Future Studies

4.1 Future Studies

I feel there is enough data and background to support individual projects for each *orf.*

Each of the individual insertion mutants *orfB* (PA1689), *orfC* (PA1688) and *orfD* (PA1687) could be complemented using the new complementation system by Choi and Schweizer (2003) to see if a single gene copy complementation will give carbohydrate uptake assay results similar to wildtype, versus the system used in this thesis which makes 8-10 copies of the gene in the cell. Each insertion mutant could have the insertion removed by using *cre* recombinase. This will leave the Hah in-frame portion in the gene. The use of antibody detection and/or metal affinity purification to harvest large amounts of protein for purification of each orf protein. Each of the proteins could then be further characterized.

In the case of *orfB* (PA1689) the project can include a literature search on UDP-glucose involvement in MDOs, lipopolysaccaride production, the association of MdoB and loss of virulence. The development of an assay to determine if the putative OrfB protein is MdoB is warranted.

In the case of *orfC* (PA1688) the project can also include an alternative method of protein expression, by recloning *orfC* into pUCP21 so it can be overexpressed in the *E. coli*

system. A verification of this protein can be done by obtaining the antibody to strictosidine synthase.

In the case of *orfD* (PA1687) the project can also include testing mutant D by the addition of exogenous spermidine and see if the complementation phenotype can be detected.

Appendix A

Cross Reference

This appendix cross references the components from all the pathways of carbohydrate uptake and metabolism in *P. aeruginosa* to the appropriate PA number from the PseudoCAP genome website. It also gives the gene position, beginning and end, and a short description of the gene (Stover *et al.*, 2000). Fig. A-1 is a code diagram which assigns a color to each specific carbohydrate uptake system, each catabolic system and regulatory genes. The color coding of these systems makes it easier to see the clustering of the genes involved in the aforementioned systems.

Gene Name	***PA#***	**position # beginning**	**position # end**	**Description**
Pgk	PA0552	611281	612444	phosphoglycerate kinase carbon compound catabolism
Fba	PA0555	613338	614402	fructose-1,6-bisphosphate aldolase, carbon compound catabolism, central intermediary metabolism
OprD	PA0958	1045314	1043983	Basic amino acid, basic peptide and imipenem outer membrane porin OprD
Pyc-B	PA1400	1521109	1524396	probable pyruvate carboxylase, energy metabolism
Pyk-I	PA1498	1627495	1626062	pyruvate kinase I, carbon compound catabolism
Gad	PA2265	2493937	2495712	gluconate dehydrogenase, carbon compound catabolism
Kgk	PA2261	2489725	2490675	2-ketogluconate kinase, carbon compound catabolism
Gcd	PA2290	2521104	2518693	glucose dehydrogenase, carbon compound catabolism

Gene Name	*PA#*	position # beginning	position # end	Description
$OprB_2$	PA2291	2522616	2521258	probable glucose-sensitive porin, transport of small molecules
GnuK	PA2321	2560144	2560665	gluconokinase, carbon compound catabolism, energy metabolism
GnuT	PA2322	2560762	2562114	gluconate permease, transport of small molecules
Mdh	PA2342	2586434	2587909	mannitol dehydrogenase, carbon compound catabolism
Frk	PA2344	2589455	2590387	fructokinase, carbon compound catabolism
Eda	PA3131	3513041	3512394	2-keto-3-deoxy-6-phosphogluconate aldolase, carbon compound catabolism, central intermediary metabolism
Zwf	PA3183	3573793	3572324	glucose-6-phosphate 1-dehydrogenase, carbon compound catabolism
HexR	PA3184	3573980	3574837	Transcriptional regulator, carbon compound catabolism
OprB	PA3186	3577276	3575912	Glucose/carbohydrate outer membrane porin,transport of small molecules
GltK	PA3187	3578480	3577320	probable ATP-binding component of ABC transporter, transport of small molecules
GltG	PA3188	3579358	3578513	probable permease of ABC sugar transporter, transport of small molecules
GltF	PA3189	3580283	3579351	probable permease of ABC sugar transporter,transport of small molecules
Gbp (GltB)	PA3190	3581646	3580384	binding protein component of ABC transporter
Sensor	PA3191	3583592	3583616	probable two-component sensor
GltR	PA3192	3584344	3583616	Two-component response regulator
Glk	PA3193	3585374	3584379	glucokinase, carbon compound catabolism
Edd	PA3194	3587303	3585477	phosphogluconate dehydratase, carbon compound catabolism
Gap	PA3195	3587433	3588437	glyceraldehyde 3-phosphate dehydrogenase, carbon compound catabolism
EnzII	PA3560	3990595	3988838	phosphotransferase system, fructose-specific IIBC component, carbon compound catabolism, transport of small molecules

Gene Name	*PA#*	position # beginning	position # end	Description
EnzI	PA3562	3994411	3991541	phosphotransferase system enzyme I, central intermediary metabolism, transport of small molecules
FruR	PA3563	3994739	3995728	fructose transport system repressor
GlpF	PA3581	4012806	4013645	glycerol uptake facilitator protein, transport of small molecules
GlpK	PA3582	4013685	4015202	glycerol kinase, central intermediary metabolism
GlpR	PA3583	4015408	4016163	Transcriptional regulator, glycerol-3-phosphate regulon repressor
GlpD	PA3584	4016441	4017979	glycerol-3-phosphate dehydrogenase, central intermediary metabolism, energy metabolism
Eno	PA3635	4069966	4068677	Enolase, energy metabolism;translation, post-translational modification, degradation;carbon compound catabolism
Pyc-A	PA3687	4130392	4127756	pyruvate carboxylase, central intermediary metabolism, energy metabolism
Pyk-II	PA4329	4856960	4858411	pyruvate kinase II, carbon compound catabolism
Pgi	PA4732	5313676	5315340	glucose-6-phosphate isomerase, carbon compound catabolism, energy metabolism
Tpi	PA4748	5333501	5332746	triosephosphate isomerase, central intermediary metabolism
Fbp	PA5110	5753474	5752464	fructose-1,6-bisphosphatase, carbon compound catabolism, central intermediary metabolism
Pgm	PA5131	5778134	5779681	phosphoglycerate mutase, carbon compound catabolism
CRC	PA5332	6002121	6002900	Regulatory gene for carbon compound catabolism, energy metabolism
Kgr				2-keto-6-phosphogluconate reductase
Fpk				fructose 1-phosphate kinase
Mbp				mannitol binding protein

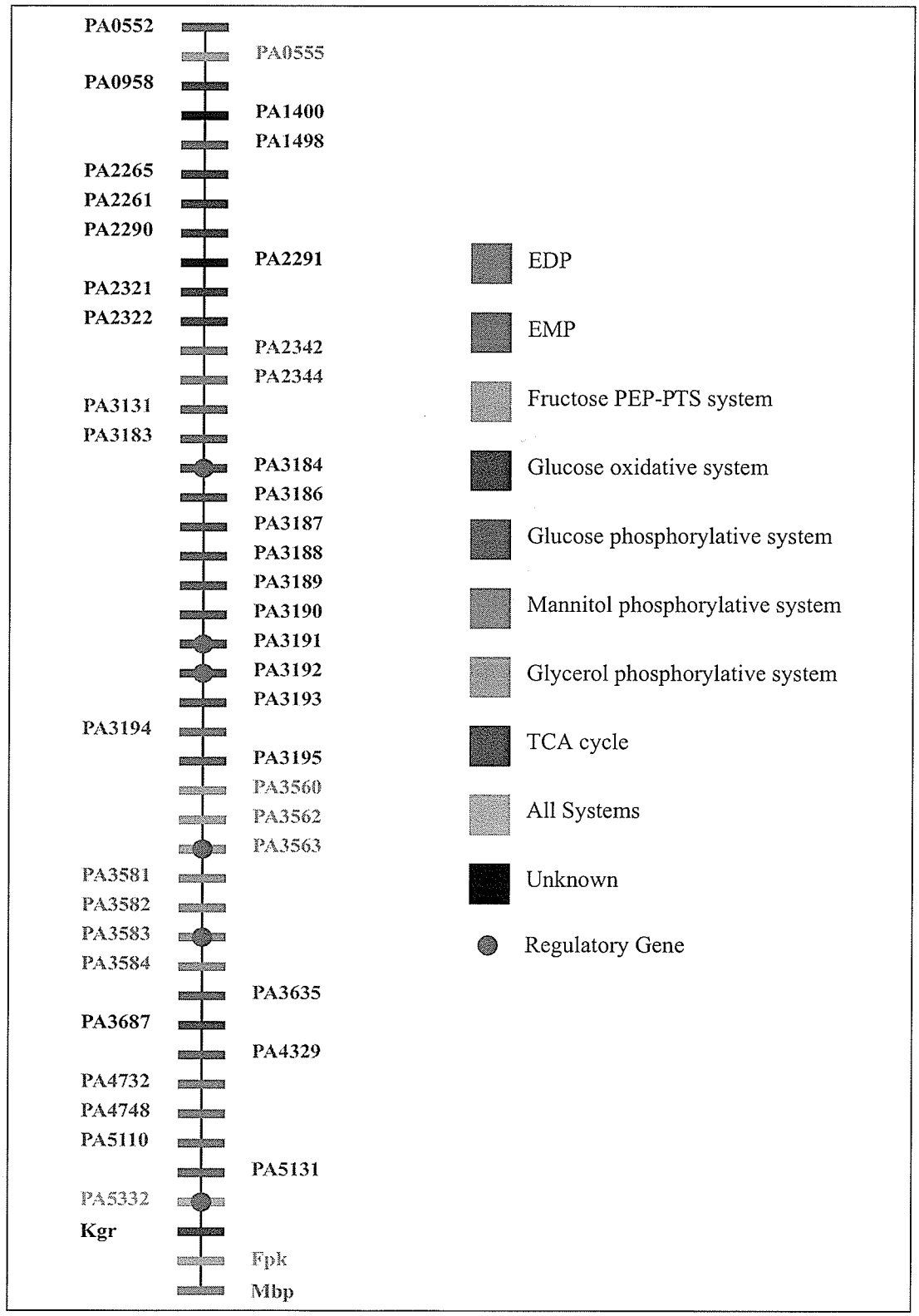

Figure A-1. Cross reference code diagram

Appendix B

pBL100, pBON and Suicide Vector Systems

B.1 Shuttle Vector pBL100

Vector pBL100 (Adewoye, 1999), constructed from plasmid pTZ18U (Mead *et al.*, 1986), houses *orf's B,C* and *D* (5.3 kb *Bgl*II genomic fragment from pE6 cosmid clone), as shown in Fig. B-1. pTZ18U (NCBI[1], Mead *et al.*, 1986) is a cloning vector derived from pUCP18/19. It contains a polylinker within α region of *lac*Z gene, blue/white screening of recombinants, high copy number and ampicillin (Ap) resistance.

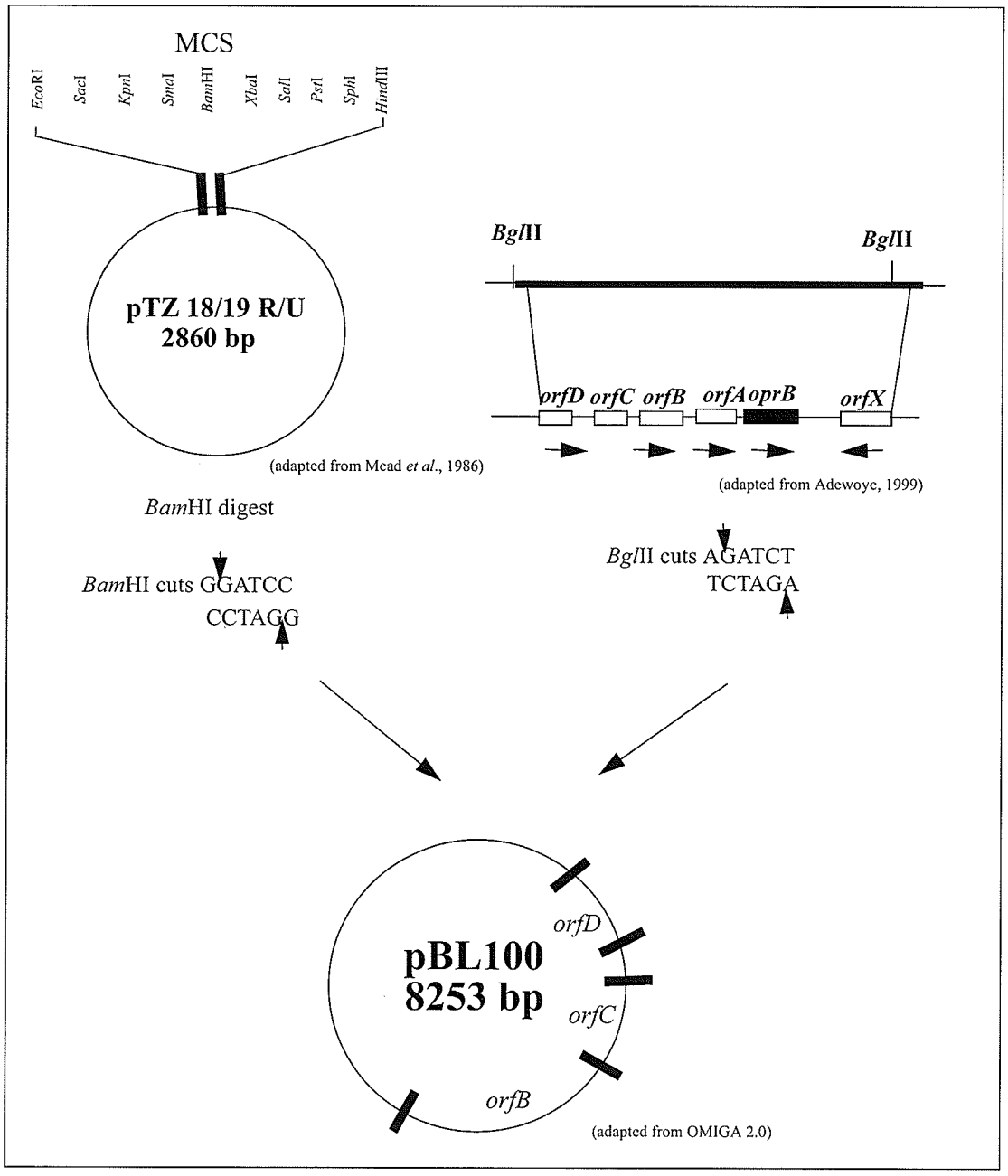

Figure B-1. The construction of pBL100

This figure was adapted from Adewoye, 1999.

B.2 pBON

The pBON vector was initially designed with the intent to remove the partial *orfD* and *orfB* regions. This segment would be inserted into pEX18Tc and pKNG100, both suicide vectors, to be used to create *P. aeruginosa* knock-out mutant (*orfB, C* and *D* removed). These tools were not used due to difficulties with the suicide vector system. Transposon insertion mutants became available from Washington State Genome Centre (Section 2.6) and were thus used instead.

The vector pBON was constructed using *Stu*I digestion of the vector pBL100 (Adewoye, 1999). *Stu*I makes four cuts into pBL100 (Fig B-2), the largest section (5831 bp) is self-ligated to produce pBON (Fig. B-3). In Fig. B-2 you see that restriction digest results in a section of *orfD* (520 bp) gene (beginning of gene) and a section of *orfB* (1053 bp end of the gene) remaining on the largest section.

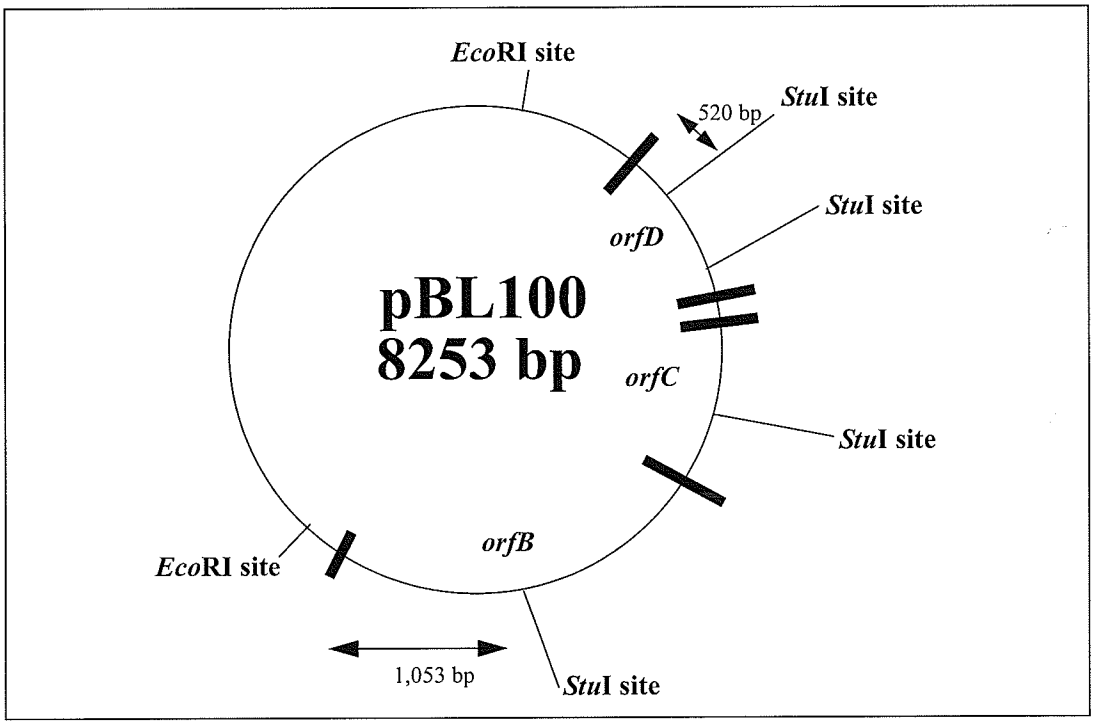

Figure B-2. Vector pBL100 with *Stu*I and *Eco*RI sites illustrated

The thick lines represent the beginning and ends of the three *orfs B*,*C* and *D* all transcribed in the clockwise direction (Adapted from OMIGA 2.0 software of Oxford Moleculars).

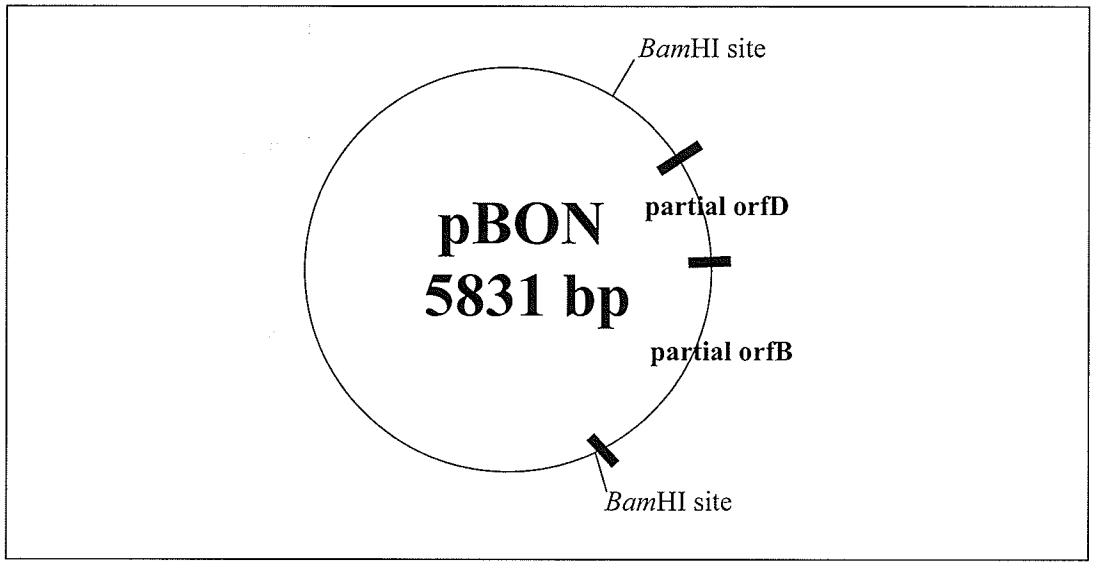

Figure B-3. pBON vector

The thick lines represent beginning and end of the partial *orfD* and *orfB*. The thin lines represent *Bam*HI restriction sites on the pBON vector (Adapted from OMIGA 2.0 software of Oxford Moleculars).

pBON was designed to be further digested using *Bam*HI restriction enzyme to remove an approximate 1.6 kb fragment. This 1.6 kb fragment would have the partial sequence of *orfD* and partial sequence of *orfB* which were inserted into cloning vectors pEX18Tc and pKNG101. These new suicide vectors are called pAK18Tc and pKK101, respectively. These two suicide vectors were to be used to make a deletion mutant (*orfB,C,D*) in *P. aeruginosa* wildtype. pBON was constructed by Bonnie Solylo, 2003.

Fig. B-4 shows pBON confirmation via restriction digest using *Pst*I, *Eco*RI (Table B-1) and PCR using the $D_{1(\text{forward primer})}$ and $B_{2(\text{reverse primer})}$ (Table 2-3) at annealing temperature 54°C to produce a 2.0 kb product.

Table B-1. Restriction enzymes and expected fragment sizes

Plasmid	Restriction Enzyme	Fragment Sizes
pBL100	*Eco*RI	4.4 kb, 3.8 kb
pBL100	*Pst*I	4.3 kb, 3.0 kb, 934 bp
pBON	*Eco*RI	3.3 kb, 2.5 kb
pBON	*Pst*I	5.8 kb

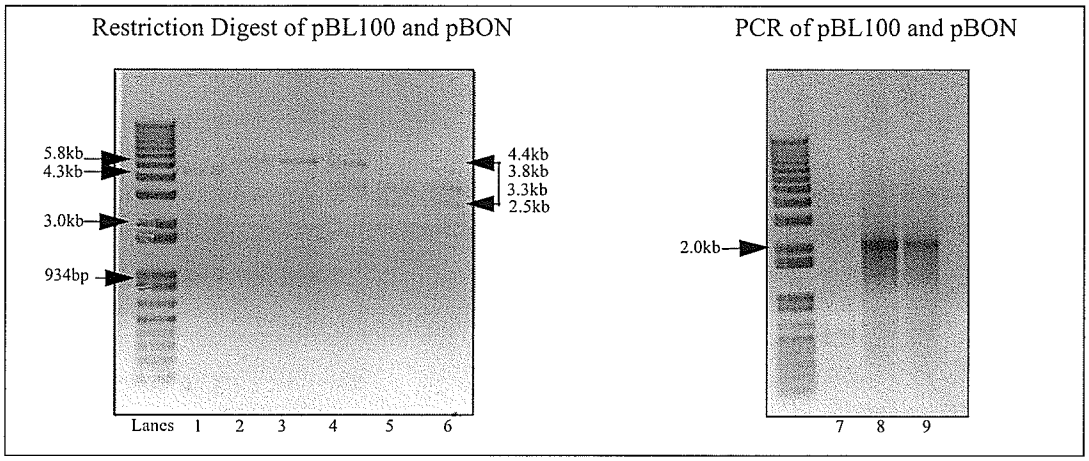

Figure B-4. Agarose gel electrophoresis of pBON, pBL100 restriction digests and PCR Lane 1 - pBL100 cut with *Pst*I, Lane 2 and 3 - pBON cut with *Pst*I, Lane 4 - pBL100 cut with *Eco*RI, Lane 5 and 6 - pBON cut with *Eco*RI, Lane 7 - pBL100 PCR, Lane 8 and 9 - pBON PCR. The sizes in restriction digest gel correspond to the following digest products: 4.3kb, 3.0kb and 935bp - pBL100 cut with *Pst*I, 5.8kb - pBON cut via *Pst*I, 4.4kb and 3.8kb - pBL100 cut via *Eco*RI, 3.3 kb and 2.5kb - pBON cut via EcoRI. The PCR gel 2.0kb corresponds to the pBON PCR product generated by D_1 and B_2 primers (Table 2-3).

B.3 Suicide vectors pEX18Tc and pKNG100

The suicide vector pEX18Tc and pKNG100 are gene replacement vectors for *P. aeruginosa* (Kaniga *et al.*, 1991, Hoang *et al.*, 1998). These vectors (Fig. B-5) incorporate the counterselectable *sacB* marker, a *lacZ*α-allele for blue/white screening, the MCS (10 unique restriction sites) of pUCP18/19, an *oriT* for conjugation-mediated plasmid transfer and carbenicillin (Cm^r), gentamicin (Gm^r), streptomycin (Sm^r) and tetracycline (Tc^r) selectable markers. (Schweizer *et al.*, 1992). *sacB* is from the bacterium *Bacillus subtilis* and is used as a counter-selectable marker which allows for positive selection of the segregation of true mutants from the more frequently occurring merodiploids. *sacB* encodes levansucrase, which confers toxicity to cells grown in sucrose, 5% (w/v).

The systems work as such, the suicide vector cannot replicate as a plasmid normally does to give the cell antibiotic resistance, thus for the cell to survive (on carbenicillin supplemented plates) the whole vector must integrate into the *P. aeruginosa* genome. Since the vector contains a 2.0 kb *Bam*HI restriction fragment insertion from pBON (which has homology to the *P. aeruginosa* genome at *orfD* and *orfB*) this increases the likelihood that integration will take place at these points of homology. The colonies which have grown on the antibiotic plate will have the insertion of the vector at either the point of homology in the *P. aeruginosa* genome or an alternate site in the genome. Since the whole vector is not wanted in the genome the *sacB* gene is used to drive excision of the plasmid from the genome. In 50% of the cases the whole vector is excised, in the remaining cases the excision of the plasmid will occur leaving in the disrupted gene insertion (e.g. 1.6 kb fragment from pBON) in the *P. aeruginosa* genome. The next step is to screen the colonies by growing on sucrose. The cells still harboring *sacB* will die (hence the name, suicide

vector). The cells that are able to grow on sucrose signify that the *sacB* gene has been excised. From these colonies screening is done by PCR using primers which verify the presence of the 1.6 kb pBON segment, it is also possible to use the PCR primers for each of the orfs to ensure none of the orfs are present in the mutant.

For this project there were problems with the sucrose excision step whereby mutants were able to grow on sucrose but *sacB* gene appeared to be present (assayed via PCR using *sacB* gene primers). At this point this line of investigation was ceased.

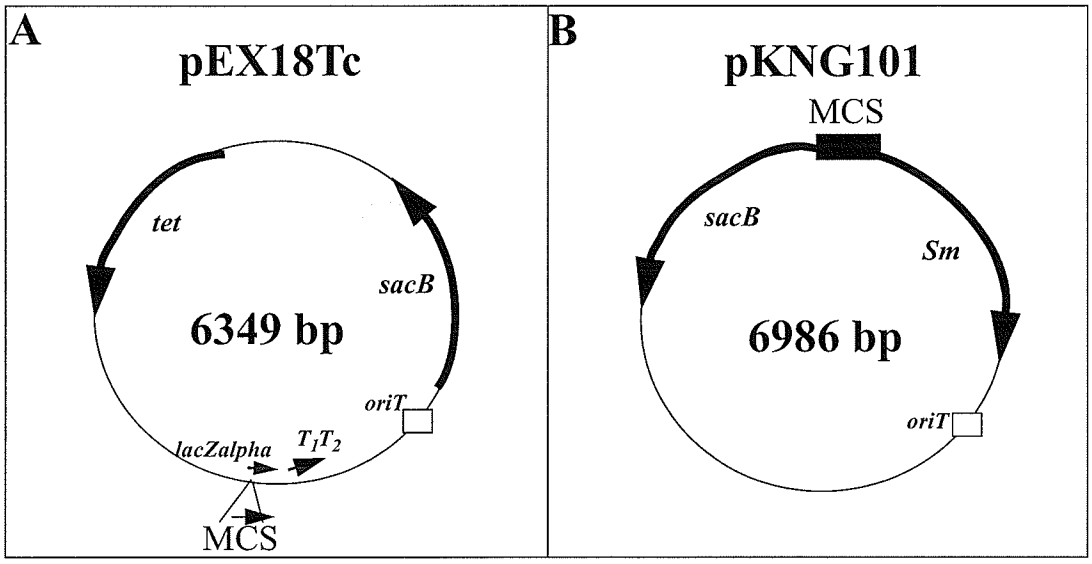

Figure B-5. Suicide vectors pEX18Tc and pKNG100

A - pEX18Tc vector, *tet* - tetracycline resistance marker, , *lacZalpha* - lacZalpha allele, T_1T_2 - double transcriptional terminators (Adapted from Hoang *et al.*, 1998). **B** - pKNG101 vector, *Sm* - streptomycin resistance marker. Common to both vectors, *sacB* - sacB gene, MCS - multi-cloning site, *oriT* - origin of transfer, arrows indicated transcriptional orientation (Adapted from Kaniga *et al.*, 1991).

Appendix C

Cloning of *orfC* and *orfD* into pUCP20

Each open reading frame (*orfC* and *D*) was inserted into the pUCP20 cloning vector and each was theoretically capable of expressing proteins within *E. coli* or *P. aeruginosa*. The partial sequence (lead strand only) of pUCP20/*orfC* gene plus sequencing data are found in Figs. 3-24 to 3-26. The partial sequence (lead strand only) of pUCP20/*orfD* gene plus sequencing data are found in Figs. 3-27 to 3-29. The pUCP20/*orfC* and pUCP20/*orfD* constructs were developed by Dr. R. Habibian (2002).

C.1 Cloning of *orfC* into pUCP20

OrfC was obtained by PCR using pBL100 as template DNA using the following primers: Forward - TACTACAACGCCGGGATCC with *Bam*HI site underlined and Reverse - GGTGGTTCGGAATTC with *Eco*RI site underlined. The PCR product was then digested using the restriction enzymes *Bam*HI and *Eco*RI . Fig. C-1 shows the ends after restriction digest of *orfC* PCR insertion sequence. The *orfC* was inserted backwards in the MCS of pUCP20 (so the end of the gene was in line with the MCS transcription start site). The consequence of this is that in *E. coli* the gene would not be expressed but in *P. aeruginosa* it would be expressed as the insertion has a putative RBS seen in Fig. 3-24.

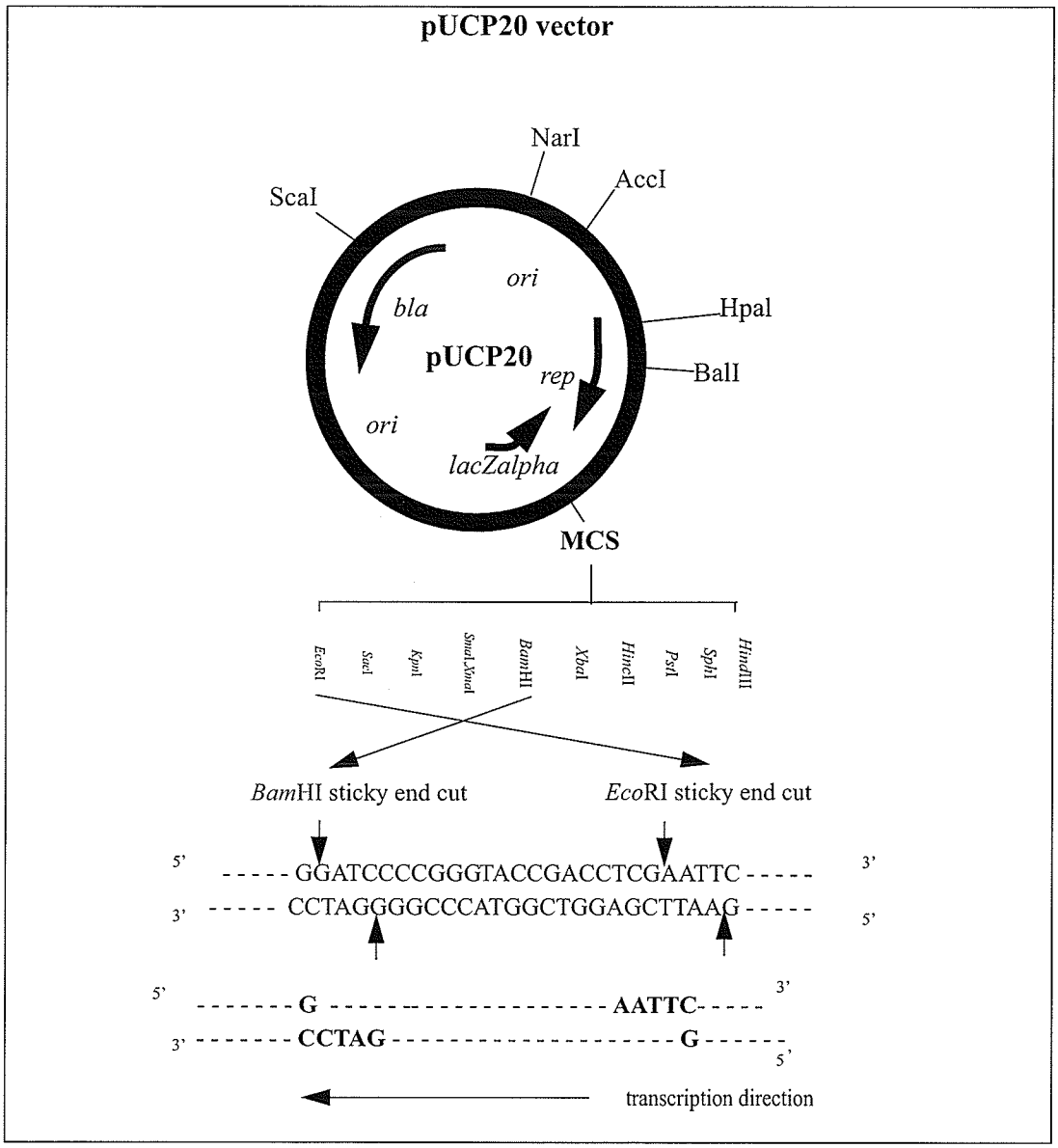

Figure C-1. pUCP20 vector with MCS restriction digest

The restriction enzyme *Eco*RI cuts between GA at consensus sequence GAATTC leaving a 3' overhang on one end of the vector. The restriction enzyme *Bam*HI cuts between GG at consensus sequence GGATCC leaving a 3' overhang on the other end of the vector [Adapted from West, *et al.*, 1994 and OMIGA 2.0 (Oxford Moleculars) computer program].

For the *orfC* gene to insert correctly the lead 5' *Bam*HI sticky end cut must attach to the 5'*Bam*HI cut of pUCP20.

C.2 Cloning of *orfD* into pUCP20

OrfD was obtained by PCR using pBL100 as template DNA with the following primers: Forward - TGGTGGAATTCGCGCCATT with *Eco*RI site underlined and Reverse - CAGGCAGGATCCTACTACG with *Bam*HI site underlined. The PCR product was then digested using the restriction enzymes *Eco*RI and *Bam*HI. Fig. C-2 shows pUCP20 vector with the restriction digest sites in relation to the MCS and the transcription direction of the plasmid.

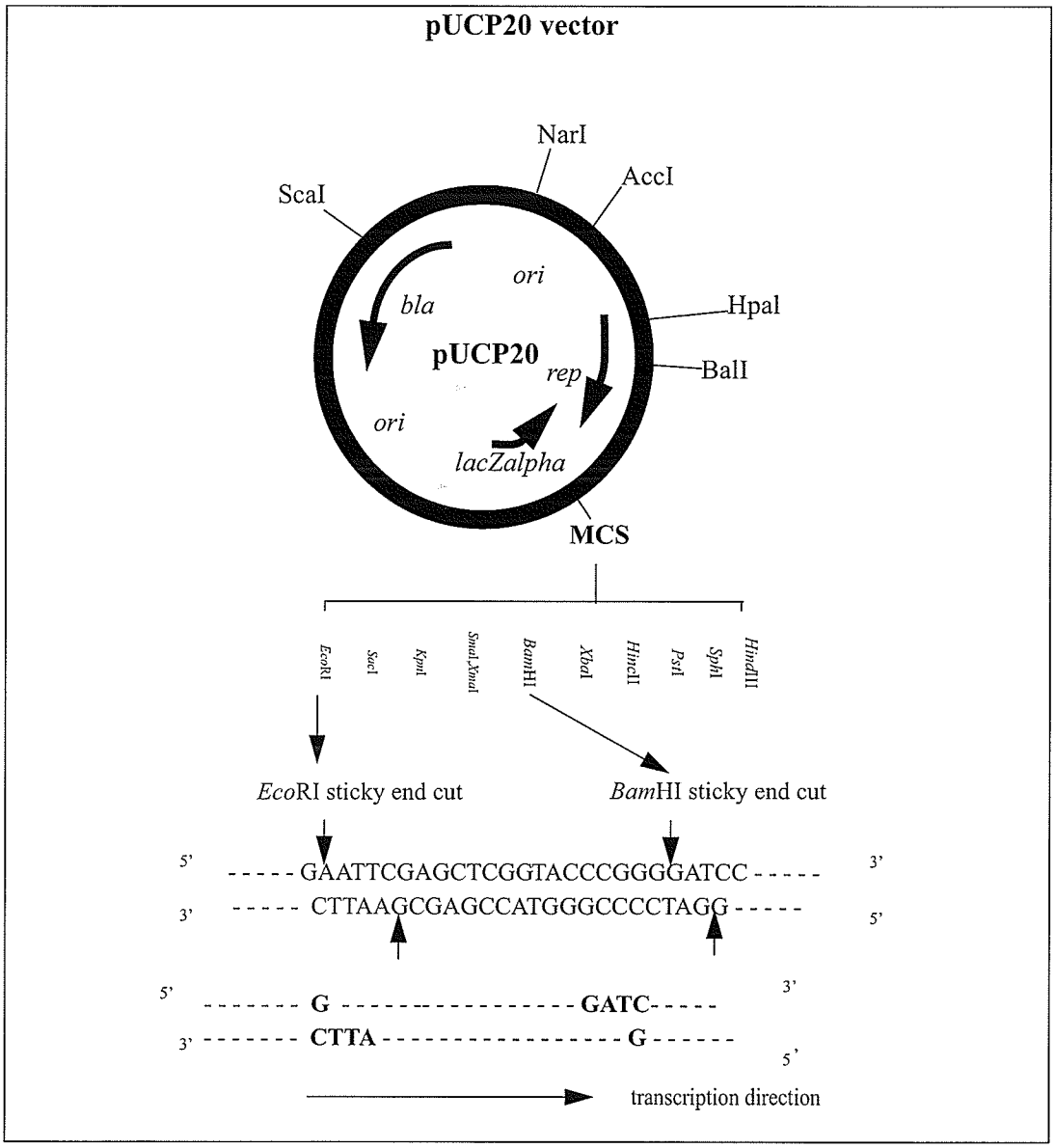

Figure C-2. pUCP20 vector with MCS restriction digest

The restriction enzyme *Eco*RI cuts between GA in the consensus sequence GAATTC leaving a 3' overhang of the vector. The restriction enzyme *Bam*HI cuts between GG in the consensus sequence GGATCC leaving a 3' overhang on the vector [Adapted from West *et al.*, 1994 and OMIGA 2.0 (Oxford Moleculars) computer program].

For the *orfD* gene to insert in the correct orientation the lead 5' *Eco*RI sticky end must attach to the 5' *Eco*RI cut of pUCP20. This attachment ensures the correct orientation for the inserted gene, in pUCP20, required for transcription.

Bibliography

Adewoye, L. O. and Worobec, E. A. 1999. Multiple environmental factors regulate the expression of the carbohydrate-selective OprB porin of *Pseudomonas aeruginosa*. Can. J. Microbiol. **45**:1033-1042.

Adewoye, L. O. 1999. Characterization of the glucose ABC transporter of *Pseudomonas aeruginosa*. Ph.D. Thesis, University of Manitoba, Winnipeg, Manitoba, Canada.

Adewoye, L. O., Campbell, J., Worobec, E. A. 1999. Identification of a *trans*-regulatory locus involved in the regulation of carbohydrate transport in *Pseudomonas aeruginosa*. Abstract #12. Pseudomonas 1999 International Meeting, Maui, Hawaii, U. S. A.

Altschul, S. F., Madden, T. L., Schaffer, A. A., Zhang, J., Zheng, Z., Miller, W., Lipmann, D. J. 1997. Gapped BLAST and PSI-BLAST: A new generation of protein database search programs. Nucleic Acids Res. **25**:3389-3402.

Ausubel, F. M., Brent, R., Kingston, R. E., Moore, D. D., Seidman, J. G., Smith, J. A., Struhl, K. (eds). 1989. Current Protocals in Molecular Biology. New York: John Wiley and Sons.

Baumann, P. and Baumann, L. 1975. Catabolism of D-fructose and D-ribose by *Pseudomonas doudoroffii*. Arch. Microbiol. **105**:225-240.

Blevins, W. T., Feary, T. W., Phibbs, P. V., Jr. 1975. 6-phosphogluconate dehydratase deficiency in pleiotropic carbohydrate-negative mutant strains of *Pseudomonas aeruginosa*. J. Bacteriol. **121**:942-949.

Bohin, J-P. and Kennedy, E. P. 1984. Regulation of the synthesis of membrane-derived oligosaccharides in *Escherichia coli*. J. Biol. Chem. **259**:8388-8393.

Brock, T. D., Madigan, M. T., Martinko, J. M., Parker, J. 1984. Biology of Microorganisms 7th ed. Prentice Hall, U.S.A. Pages: 411, 412, 418, 481, 483, 490, 518, 519, 775, 777.

Choi, K. H. and Schweizer, H. P. 2003. A versatile broad-host-range bacterial gene integration system. Abstract #72. Pseudomonas 2003 International Meeting, Quebec City, Quebec, Canada.

Cuskey, S. M., Wolff, J. A., Phibbs, P. V., Jr., Olsen, R. H. 1985a. Cloning of genes specifying carbohydrate catabolism in *Pseudomonas aeruginosa* and *Pseudomonas putida*. J. Bacteriol. **162:**865-871.

Cuskey, S. M. and Phibbs, P. V., Jr. 1985b. Chromosomal mapping of mutations affecting glycerol and glucose catabolism in *Pseudomonas aeruginosa* PAO. J. Bacteriol. **162:**872-880.

Davis, C. L. and Robb, F. T. 1985. Maintenance of different mannitol uptake systems during starvation in oxidative and fermentative marine bacteria. Applied Environ. Microbiol. **50:**743-748.

Debarbieux, L., Bohin, A., Bohin, J. P. 1997. Topological analysis of the membrane-bound glucosyltransferase, MdoH, required for osmoregulated periplasmic glucan synthesis in *Escherichia coli*. J. Bacteriol. **179:**6692-6698.

Delcour, A. H., Adler, J., Kung, C., Martinac, B. 1992. Membrane-derived oligosaccharides (MDO's) promote closing of an *Escherichia coli* porin channel. FEBS Letters. **304:**216-220.

Durham, D. R. and Phibbs, P. V., Jr. 1982. Fractionation and characterization of the phosphoenolpyruvate:fructose 1-phosphortransferase system from *Pseudomonas aeruginosa*. J. Bacteriol. **149:**534-541.

Eagon, R. G. and Williams, A. K. 1960. Enzymatic patterns of adaptation to fructose, glucose and mannose exhibited by *Pseudomonas aeruginosa*. J. Bacteriol. **79:**90-94.

Eagon, R. G. and Phibbs, P. V., Jr. 1971. Kinetics of transport of glucose, fructose, and mannitol by *Pseudomonas aeruginosa*. Can. J. Biochem. **49:**1031-1041.

Eisenberg, R. C. and Phibbs, P. V., Jr. 1982. Characterization of an inducible mannitol-binding protein from *Pseudomonas aeruginosa*. Curr. Microbiol. **7:**229-234.

Fiedler, W. and Rotering, H. 1985. Characterization of *Escherchia coli* MdoB mutant strain unable to transfer sn-1-phosphoglycerol to membrane-derived oligosaccharides. J. Biol. Chem. **260:**4799-4806.

Geiger, O., Russo, F. D., Silhavy, T. J., Kennedy, E. P. 1992. Membrane-derived oligosaccharides affect porin osmoregulation only in media of low ionic strength. J. Bacteriol. **174:**1410-1413.

Guyman, L. F. and Eagon, R. G. 1974. Transport of glucose, gluconate, and methyl α-D-glucoside by *Pseudomonas aeruginosa.* J. Bacteriol. **117:**1261-1269.

Hampp, N. and Zenk, M. H. 1988. Homogeneous strictosidine synthase from cell suspension cultures of *Rauvolfia serpentina*. Phytochem. **27:**3811-3815.

Hancock, R. E. W. and Carey, A. M. 1979. Outer membrane of *Pseudomonas aeruginosa*: heat-and 2-mercaptoethanol-modifiable proteins. J. Bacteriol. **140:**902-910.

Hancock, R. E. W. and Carey, A. M. 1980. Protein D1-a glucose-inducible, pore-forming protein from the outer membrane of *Pseudomonas aeruginosa*. FEMS Microbiol. Letters **8:**105-109.

Hemscheidt, T. and Zenk, M. H. 1980. Glucosidases involved in indole alkaloid biosynthesis of *Catharanthus* cell cultures. FEBS Letters. **110:**187-191.

Higgins, C. F., Hyde, S. C., Mimmack, M. M., Gileadi, U., Gill, D. R., Gallagher, M. P. 1990. Binding protein-dependent transport systems. J. Bioenerg. Biomemb. **22:**571-592.

Huang, H. and Hancock, R. E. W. 1993. Genetic definition of the substrate selectivity of outer membrane porin protein OprD of *Pseudomonas aeruginosa*. J. Bacteriol. **175:**7793-7800.

Hunt, J. C. and Phibbs, P. V., Jr. 1983. Regulation of alternate peripheral pathways of glucose catabolism during aerobic and anaerobic growth of *Pseudomonas aeruginosa*. J. Bacteriol. **154:**793-802.

Hoang, T. T., Karkhoff-Schweizer, R. R., Kutchma, A. J., Schweizer, H. P. 1998. A broad-host- range Flp-*FRT* recombination system for site-specific excision of chromosomally-located DNA sequences: application for isolation of unmarked *Pseudomonas aeruginosa* mutants. Gene **212:**77-86.

Hylemon, P. B. and Phibbs, P. V., Jr. 1972. Independent regulation of hexose catabolizing enzymes and glucose transport activity in *Pseudomonas aeruginosa*. Biochem Biophy. Res. Comm. **48:**1041-1048.

Jackson, B. J. and Kennedy, E. P. 1983. The biosynthesis of membrane-derived oligosaccharides. J. Biol. Chem. **258:**2394-2398.

Jackson, B. J., Bohin, J-P., Kennedy, E. P. 1984. Biosynthesis of membrane-derived oligosaccharides: characterization of *mdoB* mutants defective in phosphoglycerol transferase I activity. J. Bacteriol. **160:**976-981.

Jackson, B. J., Gennity, J. M., Kennedy, E. P. 1986. Regulation of the balanced synthesis of membrane phospholipids. J. Biol. Chem. **261:**13464-13468.

Jacobs, M. A., Alwood, A., Thaipisuttikul, I., Spencer, D., Haugen, E., Ernst, S., Will, O., Kaul, R., Raymond, C., Levy, R., Chun-Rong, L., Guentner, D., Bovee, D., Olson, M. V., Manoil, C. 2003. Comprehensive transposon mutant library of *Pseudomonas aeruginosa*. Proc. Natl. Acad. Sci. USA. **24:**14339-14344.

Jermyn, M. A. 1960. Studies on the glucono-δ-lactonase of *Pseudomonas fluorescens*. Biochem. et Biophys. ACTA. **37:**78-92.

Jin, Y., Bok, J. W., Guzman-de-Pena, D., Keller, N. P. 2002. Requirement of spermidine for developmental transitions in *Aspergillus nidulans*. Mol. Microbiol. **46:**801-812.

Kallio, A. and McCann, P. P. 1981. Difluoromethylornithine irreversibly inactivates ornithine decarboxylase of *Pseudomonas aeruginosa*, but does not inhibit the enzymes of *Escherichia coli*. Biochem J. **200:**69-75.

Kaniga, K., Delor, I., Cornelis, G. R. 1991. A wide-host-range suicide vector for improving reverse genetics in Gram-negative bacteria: inactivation of the *blaA* gene of *Yersinia enterocolitica*. Gene **109:**137-141.

Kennedy, E. P. 1982. Osmotic regulation and the biosynthesis of membrane-oligosaccharides in *Escherichia coli*. Proc. Natl. Acad. Sci. USA. **79:**1092-1095.

Kutchan, T. M. 1993. Strictosidine: from alkaloid to enzyme to gene. Phytochem. **32:**493-506.

Kutcher, K. L. 2004. Molecular characterization of GltF and GltG of the *Pseudomonas aeruginosa* glucose ABC transporter. M.Sc. Thesis, University of Manitoba, Winnipeg, Manitoba, Canada.

Kyte, J. and Doolittle, R. F. 1982. A simple method for displaying the hydropathic character of a protein. J. Mol. Bio. **157:**105-132.

Lacroix, J-M., Lanfroy, E., Cogez, V., Lequette, Y., Bohin, A., Bohin, J. P. 1999. The MdoC gene of *Escherchia coli* encodes a membrane protein that is required for succinylation of osmoregulated periplasmic glucans. J. Bacteriol. **181:**3626-3631.

Lu, C-D., Itoh, Y., Nakada, Y., Jiang, Y. 2002. Functional analysis and regulation of the divergent *spuABCDEFGH-spuI* operons for polyamine uptake and utilization in *Pseudomonas aerugionosa* PA01. J. Bacteriol. **184:**3765-3773.

Lutenberg, B. and Van Alpen, L. 1983 Molecular architecture and functioning of the outer membrane of *Escherichia coli* and other Gram-negative. Biochim. Biophys. ACTA. **737:**51-115.

MacGregor, C. H., Wolff, J. A., Arora, S. K., Phibbs, P. V., Jr. 1991. Cloning of a catabolite repression control (*crc*) gene from *Pseudomonas aeruginosa*, expression of the gene in *Escherichia coli*, and identification of the gene product in *Pseudomonas aeruginosa*. J. Bacteriol. **173:**7204-7212.

Mead, A. D., Szczesna-Skorupa, E., Kemper, B. 1986. Single-stranded DNA 'blue' T7 promoter plasmids: a versatile tandem promoter system for cloning and protein engineering. Protein Engineering **1:**67-74.

Midgley, M. and Dawes, E. A. 1973. The regulation of transport of glucose and methyl α-glucoside in *Pseudomonas aeruginosa*. Biochem. J. **132:**141-154.

Mims, C. A., Playfair, J. H. L., Roitt, I. M., Wakelin, D., Williams, R., Anderson, R. M. 1993. In Medical Microbiology. Mosby: London, U.K. Pages 22.18, 33.5, 33.6, A.24, A.25.

Mitchell, C. G. and Dawes, E. A. 1982. The role of oxygen in the regulation of glucose metabolism, transport and the tricarboxylic acid cycle in *Pseudomonas aeruginosa*. J. Gen. Micro. **128:**49-59.

Olsen, R. H., DeBusscher, G., McCombie, R. W. 1982. Development of broad-host-range vectors and gene banks: self-cloning of the *Pseudomonas aeruginosa* PAO chromosome. J. Bacteriol. **150:**60-69.

Osborn, M. J., Rosen, L., Rothfield, L., Zeleznick, L. D., Horecker, B. L. 1964. Lipopolysaccharide of the Gram-negative cell wall. Science **145:**783-789.

O'Toole, G., Gibbs, K. A., Hager, P. W., Phibbs, P. V., Jr. Kolter, R. 2000. The global carbon metabolism regulator Crc is a component of a signal transduction pathway required for biofilm development by *Pseudomonas aeruginosa*. J. Bacteriol. **182:**425-431.

Page, R., Altabe, S., Hugouvieux-Cotte-Pattat, N., Lacroix, J. M., Robert-Baudouy, J., Bohin, J. P. 2001. Osmoregulated periplasmic glucan synthesis is required for *Erwinia chrysanthemi* pathogenicity. J. Bacteriol. **183:**3134-3141.

Pfitzner, U. and Zenk, M. H. 1989. Homogeneous strictosidine synthase isoenzymes from cell suspension cultures of *Catharanthus roseus*. Planta Med. **55:**525-530.

Phibbs, P. V., Jr. and Eagon, R. G. 1970. Transport and phosphorylation of glucose, fructose, and mannitol by *Pseudomonas aeruginosa*. Arch. Biochem. Biophys. **138:**470-482.

Phibbs, P. V., Jr. McCowen, S. M., Feary, T. W., Blevins, W. T. 1978. Mannitol and fructose catabolic pathways of *Pseudomonas aeruginosa* carbohydrate-negative mutants and pleiotropic effects of certain enzyme deficiencies. J. Bacteriol. **133:**717-728.

Pitout, J. D., Thomson, K. S., Hanson, N. D., Ehrhardt, A. F., Coudron, P., Sanders, C. C. 1998. Plasmid-mediated resistance to expanded-spectrum cephalosporins among *Enterobacter aerogenes* strains. Antimicro. Agents and Chemother. **42:**596-600.

Powell, B. S., Rogowski, P. M., Kado, C. I. 1989. virG of *Agrobacterium tumefaciens* plasmid pTiC58 encodes a DNA-binding protein. Molec. Microbiol. **3:**411-419.

Rajagopal, S., Eis, N., Bhattacharya, M., Nickerson, K. W. 2003. Membrane-derived oligosaccharides (MDOs) are essential for sodium dodecyl sulfate resistance in *Escherichia coli*. FEMS Microbiol. Lett. **223:**25-31.

Roehl, R. A. and Phibbs, P. V., Jr. 1982. Characterization and genetic mapping of fructose phosphotransferase mutations in *Pseudomonas aeruginosa.* J. Bacteriol. **149:**897-905.

Roehl, R. A., Feary, T. W., Phibbs, P. V., Jr. 1983. Clustering of mutations affecting central pathway enzymes of carbohydrate catabolism in *Pseudomonas aeruginosa.* J. Bacteriol. **156:**1123-1129.

Rosenberg, S. L. and Hegeman, G. D. 1971. Genetics of the mandelate pathway in *Pseudomonas aeruginosa.* J. Bacteriol. **108:**1270-1276.

Rumley, M. K., Therisod, H., Weissborn, A. C., Kennedy, E. P. 1992. Mechanisms of regulation of the biosynthesis of membrane-derived oligosaccharides in *Escherchia coli.* J Biol. Chem. **267:**11806-11810.

Sage, A. E., Proctor, W. D., Phibbs, P. V., Jr. 1996. A two-component response regulator, *gltR*, is required for glucose transport activity in *Pseudomonas aeruginosa* PAO1. J. Bacteriol. **178:**6064-6066.

Sambrook, J., Fritsch, E. F., Maniatis, T. 1989. Molecular cloning: a laboratory manual, 2nd ed. Cold Spring Harbor Laboratory Press, Cold Spring Harbor, N.Y., U.S.A.

Saravolac, E. G., Taylor, N. F., Benz, R., Hancock, R. E. W. 1991. Purification of glucose-inducible outer membrane protein oprB of *Pseudomonas putida* and reconstitution of glucose- specific pores. J. Bacteriol. **173:**4970-4976.

Sawyer, M. H., Baumann, P., Baumann, L., Berman, S. M., Canovas, J. L., Berman, R. H. 1977. Pathways of D-fructose catabolism in species of *Pseudomonas*. Arch. Microbiol. **112:**49-55.

Schneider, J. E., Reinhold, V., Rumley, M. K., Kennedy, E. P. 1979. Structual studies of the membrane-derived oligosaccharides of *Escherchia coli*. J. Biol. Chem. **254**:10135-10138.

Schulman, H. and Kennedy, E. P. 1977. Identification of UDP-glucose as an intermediate in the biosynthesis of trhe membrane-derived oligosaccharides of *Escherichia coli*. J. Biol. Chem. **252:**6299-6303.

Schulman, H. and Kennedy, E. P. 1979. Localization of membrane-derived oligosaccarides in the outer envelope of *Escherchia coli* and their occurence in other Gram-negative bacteria. J. Bacteriol. **137:**686-688.

Schweizer, H. P. 1991. The *agmR* gene, an environmentally responsive gene, complements defective *glpR*, which encodes the putative activator for glycerol metabolism in *Pseudomonas aeruginosa*. J. Bacteriol. **173:**6798-6806.

Schweizer, H. P. and Hoang, T. T. 1995. An improved system for gene replacement and *xyl*E fusion analysis in *Pseudomonas aeruginosa*. Gene **158:**15-22.

Schweizer, H. P., Jump, R., Po, C. 1997. Structure and gene-polypeptide relationships of the region encoding glycerol diffusion facilitator (glpF) and glycerol kinase (glpK) of *Pseudomonas aeruginosa*. Microbiology. **143:**1287-1297.

Siegel, L. S. and Phibbs, P. V., Jr. 1979. Glycerol and L-α-glycerol-3-phosphate uptake by *Pseudomonas aeruginosa*. Curr. Microbiology. **2:**251-256.

Sly, L. M., Worobec, E. A., Perkins, R. E., Phibbs, P. V., Jr. 1993. Reconstitution of glucose uptake and chemotaxis in *Pseudomonas aeruginosa* glucose transport defective mutants. Can. J. Micro. **39:**1079-1083.

Stinnett, J. D., Guymon, L. F., Eagon, R. G. 1973. A novel technique for the preparation of transport-active membrane vesicles from *Pseudomonas aeruginosa*: observations on gluconate transport. Biochem. Biophys. Res. Comm. **52:**284-290.

Stinson, M. W., Cohen, M. A., Merrick, J. M. 1976. Isolation of dicarboxylic acid- and glucose binding proteins from *Pseudomonas aeruginosa*. J. Bacteriol. **128:**573-579.

Stinson, M.W., Cohen, M. A., Merrick M. A. 1977. Purification and properties of the periplasmic glucose-binding protein of *Pseudomonas aeruginosa*. J. Bacteriol. **131:**672-681.

Stockigt, J. and Zenk, M. H. 1977. Isovincoside (strictosidine), the key intermediate in the enzymatic formation of indole alkaloids. FEBS Lett. **79:**233-237.

Stover, C. K., Pham, X. Q., Erwin, A. L., Mizoguchi, S. D., Warrener, P., Hickey, M. J., Brinkman, F. S. L., Hufnagle, W. O., Kowalik, D. J., Lagrou, M., Garber, R. L., Goltry, L., Tolentino, E., Westbrock-Wadman, S., Yuan, Y., Brody, L. L., Coulter,

S. N., Folger, K. R., Kas, A., Larbig, K., Lim, R., Smith, K., Spencer, D., Wong, K-S., Wu, Z., Paulsen, I. T., Reizer J., Saier, M. H., Hancock, R. E. W., Lory, S., Olson, M. V. 2000. Complete genome sequence of *Pseudomonas aeruginosa* PA01, an opportunistic pathogen. Nature **406:** 959-964.

Tabor-White, C. and Tabor, H. 1984. Polyamines. Annu. Rev. Biochem. **53:**749-790.

Tabor-White, C. and Tabor, H. 1985. Polyamines in microorganisms. Microbiol. Rev. **49:**81-99.

Temple, L., Cuskey, S. M., Perkins, R. E., Bass, R. C., Morales, N. M., Christie, G. E., Olsen, R. H., Phibbs, P. V., Jr. 1990. Analysis of cloned structural and regulatory genes for carbohydrate utilization in *Pseudomonas aeruginosa* PAO. J. Bacteriol. **172:**6396-6402.

Temple, L. M. , Sage, A. E., Schewizer, H. P., Phibbs, P. V., Jr. 1998. Carbohydrate catabolism in *Pseudomonas aeruginosa*. In Biotechnology Handbooks: *Pseudomonas*, vol. 10, pp.35-72. Edited by T. C. Montie. Plenum Press, New York.

Tiwari, N. P. and Campbell, J. J. R. 1969. Enzymatic control of the metabolic activity of *Pseudomonas aeruginosa* grown in glucose or succinate media. Biochim. Biohys. Acta. **192:**395-401.

Trias, J., Rosenberg, E. Y., Nikaido, H. 1988. Specificity of the glucose channel formed by protein D1 of *Pseudomonas aeruginosa*. Biochim. Biophys. Acta **938:**493-496.

Tsay, S., Brown, K. K., Gaudy, E. T. 1971. Transport of glycerol by *Pseudomonas aeruginosa*. J. Bacteriol. **108:**82-88.

Valentine, P. J., Devore, B. P., Heffron, F. 1998. Identification of three highly attenuated *Salmonella typhimurium* mutants that are more immunogenic and protective in mice than a prototypical *aroA* mutant. Infect. Immun. **66:**3378-3383.

Van Dijken, J. P. and Quayle, J. R. 1977. Fructose metabolism in four *Pseudomonas* species. Arch. Microbiol. **114:**281-286.

Von Heige, G. 1986. A new method for prediction signal sequence cleavage sites. Nucleic Acid Res. **14:**4683-4690.

Weissenborn, D. L., Wittekindt, N., Larson, T. J. 1992. Structure and regulation of the *glpFK* operon encoding glycerol diffusion facilitator and glycerol kinase of *Escherichia coli* K-12. J. Biol. Chem. **267:**6122-6131.

West, S. E. H., Schweizer, H. P., Dall, C., Sample, A. K., Runyen-Janecky, L. J. 1994. Construction of improved *Escherichia-Pseudomonas* shuttle vectors derived from pUC18/19 and sequence of the region required for their replication in *Pseudomonas aeruginosa*. Gene **148:**81-86.

Williams, S. G., Greenwood, J. A., Jones, C.W. 1994. The effect of nutrient limitation on glycerol uptake and metabolism in continuous cultures of *Pseudomonas aeruginosa*. Microbiology **140:**2961-2969.

Whiting, P. H., Midgley, M., Dawes, E. A. 1976a. The regulation of transport of glucose, gluconate and 2-oxogluconate and of glucose catabolism in *Pseudomonas aeruginosa*. Biochem. J. **154:**659-668.

Whiting, P H., Midgley, M., Dawes, E. A. 1976b. The role of glucose limitation in the regulation of the transport of glucose, gluconate and 2-oxogluconate, and of glucose metabolism in *Pseudomonas aeruginosa*. J. Gen. Micro. **92:**304-310.

Wylie, J. L., Bernegger-Egli, C., O'Neil, J. D. J., Worobec, E. A. 1993. Biophysical characterization of OprB, a glucose-inducible porin of *Pseudomonas aeruginosa*. J. Bioenerg. Biomembr. **25:**547-556.

Wylie, J. L. and Worobec, E. A. 1993. Substrate specificity of the high-affinity glucose transport system of *Pseudomonas aeruginosa*. Can. J. Microbiol. **39:**722-725.

Wylie, J. L. and Worobec, E. A. 1994. Cloning and nucleotide sequence of the *Pseudomonas aeruginosa* glucose-selective OprB porin gene and distribution of OprB within the family *Pseudomonadaceae*. Eur. J. Biochem. **220:**505-512.

Wylie, J. L. and Worobec, E. A. 1995. The OprB porin plays a central role in carbohydrate uptake in *Pseudomonas aeruginosa*. J. Bacteriol. **177:**3021-3026.